ABSTRACT

Title of dissertation: WIRELESS NETWORK COCAST: COOPERATIVE COMMUNICATIONS WITH SPACE-TIME NETWORK CODING

Hung-Quoc Duc Lai, Doctor of Philosophy, 2011

Dissertation directed by: Professor K. J. Ray Liu
Department of Electrical and Computer Engineering

Traditional cooperative communications can greatly improve communication performance. However, transmissions from multiple relay nodes are challenging in practice. Single transmissions using time-division multiple access cause large transmission delay, but simultaneous transmissions from two or more nodes using frequency-division multiple access (FDMA), code-division multiple access (CDMA), or distributed space-time codes are associated with the issues of imperfect frequency and timing synchronization due to the asynchronous nature of cooperation.

In this dissertation, we propose a novel concept of wireless network cocast (WNC) and develop its associated space-time network codes (STNCs) to overcome the foretold issues. In WNC networks, each node is allocated a time slot for its transmission and thus the issues of imperfect synchronization are eliminated. To reduce the large transmission delay, each relay node forms a unique signal, a combination of the overheard information, and transmits it to the intended destination. The combining functions at relay nodes form a STNC that ensures full spatial diver-

sity for the transmitted information as in traditional cooperative communications. Various traditional combining techniques are utilized to design the STNCs, including FDMA-like and CDMA-like techniques and transform-based techniques with the use of Hadamard and Vandermonde matrices. However, a major distinction is that the combination of information from different sources happens within a relay node instead of through the air as in traditional cooperative communications.

We consider a general case of multiuser relay wireless networks, where user nodes transmit and receive their information to and from a common base node with the assistance from relay nodes. We then apply the STNCs to multiuser cooperative networks, in which the user nodes are also relay nodes helping each other in their transmission. Since the cooperative nodes are distributed around the network, the node locations can be an important aspect of designing a STNC. Therefore, we propose a location-aware WNC scheme to reduce the aggregate transmit power and achieve even power distribution among the user nodes in the network.

WNC networks and its associated STNCs provide spatial diversity to dramatically reduce the required transmit power. However, due to the additional processing power in receiving and retransmitting each other's information, not all nodes and WNC networks result in energy efficiency. Therefore, we first examine the power consumption in WNC networks. We then offer a TDMA-based merge process based on coalitional formation games to orderly and efficiently form cooperative groups in WNC networks. The proposed merge process substantially reduces the network power consumption and improves the network lifetime.

WIRELESS NETWORK COCAST: COOPERATIVE COMMUNICATIONS WITH SPACE-TIME NETWORK CODING

by

Hung-Quoc Duc Lai

Dissertation submitted to the Faculty of the Graduate School of the
University of Maryland, College Park in partial fulfillment
of the requirements for the degree of
Doctor of Philosophy
2011

Advisory Committee:
Professor K. J. Ray Liu, Chair/Advisor
Professor Alexander Barg
Professor Min Wu
Professor Dianne O'Leary
Professor Lawrence Washington

Preface

This dissertation was submitted to the Faculty of the Department of Electrical and Computer Engineering at the University of Maryland in partial fulfillment of the requirements for the degree of Doctor of Philosophy (Ph.D.). The studies were carried out over a period of over three years, from September 2007 to December 2010. The research was mainly supported by the In-house Laboratory Independent Research (ILIR) program at the United States Army Research, Development, and Engineering Command (RDECOM) Communications-Electronics Research, Development, and Engineering Center (CERDEC).

Hung-Quoc Lai

College Park, April 21, 2011

Dedication

To my wife Lethy and my beloved children:
Quoc-Viet, Quoc-Kiet, and Minh-Chau

Acknowledgements

As the first person in my extended family to receive a Ph.D. degree, I owe my gratitude to all the people who have helped me through this long journey, in one way or another, making this great achievement as much a significant life experience as a challenging but rewarding intellectual experience.

First and foremost, I would like to express my deep gratitude to my advisor, Professor K. J. Ray Liu for his care, guidance, and support. I first knew Professor Liu in Summer 2003 when I worked under his supervision in the Maryland Engineering Research Internship Teams (MERIT) program at the Department of Electrical and Computer Engineering, University of Maryland. His research work and his erudition always inspire me and were an encouragement for me to continue my education with my Ph.D. study after I completed my undergraduate. It has been a pleasure to work with and learn from such an extraordinary individual.

I would also like to thank the other members of my dissertation committee. Special thanks are due to Professor Alexander Barg and Professor Min Wu for their guidance in my research proposal. Their knowledge and insights were extremely valuable and greatly enriched my work. I also want to thank Professor Dianne O'Leary and Professor Lawrence Washington for agreeing to serve on my dissertation committee. To all the committee members, I greatly appreciate their invaluable time reviewing and commenting the manuscript.

My colleagues in Signals and Information Group at the University of Maryland have enriched my graduate life in many ways and deserve a special mention. I would

like to thank every member in the group for their friendship, encouragement, and help. I have learned a lot from each one of them, and for that I am deeply grateful. I specially thank Dr. Ahmed Ibrahim, Ms. Zhenzhen Gao, and Mr. Yan Chen for the research discussions that were all inspiring for me.

I would also like to thank Ms. Dorothea Brosius at the Institute for Electronics and Applied Physics, University of Maryland for providing the LaTex template, which made putting this dissertation together an easy effort.

I would like to acknowledge the financial support from the Gates Millennium Scholars for my undergraduate and graduate study. Without the support, it would be difficult for me to follow this program and complete this dissertation.

I owe my deepest thanks to my parents who bore me to this life and gave me a chance to come to the United States for a better education and life. It is a sadness in this achievement without my dad. Nevertheless, I knew he would greatly rejoice at my accomplishment.

I would also like to express my sincere appreciation to my parents-in-law in their encouragement. As teachers, they have inspired me on the love for education.

I would also like to express my deep gratitude to my aunt who raised me through my difficult childhood. Without her care and love, I would not have my early education, the first step to this accomplishment.

My deepest thanks are also given to my wife for her endless love and support. She has always stood by me, shared with me the fruits of life as well as its bitterness, and encouraged me in my work. Without her sacrifice, especially during this year when I composed this dissertation and prepared for the examination, it would be

hard for me to complete the Ph.D. program. Words cannot express the gratitude I owe her.

Lastly, all praise is due to God for making me be able to achieve this important step in life.

Table of Contents

List of Figures

List of Abbreviations

ADC	Analog-to-Digital Converter
AF	Amplify-and-Forward
AWGN	Additive White Gaussian Noise
BER	Bit Error Rate
BPSK	Binary Phase-Shift Keying
CDMA	Code-Division Multiple Access
CMOS	Complementary Metal-Oxide-Semiconductor
DAC	Digital-to-Analog Converter
DF	Decode-and-Forward
DSTBC	Distributed Space-Time Block Code
DSTC	Distributed Space-Time Code
DTX	Direct Transmission
FDMA	Frequency-Division Multiple Access
IFA	Intermediate-Frequency Amplifier
INC	Immediate-Neighbor Cooperation
ISI	Inter-Symbol Interference
LA-WNC	Location-Aware Wireless Network Cocast
LNA	Low Noise Amplifier
M2P	Multipoint-to-Point
MAX	Maximal Cooperation
MIMO	Multiple-Input Multiple-Output
ML	Maximum Likelihood
MMSE	Minimum Mean Square Error
OFDM	Orthogonal Frequency-Division Multiplexing
OFDMA	Orthogonal Frequency-Division Multiple Access
P2M	Point-to-Multipoint
PA	Power Amplifier
PAPR	Peak-to-Average-Power Ratio
PEP	Pairwise Error Probability
PSK	Phase-Shift Keying
QAM	Quadrature Amplitude Modulation
QPSK	Quadrature Phase-Shift Keying
RF	Radio-Frequency
RTS	Request-To-Send
SER	Symbol Error Rate
SINR	Signal-to-Interference-plus-Noise Ratio
SNR	Signal-to-Noise Ratio
STBC	Space-Time Block Code
STNC	Space-Time Network Code
TDMA	Time-Division Multiple Access
WNC	Wireless Network Cocast
WNCR	Wireless Network Cocast - Relay

Chapter 1

Introduction

1.1 Motivation

It is well-known that the performance of communication systems degrades greatly when operating in radio-frequency (RF) environments characterized by multipath propagation such as urban environments. Diversity techniques like time, frequency, and spatial diversity can be utilized to mitigate the multipath effect. The recent multiple-input multiple-output (MIMO) technology [1], [2], [3], in which communication devices are equipped with multiple transmit and/or multiple receive antennas, can significantly increase communication reliability through the use of spatial diversity. For instance, space-time codes, which exploit space and time diversity, were proposed in [4], [5], [6], [7], [8] for frequency flat fading channels. In case of frequency selective channels such as those experienced in broadband wireless communication systems, the frequency domain is taken into designing space-frequency codes [9], [10] for MIMO orthogonal frequency-division multiplexing (OFDM) systems. When long delay and complexity in decoding are allowable, space-time-frequency codes can be used over several OFDM symbols to achieve space, time, and frequency diversity [11], [12].

Although MIMO provides spatial diversity to improve communication performance, the use of MIMO technology possesses a number of issues in practical applications whose size, weight, and power are dominant factors in choosing a technology as in military hand-held and man-packed devices. First, the required separation among antennas, usually at least a half of wavelength, makes MIMO unsuitable for low transmit frequencies, which are used to have low free-space path loss and thus a longer battery life. Second, the use of multiple RF chains at a device increases the size and weight of the device and thus limits certain MIMO applications such as those in wireless sensor networks and military hand-held devices.

To overcome the MIMO issues while maintaining MIMO benefits in improving reliability, cooperative communications [13] have recently received much attention. Cooperative communications make use of broadcast nature of wireless transmission with nodes in a network acting as relays retransmitting overheard information to the intended destination. The distributed antennas from the source and the relays form a virtual antenna array, and spatial diversity is achieved without the need to use multiple antennas at the source node.

Various cooperative diversity protocols have been proposed and analyzed in [14], [15], [16], [17], [18], [19]. Several strategies for single-relay cooperative communications such as decode-and-forward (DF) and amplify-and-forward (AF) were introduced in [14], and their performance in terms of outage behavior was analyzed. In DF protocol, each relay decodes the overheard symbol from the source, re-encodes it, and then forwards it to the destination. AF protocol is a simpler technique, in which each relay simply amplifies the overheard signal and forwards

it to the destination. In [15], user cooperation strategy and performance analysis of a code-division multiple access system for two cooperative users were presented. Symbol error rate (SER) performance for multi-relay DF protocols was analyzed in [16]. Outage analysis for multi-relay AF relay networks was studied in [17]. In [16] and [17], optimal power allocation was also derived for DF and AF protocols. Various relay selection schemes were proposed in [18] that achieve high bandwidth efficiency and full diversity order. Finally in [19], distributed space-time-coded DF and AF protocols, which are based on conventional MIMO space-time coding, were proposed and their outage performance was analyzed.

Cooperative communications often consist of two phases: the source transmission phase and the relay transmission phase [16], [17], [19]. In the first phase, a source broadcasts its information to relays, which then forward the overheard information to the destination in the second phase. Much research in cooperative communications has focused on simultaneous transmissions from two or more nodes by using frequency-division multiple access (FDMA), code-division multiple access (CDMA), or distributed space-time codes (DSTCs) with an assumption of perfect frequency and timing synchronization [16], [17], [19], [20]. However, such an assumption is difficult to be met in practice due to the asynchronous nature of distributed antennas, especially in mobile conditions where nodes move at different speeds and in different directions. For timing synchronization, the coordination to make signals received simultaneously at the destination is challenging due to differences in propagation time among nodes, processing time in each radio, and timing estimation error. The frequency synchronization issue occurs when each node has an

independent local oscillator generating a transmit frequency with certain variation to the nominal. The transmit frequencies from different nodes, therefore, are different. Moreover, signals from nodes in mobile conditions with different directions and speeds are under different Doppler effects. Together, various frequency mismatches occur at once at the destination and make it difficult to estimate and compensate all the frequency offsets. The imperfect synchronization causes the inter-symbol interference (ISI), which is the source of system performance degradation [21], [22].

The issues of imperfect frequency and timing synchronization prohibit two or more nodes from transmitting at the same time. To overcome these issues, time-division multiple access (TDMA) [16], where each relay node take turn to forward the overheard symbols, would be the most commonly-used technique in many applications. A phased-locked loop device at a receiver can easily overcome the frequency mismatch and timing error from a single arriving signal. However, TDMA requires large transmission delays, especially for networks with large numbers of source nodes and relay nodes. Therefore, there is an essential need to overcome the issues of imperfect frequency and timing synchronization while maintaining the spatial diversity and reducing the total required time slots.

Many previous work consider cooperative communications as a direct extension of MIMO communications, leveraging the distributed antennas in a network to achieve the MIMO benefits. Hence the issues of imperfect synchronization due to the simultaneous transmissions from multiple nodes arise and prevent cooperative communications from emerging in practice. To address these issues, a number of methods in previous work have been proposed [23], [24], [25], [26], [27]. For mitigat-

ing the issue of timing synchronization, an artificial delay is assigned to each relay, and the destination uses a joint decision feedback equalizer to detect the transmitted information [23]. With a careful design of the artificial delay, full spatial diversity can be achieved. In [24], a family of distributed space-time trellis codes was proposed to provide full spatial diversity. However, the complexity of the decoder increases exponentially with the synchronization mismatch. In [25], delay-tolerant distributed threaded algebraic space-time codes were proposed. The codes associate with symbol repetition to maintain full spatial diversity and thus lead to substantial rate loss. To overcome the issue of frequency synchronization, distributed carrier synchronization was proposed in [26], [27], in which the transmit frequency of relay nodes is locked into the reference frequency of a master node. Each of these foretold approaches addresses the issue of either the frequency synchronization or the timing mismatch, not both. In addition, these approaches just mitigate the issues, not completely eliminate them.

1.2 Dissertation Outline and Contributions

In this dissertation, we propose a novel concept of wireless network cocast (WNC) and develop its associated space-time network codes (STNCs) to achieve the objectives of eliminating the issues of imperfect frequency and timing synchronization while maintaining the full spatial diversity in cooperative communications with low transmission delays. Cocast, an abbreviation of *co*operative *cast*, is a newly defined transmission method, in which information from different source nodes are

jointly combined within a relay and transmitted to the intended destinations. The novelty of this work is that it lays out a new framework for the cooperation among nodes in a network and proposes solutions to overcome the said issues. In the following, we provide synopses of our main contributions in the subsequent chapters of this dissertation.

1.2.1 Wireless Network Cocast and Space-Time Network Coding (Chapter 2)

In this chapter, we describe the novel concept of WNC and propose a number of STNCs based on FDMA-like and CDMA-like combining techniques. We consider two general cases of multipoint-to-point (M2P) and point-to-multipoint (P2M), where user nodes transmit and receive their information to and from a common base node, respectively, with the assistance from relay nodes. Both DF and AF protocols in cooperative communications are considered. We derive the exact and the asymptotic SER expressions[1] for general phase shift keying (PSK) modulation for DF protocol. For AF protocol, we offer a conditional SER expression given the channel knowledge. The STNCs are then applied into networks, in which the user nodes are also relay nodes helping each other in their transmission. We study the performance improvement of the WNC networks over direct transmission (DTX) networks, where a user node transmits directly to the base node without assistance from any other nodes. Simulations show that given the same quality of service rep-

[1] Asymptotic SER performance is a performance at high signal-to-noise ratio.

resented by a SER, the use of WNC schemes results in a great improvement in terms of power saving, range extension, and transmission rate [28], [29], [30].

1.2.2 Location-Aware Cooperative Communications with Linear Network Coding (Chapter 3)

In wireless networks, reducing aggregate transmit power and in many cases, having even power distribution increase the network lifetime. The conventional DTX scheme results in high aggregate transmit power and uneven power distribution. In this chapter, we propose a number of location-aware cooperation-based schemes namely immediate-neighbor cooperation (INC), maximal cooperation (MAX), and WNC that take into account the node locations to reduce aggregate transmit power and achieve even power distribution. The INC scheme utilizes single-relay cooperative communication, resulting in good reduction of aggregate transmit power and low transmission delay; however, power distribution is still uneven. In the MAX scheme, multi-relay cooperative communication is leveraged to provide *incremental diversity* to achieve even power distribution and substantial reduction in aggregate transmit power. Transmission delay in the MAX scheme, however, grows quadratically with the number of user nodes in the network. As a result, we utilize the concept of WNC to propose a location-aware WNC (LA-WNC) scheme that achieves incremental diversity as in MAX and low transmission delay as in INC. Performance evaluation in uniformly distributed networks shows that the INC, MAX, and WNC schemes substantially reduce aggregate transmit power while the MAX and WNC schemes

also provide even power distribution [31], [32].

1.2.3 Transform-based Space-Time Network Coding (Chapter 4)

In Chapter 2, FDMA-like and CDMA-like combining techniques are used to develop STNCs for WNC networks. Although these STNCs help reducing the transmission delays, they do not achieve better spectral efficiency over the traditional TDMA scheme in cooperative communications. In this chapter, a STNC based on transform-based coding, whose coding matrices take a form of Hadamard or Vandermonde matrices and compose a set of parameters that are optimized for conventional signal constellations, is proposed to improve the spectral efficiency of the combining signals at relay nodes. We analyze the pairwise error probability (PEP) performance of the proposed STNC and derive the design criteria of the network coding matrix to achieve full diversity. We also perform simulations to validate the performance of the proposed STNC. In addition, performance comparison between the proposed STNC and a distributed space-time block code (DSTBC) scheme, which operates under timing synchronization errors, is investigated through simulations [33].

1.2.4 Coalition Formation Games for Energy Efficient Wireless Network Cocast (Chapter 5)

WNC networks and its associated STNCs provide spatial diversity to combat channel fading and thus dramatically reduce the required transmit power in comparison with DTX networks. However, due to the additional processing power

in receiving and retransmitting each other's information, not all nodes and WNC networks result in energy efficiency. In this chapter, we first examine the power consumption in WNC and DTX networks. The power consumption includes the processing power at the transmitter and receiver radio-frequency components and the required transmit power to convey information over the medium between the transmitter and receiver. We then offer a TDMA-based merge process based on coalitional formation games to orderly and efficiently form cooperative groups in WNC networks. A node is merged into a cooperative group only if the merge leads to power saving for the group without causing additional power burden to the individual members. Simulation is provided to corroborate the energy efficient WNC networks. From the simulation, there is a substantial reduction in network power consumption when using the proposed merge process. In addition, the merge process also improves the network lifetime.

Chapter 2

Wireless Network Cocast and Space-Time Network Coding

In this chapter, we present a novel concept of WNC and propose its associated STNCs to overcome the issue of imperfect frequency and timing synchronization while maintaining the spatial diversity and reducing the transmission delays in cooperative communications. We consider two general cases of M2P and P2M transmissions, where N user nodes transmit and receive their information to and from a common base node, respectively, with the assistance from R relay nodes. We denote them as M2P-WNCR and P2M-WNCR, where "R" implies the use of independent relay nodes. Both DF and AF protocols in cooperative communications are considered in the general WNCR schemes. We derive the exact and the asymptotic SER expressions for general $\mathcal{M}$-PSK modulation for DF protocol. The extension to general quadrature-amplitude modulation (QAM) can follow directly. For AF protocol, we offer a conditional SER expression given the channel knowledge.

The STNCs of WNCR schemes provide general codings that can be applied in many wireless network settings. The most interesting setting is where a group of user nodes located in a close proximity to one another as in a cluster cooperate together to improve their performance. An example can be found in wireless sensor networks or cellular networks with transmission exchange between sensors and a

fusion center or between a base station and users. In this case, the user nodes can also be relays, helping one another in transmissions between themselves and the base node. We refer this network setting as clustering setting, and the application of WNCR schemes in this network are denoted as WNC schemes. We study the performance improvement using WNC schemes over DTX scheme, where a user node transmits directly to the base node without assistance from any other nodes. Simulations show that given the same quality of service represented by a SER, the use of WNC schemes results in a great improvement in terms of power saving, range extension, and transmission rate.

Notation: Lower and upper case bold symbols denote column vectors and matrices, respectively. *, $^\mathcal{T}$, and $^\mathcal{H}$ denote complex conjugate, transpose, and Hermitian transpose, respectively. $\text{diag}\{.\}$ represents a diagonal matrix. $|.|$ denotes the magnitude or the size of a set. $\mathcal{CN}(0, \sigma^2)$ is the circular symmetric complex Gaussian random variable with zero mean and variance σ^2. r refers to the index of a relay node, and n denotes the index of a transmitted symbol of interest and also the index of a user node. a_{uv} with generic indices u and v denotes a signal coefficient.

2.1 A Concept and System Models

Let us consider a multiuser relay wireless network that comprises of N user nodes denoted as $U_1, U_2, ..., U_N$ having their own information that need to be delivered to a common base node U_0 as shown in Figure 2.1. Moreover, we assume

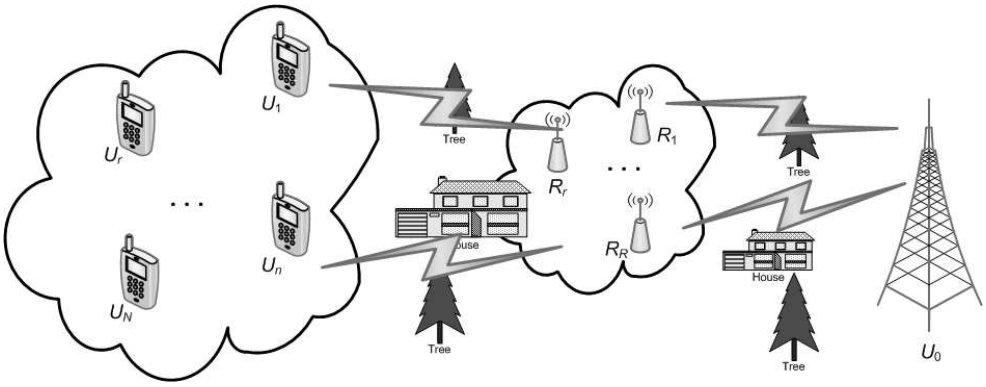

Figure 2.1: A multiuser relay wireless network.

R relay nodes, denoted as $R_1, R_2, ..., R_R$, helping the user nodes in forwarding the transmitted information. Without loss of generality, the transmitted information can be represented by symbols, denoted as $x_1, x_2, ..., x_N$. Nevertheless, the user nodes and relay nodes in practice will transmit the information in packets that contains a large number of symbols. The destination will collect all the transmitted packets and then jointly detect the transmitted information as in traditional network coding [34], [35], [36]. Note that the relay nodes can be the user nodes themselves or they can be nodes dedicated to only relaying information for others such as relay towers.

We realize that after the source transmission phase, in which the N source nodes broadcast their information, the relay nodes possess a set of overheard symbols, denoted as a vector $\mathbf{x} = [x_1, x_2, ..., x_N]^{\mathcal{T}}$, from the user nodes. Instead of allowing multiple relay nodes transmitting at the same time as in the traditional cooperative communications, each relay node forms a single signal by encoding the set of overheard symbols, denoted as $f_r(\mathbf{x})$ for relay node R_r for $r = 1, 2, ..., R$ and

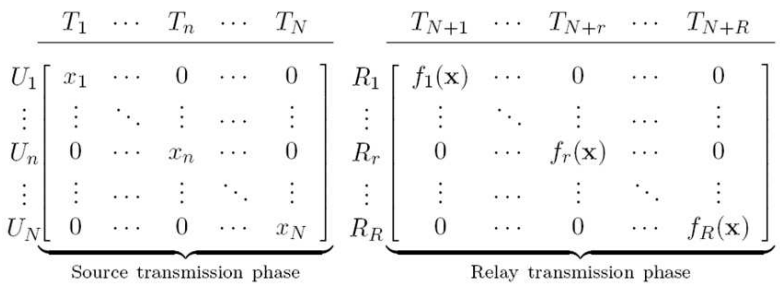

Figure 2.2: A general framework of space-time network coding.

transmits it to the intended destination in its own dedicated time slot. The transmissions from the N user nodes and R relay nodes in the source and relay transmission phases, respectively, are illustrated in Figure 2.2. Each set of encoding functions f_r's, denoted as $\{f_r\}_{r=1}^{R}$, will form a STNC that governs the cooperation and the transmission among the nodes in the network. The STNC will provide appropriate spatial diversity with only $(N + R)$ time slots, a reduction from $2N$ time slots in the traditional CDMA and FDMA cooperative communications for N being usually greater than R and from $N(R+1)$ time slots in the traditional TDMA cooperative communications. Moreover, the foretold issue of imperfect frequency and timing synchronization is overcome because a single transmission is granted at any given time slot in the network.

The concept of our proposed STNCs is very general. Fundamentally, it involves combining information from different sources at a relay node as in traditional network coding, which gives rise to the concept of network coding, and transmitting the combined signal in a dedicated time slot, which makes the space-time concept. Note that the proposed space-time network coding is different from the traditional

network coding in several aspects. Unlike traditional network coding [34], [35], [36], in which the combination of packets is performed at the bit level with Galois field operations and occurs at the network layer, the overheard information in our proposed STNCs is combined at the symbol level of the physical layer. In addition, traditional network coding is to improve the network throughput while our proposed STNC schemes, in contrast, is intended to improve the communication reliability. Lastly, while the traditional network coding is invariant in terms of node locations, the space dimension (or node locations), due to the distribution of nodes around wireless networks, can be an important aspect of designing a STNC as we will see in Chapter 3.

We expect that various traditional combining techniques can be used; however, a major distinction is that the combining of symbols from different sources, giving rise to the received signal at a destination, happens within a transmitter instead of through the air. These techniques could include CDMA-like, FDMA-like, and TDMA-like techniques. As the names suggest, each source information in CDMA-like technique is assigned a spreading code [37], [38] while FDMA-like technique uses a group of subcarriers as in the well-known orthogonal frequency-division multiple access (OFDMA) [39]. In TDMA-like technique, each relay is assigned a large time slots to be able to concatenate the N symbols along the time axis for transmission. As in the traditional TDMA scheme, the TDMA-like scheme can overcome the imperfect synchronization issue but also leads to the issue of long transmission delay due to the concatenation of symbols along the time axis. The combining techniques could also be transform-based techniques [40], [41], [42] with the use of Hadamard or

Vandermonde matrices. In addition, they could probably be the traditional network coding [34], [35], [36], which linearly combines symbols from different sources over Galois field. Clearly, each combining technique requires an appropriate multi-user detection technique to separate the transmitted symbols from single coded-signals.

The STNCs that we propose in this chapter are the CDMA-like, FDMA-like, and TDMA-like techniques. Although they are expected to provide comparable SER performance, we favor the first two techniques since they can provide lower transmission delay in comparison with the third one. CDMA and FDMA has been used in cooperative communications [15], [20], [16], where multiple relay nodes transmit at the same time with the assumption of perfect synchronization. This assumption is hard to be met in practice as we discussed in Chapter 1. In our work, each relay node forms a linearly-coded signal from the overheard symbol within the node itself and transmits the signal in its assigned time slot. Note that our proposed CDMA-like, FDMA-like, and TDMA-like schemes do not provide more bandwidth efficiency, measured by the number of bits per second per Hertz (bit/s/Hz), than the traditional TDMA, FDMA, and CDMA schemes in cooperative communications. In multinode transmissions, time, frequency, and code are interchangeable resources. To reduce the number of required time slots, more frequency resource is needed. However, the use of these resources is governed by practical applications and constraints. For example in traditional non-cooperative networks, FDMA such as the OFDMA employed in WiMAX systems [39] is preferred over TDMA for applications that require low transmission delay. On the other hand, CDMA system with its spreading techniques is in favor due to its ability to overcome intentional

interference such as jamming signals in military applications. Our proposed scheme is to solve a practical issues of imperfect synchronization and large transmission delay in the traditional TDMA, FDMA, and CDMA schemes.

The general framework in Figure 2.2 can be applied in M2P and P2M transmissions, and we denote these schemes as M2P-WNCR and P2M-WNCR. In M2P-WNCR, the N user nodes $U_1, U_2, ..., U_N$ transmit their symbols $x_1, x_2, ..., x_N$, respectively, to the base node U_0 while the user nodes are the destinations for these symbols from the base node in P2M-WNCR. The channels are modeled as narrowband Rayleigh fading with additive white Gaussian noise (AWGN). Quasi-static channels are assumed, where they remain constant over each time slot and change independently between consecutive slots. The channel coefficient between an arbitrary receiver u and transmitter v is defined as $h_{uv} \sim \mathcal{CN}(0, \sigma_{uv}^2)$, where $\sigma_{uv}^2 = d_{uv}^{-\alpha}$ is the channel variance with d_{uv} and α being the distance between the two nodes and the path loss exponent, respectively. The transmit power P_n associated with transmitted symbol x_n is distributed among the source node (U_n or U_0 in M2P-WNCR or P2M-WNCR, respectively) and the relay nodes. We have $P_n = P_{nn} + \sum_{r=1}^{R} P_{rn}$, where P_{nn} and P_{rn} are the power allocated at the source U_n or U_0 and the relay R_r, respectively.

In the CDMA-like STNC, each symbol x_n is assigned a complex-valued signature waveform (also called a spreading code) $s_n(t)$ to protect it against the interference from other symbols. The cross-correlation between $s_n(t)$ and $s_m(t)$ is defined as $\rho_{nm} = \langle s_n(t), s_m(t) \rangle \triangleq \frac{1}{T} \int_0^T s_n(t) s_m^*(t) dt$, the inner product between $s_n(t)$ and $s_m(t)$ with the symbol interval T and * representing the complex conjugate. We

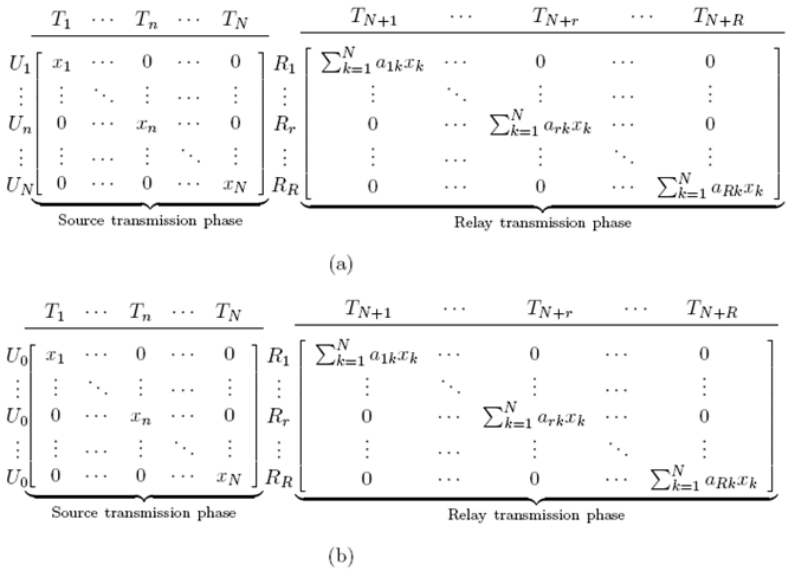

Figure 2.3: Space-time network codes for (a) M2P-WNCR and (b) P2M-WNCR schemes.

assume $\rho_{nn} = \|s_n(t)\|^2 = 1$. In the FDMA-like and TDMA-like, $s_n(t)$ represents the dedicated carrier and the symbol duration associated with symbol x_n. In this work, orthogonal and nonorthogonal codes refer to the cross-correlation characteristics of the signature waveforms. When $\rho_{nm} \neq 0$ for $m \neq n$, we have the nonorthogonal code. We assume that the relay nodes know the signature waveforms associated with the user nodes. In the sequel, we will describe in details the STNCs for WNCR schemes.

2.1.1 Space-Time Network Code for M2P-WNCR Transmissions

Figure 2.3(a) illustrates the transmissions in the source and relay transmission phases of the M2P-WNCR, in which the N user nodes $U_1, U_2, ..., U_N$ transmit their symbols to the common base node U_0. As shown in the figure, the STNC requires

$(N + R)$ time slots to complete the transmissions and guarantees a single transmission in the network at any given time slot to eliminate the issue of imperfect synchronization in traditional cooperative communications. In the source transmission phase, user node U_n for $n = 1, 2, ..., N$ is assigned a time slot T_n to broadcast its symbol x_n to the base node and all relay nodes. The signals received at U_0 and R_r are

$$y_{0n}(t) = h_{0n}\sqrt{P_{nn}}x_n s_n(t) + w_{0n}(t) \tag{2.1}$$

and

$$y_{rn}(t) = h_{rn}\sqrt{P_{nn}}x_n s_n(t) + w_{rn}(t), \tag{2.2}$$

respectively, where $w_{0n}(t)$ and $w_{rn}(t)$ are zero-mean and N_0-variance AWGN. At the end of this phase, each relay node R_r for $r = 1, 2, ..., R$ possesses a set of N symbols $x_1, x_2, ..., x_N$ from the user nodes. In the relay transmission phase, R_r forms a single linearly-coded signal, a linear combination of these symbols, and transmits the signal to the base node in its dedicated time slot T_r. R_r can simply amplify the signal in (2.2) and combine with others to form the linearly-coded signal, the so called AF protocol. It can also detect the symbol x_n based on (2.2), whose detection will be discussed later in Section 2.2, and re-encode it in the linearly-coded signal if the decoding is successful, the so called DF protocol. A detection state, a success or a failure in detecting a symbol, can be determined based on the amplitude of the estimated channel coefficient [14] or the received signal-to-noise ratio (SNR) [16]. Notice that this DF scheme is also called the selective-relaying protocol in the literature [14]. In practice, information is transmitted in packets [43] that contain a

large number of symbols. Each packet is detected as a whole and a cyclic redundancy check [44] is sufficient to determine the detection state of the packet.

The received signal at U_0 from R_r in the relay transmission phase is

$$y_{0r}(t) = h_{0r} \sum_{k=1}^{N} \sqrt{\widetilde{P}_{rk}} x_k s_k(t) + w_{0r}(t), \tag{2.3}$$

including symbol x_n when $k = n$. In (2.3),

$$\widetilde{P}_{rk} = \begin{cases} P_{rk} & \text{if } R_r \text{ decodes } x_k \text{ correctly} \\ 0 & \text{otherwise} \end{cases} \tag{2.4}$$

for the case of DF and

$$\widetilde{P}_{rk} = \frac{P_{rk} P_{kk} |h_{rk}|^2}{P_{kk} |h_{rk}|^2 + N_0} \tag{2.5}$$

for the case of AF and $w_{0r}(t)$ is zero-mean and $N_0 f_{0r}$-variance AWGN, where

$$f_{0r} = \begin{cases} 1 & \text{for DF} \\ 1 + \sum_{k=1}^{N} \frac{P_{rk} |h_{0r}|^2}{P_{kk} |h_{rk}|^2 + N_0} & \text{for AF} \end{cases} \tag{2.6}$$

is a factor representing the impact on U_0 performance due to the noise amplification at R_r. Notice that in (2.3), U_0 receives a combined signal of multiple transmitted symbols that is formed within a relay node, not through the air as in traditional CDMA or FDMA schemes, where the symbols are from different relays, and hence overcomes the prominent issue of imperfect frequency and timing synchronization in these technologies.

2.1.2 Space-Time Network Code for P2M-WNCR Transmissions

P2M-WNCR also consists of a source transmission phase and a relay transmission phase, in which the base node U_0 transmits symbols $x_1, x_2, ..., x_N$ to the N

user nodes $U_1, U_2, ..., U_N$. Figure 2.3(b) illustrates the transmissions in the source and relay transmission phases of the P2M-WNCR. The STNC also requires $(N+R)$ time slots to complete the transmissions, and the foretold issue of imperfect synchronization is eliminated.

As shown in the figure, the signal model for this STNC can be derived in the same manner of that in M2P-WNCR scheme. The received signals at user node U_n and relay node R_r in the source transmission phase are

$$y_{n0}(t) = h_{n0}\sqrt{P_{nn}}x_n s_n(t) + w_{n0}(t) \tag{2.7}$$

and

$$y_{r0}(t) = h_{r0}\sqrt{P_{nn}}x_n s_n(t) + w_{n0}(t), \tag{2.8}$$

respectively, where $w_{n0}(t)$ and $w_{r0}(t)$ are zero-mean and N_0-variance AWGN. In the relay transmission phase, the received signal at U_n from R_r is

$$y_{nr}(t) = h_{nr}\sum_{k=1}^{N}\sqrt{\widetilde{P}_{rk}}x_k s_k(t) + w_{nr}(t), \tag{2.9}$$

which includes the intended symbol x_n for U_n. In (2.9), $\widetilde{P}_{rk}$ follows (4.4) for the case of DF and

$$\widetilde{P}_{rk} = \frac{P_{rk}P_{kk}|h_{r0}|^2}{P_{kk}|h_{r0}|^2 + N_0} \tag{2.10}$$

for the case of AF and $w_{nr}(t)$ is zero-mean and $N_0 f_{nr}$-variance AWGN, where

$$f_{nr} = \begin{cases} 1 & \text{for DF} \\ 1 + \sum_{k=1}^{N}\frac{P_{rk}|h_{nr}|^2}{P_{kk}|h_{r0}|^2+N_0} & \text{for AF} \end{cases} \tag{2.11}$$

is a factor representing the impact on U_n due to the noise amplification at R_r.

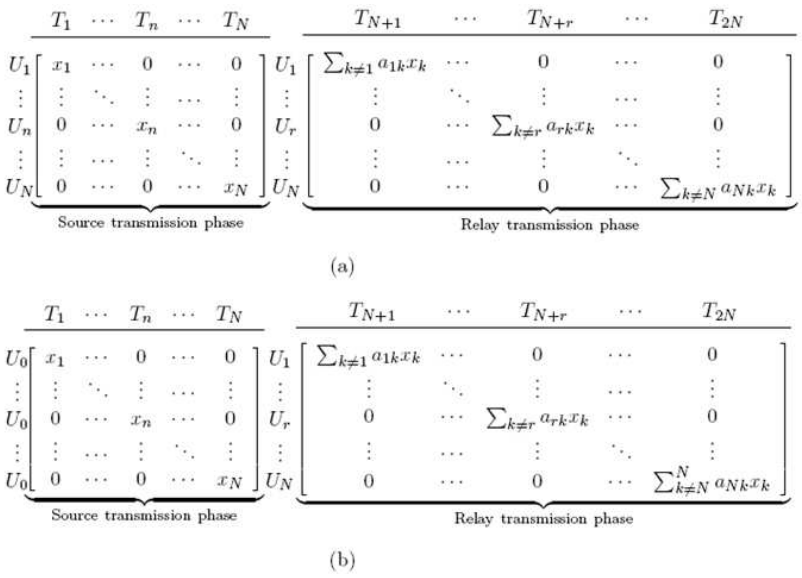

Figure 2.4: Space-time network codes for (a) M2P-WNC and (b) P2M-WNC schemes.

2.1.3 Other Space-Time Network Codes

The STNCs in the general WNCR schemes provide general codings that can be applied in many wireless network settings. The most interesting setting is where a group of user nodes located in a close proximity to one another as in a cluster cooperate together to improve their performance. In this case, the user nodes also act as relays, helping one another in transmissions between themselves and the base node. We refer this network setting as clustering setting, and the application of WNCR schemes in this network are denoted as WNC schemes. The STNCs in Figure 2.3 can be rewritten as in Figure 2.4.

M2P-WNC and P2M-WNC can be directly applied to multipoint-to-multipoint (M2M) transmissions, where multiple nodes form pair to exchange information as in

ad hoc networks. To illustrate the application, let us consider a network comprised of $2N$ nodes, separated into two clusters of transmitters and receivers, each with N nodes. In the case of using M2P-WNC, the N transmitters cooperate to one another as the user nodes in M2P-WNC. The transmitters first exchange the transmitted symbols in the source transmission phase. They then form the linearly-coded signals and broadcast them to the N receivers in the relay transmission phase. On the other hand when using P2M-WNC, the N transmitters acting as the base node in P2M transmissions. The transmitters take turn to broadcast their symbols to the N receivers in the source transmission phase. As in P2M-WNC, the receivers cooperate with one another, forming a linearly-coded signal and exchanging the signals among themselves in the relay transmission phase. In both cases, a receiver applies a detection technique presented later in Section 2.2 to detect its intended symbol and discards the unwanted ones.

2.2 Signal Detection

To detect a desired symbol, we assume that receivers have a full knowledge of the channel state information, which can be acquired using a preamble in the transmitted signal as usually done in systems such as 802.11 [43]. In the case of DF protocol, we also assume that a destination knows the detection states at the relay nodes. This can be done by using an N-bit indicator in the relaying signal. Notice that in practice, information is transmitted in packets [43] that contain a large number of symbols. Each packet is detected as a whole, and a cyclic redundancy

check [44] is sufficient to determine the detection state of the packet. Thus one bit per packet results in a minimal overhead.

As shown in Section 4.1, the transmission of symbol x_n in WNCR schemes shares a similar signal model, regardless where it is transmitted from. The symbol is first transmitted by the source node U_n or U_0 in M2P or P2M transmissions, respectively, and then forwarded by the relay nodes $R_1, R_2, ..., R_R$ to the destination node U_0 or U_n. Thus the same detection technique can be used in the two STNCs. In this section, we present a detailed signal detection in M2P-WNCR, and the detection in P2M-WNCR can follow in a straight manner. To achieve a tractable performance analysis, we use a multi-user detection technique that includes a decorrelator and a maximal-ratio combining detector. Nevertheless, one can use minimum mean-square error (MMSE) detector, which is optimal among linear detectors. At high SNR, however, we expect that MMSE detector and our multiuser detector have comparable performance. The detection for an arbitrary symbol x_n is as follows.

After the completion of the two phases, the base node U_0 in M2P-WNCR receives $(R+1)$ signals that contain symbol x_n. From these signals, it extracts $(R+1)$ soft symbols and uses a maximal-ratio combiner to detect the symbol. The first soft symbol of x_n comes directly from the source node U_n in the source transmission phase by applying matched-filtering to signal $y_{0n}(t)$ in (2.1) with respect to signature waveform $s_n(t)$ to obtain

$$y_{0nn} = \langle y_{0n}(t), s_n(t) \rangle = h_{0n}\sqrt{P_{nn}}x_n + w_{0nn}. \tag{2.12}$$

The remaining R soft symbols are collected from the R relaying signals $y_{0r}(t)$ in

(2.3) in the relay transmission phase as follows. For each signal $y_{0r}(t)$, U_0 applies a bank of matched-filtering to the signal with respect to signature waveforms $s_m(t)$ for $m = 1, 2, ..., N$ to obtain

$$y_{0rm} = \langle y_{0r}(t), s_m(t) \rangle = h_{0r} \sum_{k=1}^{N} \sqrt{\widetilde{P}_{rk}} x_k \rho_{km} + w_{0rm}. \tag{2.13}$$

Then it forms an $N \times 1$ vector comprised of the y_{0rm}'s as

$$\mathbf{y}_{0r} = h_{0r} \mathbf{R} \mathbf{A}_r \mathbf{x} + \mathbf{w}_{0r}, \tag{2.14}$$

where $\mathbf{y}_{0r} = [y_{0r1}, y_{0r2}, ..., y_{0rN}]^{\mathcal{T}}$, $\mathbf{A}_r = \text{diag}\left\{\sqrt{\widetilde{P}_{r1}}, \sqrt{\widetilde{P}_{r2}}, ..., \sqrt{\widetilde{P}_{rN}}\right\}$, $\mathbf{x} = [x_1, x_2, ...$ $x_N]^{\mathcal{T}}$, $\mathbf{w}_{0r} = [w_{0r1}, w_{0r2}, ..., w_{0rN}]^{\mathcal{T}} \sim \mathcal{CN}(\mathbf{0}, N_0 f_{0r} \mathbf{R}_r)$ with f_{0r} in (2.6), and

$$\mathbf{R} = \begin{bmatrix} 1 & \rho_{21} & \cdots & \rho_{N1} \\ \rho_{12} & 1 & \cdots & \rho_{N2} \\ \vdots & \vdots & \ddots & \vdots \\ \rho_{1N} & \rho_{2N} & \cdots & 1 \end{bmatrix}. \tag{2.15}$$

Assume that $\mathbf{R}$ is invertible with the inverse matrix $\mathbf{R}^{-1}$. This assumption is easy to achieve since the combining of symbols is done within a relay node. The signal vector $\mathbf{y}_{0r}$ is then decorrelated to obtain

$$\widetilde{\mathbf{y}}_{0r} = \mathbf{R}^{-1} \mathbf{y}_{0r} = h_{0r} \mathbf{A}_r \mathbf{x} + \widetilde{\mathbf{w}}_{0r}, \tag{2.16}$$

where $\widetilde{\mathbf{w}}_{0r} \sim \mathcal{CN}(\mathbf{0}, N_0 f_{0r} \mathbf{R}^{-1})$. Since $\mathbf{A}_r$ is a diagonal matrix, the soft symbol of x_n from R_r is

$$\widetilde{y}_{0rn} = h_{0r} \sqrt{\widetilde{P}_{rn}} x_n + \widetilde{w}_{0rn}, \tag{2.17}$$

where $\widetilde{w}_{0r} \sim \mathcal{CN}(0, N_0 f_{0r} \varepsilon_n)$ with ε_n being the nth diagonal element of matrix $\mathbf{R}^{-1}$ associated with symbol x_n. Since there are R relaying signals from R_r's, $r = 1, 2, ..., R$, U_0 obtains R soft symbols of x_n in the above manner.

From the soft symbols of x_n in (2.12) and (2.17), U_0 forms an $(R+1)\times 1$ signal vector

$$\mathbf{y}_{0n} = \mathbf{a}_{0n}x_n + \mathbf{w}_{0n}, \tag{2.18}$$

where $\mathbf{a}_{0n} = \left[h_{0n}\sqrt{P_{nn}}, h_{01}\sqrt{\widetilde{P}_{1n}}, ..., h_{0r}\sqrt{\widetilde{P}_{rn}}, ..., h_{0R}\sqrt{\widetilde{P}_{Rn}}\right]^{\mathcal{T}}$ and $\mathbf{w}_{0n} \sim \mathcal{CN}(0, \mathbf{K}_{0n})$. We can show that $\mathbf{K}_{0n} = \text{diag}\{N_0, N_0 f_{01}\varepsilon_n, ..., N_0 f_{0r}\varepsilon_n, ..., N_0 f_{0R}\varepsilon_n\}$. Let $\mathbf{b}_{0n} = \left[h_{0n}\sqrt{P_{nn}}/N_0, h_{01}\sqrt{\widetilde{P}_{1n}}/(N_0 f_{01}\varepsilon_n), ..., h_{0r}\sqrt{\widetilde{P}_{rn}}/(N_0 f_{0r}\varepsilon_n), ..., h_{0R}\sqrt{\widetilde{P}_{Rn}}/(N_0 f_{0R}\varepsilon_n)\right]^{\mathcal{T}}$. Then the desired symbol x_n can be detected based on

$$\widehat{x}_{0n} \triangleq \mathbf{b}_{0n}^{\mathcal{H}}\mathbf{y}_{0n} = a_{0n}x_n + w_{0n}, \tag{2.19}$$

where

$$a_{0n} \triangleq \mathbf{b}_{0n}^{\mathcal{H}}\mathbf{a}_{0n} = \frac{P_{nn}|h_{0n}|^2}{N_0} + \sum_{r=1}^{R}\frac{\widetilde{P}_{rn}|h_{0r}|^2}{N_0 f_{0r}\varepsilon_n} \tag{2.20}$$

and $w_{0n} \triangleq \mathbf{b}_{0n}^{\mathcal{H}}\mathbf{w}_{0n} \sim \mathcal{CN}(0, \sigma_{0n}^2)$ with $\sigma_{0n}^2 = a_{0n}$.

The detection of x_n at the relay node R_r can follow a matched-filtering applied to signal $y_{rn}(t)$ in (2.2) with respect to the signature waveform $s_n(t)$ as

$$y_{rn} = \langle y_{rn}(t), s_n(t)\rangle = h_{rn}\sqrt{P_{nn}}x_n + w_{rn}, \tag{2.21}$$

where $w_{rn} \sim \mathcal{CN}(0, N_0)$.

2.3 Performance Analysis

In this section, we derive the exact and the asymptotic SER expressions for the use of $\mathcal{M}$-PSK modulation in DF protocol in M2P-WNCR. The performance analysis for the case of P2M-WNCR, M2P-WNC, and P2M-WNC can easily follow, and thus we will offer only the final expressions for use in later sections. Notice that

a similar approach can be used to obtain SER expressions for the case of $\mathcal{M}$-QAM modulation. For AF protocol, we offer the conditional SER expression given the channel knowledge.

2.3.1 Exact SER Expressions

For M2P-WNCR, the detection in (2.19) provides the maximal conditional signal-to-interference-plus-noise ratio (SINR) γ_{0n} corresponding to the desired symbol x_n as

$$\gamma_{0n} = \frac{a_{0n}^2}{\sigma_{0n}^2} = \frac{P_{nn}|h_{0n}|^2}{N_0} + \sum_{r=1}^{R} \frac{\widetilde{P}_{rn}|h_{0r}|^2}{N_0 f_{0r}\varepsilon_n}. \tag{2.22}$$

For DF protocol, let $\beta_{rn} \in \{0, 1\}$ for $r = 1, 2, ..., R$ represent a detection state associated with x_n at R_r. Because R_r forwards x_n only if it has successfully detected the symbol, $\widetilde{P}_{nr} = P_{nr}\beta_{rn}$. All β_{rn}'s form a decimal number $S_n = [\beta_{1n}...\beta_{rn}...\beta_{Rn}]_2$, where $[.]_2$ denotes a base-2 number, that represents one of 2^R network detection states associated with x_n of the R relay nodes R_r's. Because the detection is independent from one relay node to the others, β_{rn}'s are independent Bernoulli random variables with a distribution

$$G(\beta_{rn}) = \begin{cases} 1 - SER_{rn} & \text{if } \beta_{rn} = 1 \\ SER_{rn} & \text{if } \beta_{rn} = 0 \end{cases}, \tag{2.23}$$

where SER_{rn} is the SER of detecting x_n at R_r. Hence the probability of x_n detection in state S_n is

$$Pr(S_n) = \prod_{r=1}^{R} G(\beta_{rn}). \tag{2.24}$$

Given a detection state S_n, we rewrite (2.22) as

$$\gamma_{0n|S_n} = \frac{P_{nn}|h_{0n}|^2}{N_0} + \sum_{r=1}^{R} \frac{P_{rn}\beta_{rn}|h_{0r}|^2}{N_0\varepsilon_n}, \tag{2.25}$$

where we have used $f_{0r} = 1, \forall r$ for DF protocol.

In general, the conditional SER for $\mathcal{M}$-PSK modulation with conditional SNR γ for a generic set of channel coefficients $\{h_{uv}\}$ is given by [45]

$$SER_{\,|\{h_{uv}\}} = \Psi(\gamma) \triangleq \frac{1}{\pi}\int_0^{(\mathcal{M}-1)\pi/\mathcal{M}} \exp\left(-\frac{b\gamma}{\sin^2\theta}\right) d\theta, \tag{2.26}$$

where $b = \sin^2(\pi/\mathcal{M})$. Based on (4.1), the SNR of detecting x_n at R_r given the channel gain is $\gamma_{rn} = P_{nn}|h_{rn}|^2/N_0$. By averaging (2.26) with respect to the exponential random variable $|h_{nr}|^2$, the SER in detecting x_n at R_r can be shown as [45]

$$SER_{rn} = F\left(1 + \frac{bP_{nn}\sigma_{rn}^2}{N_0\sin^2\theta}\right), \tag{2.27}$$

where

$$F\left(x(\theta)\right) = \frac{1}{\pi}\int_0^{(\mathcal{M}-1)\pi/\mathcal{M}} \frac{1}{x(\theta)} d\theta. \tag{2.28}$$

Given a detection state S_n, which can take 2^R values, the conditional SER in detecting x_n at U_0 can be calculated using the law of total probability [46] as

$$SER_{n|\{h_{0n},\ h_{0r},\ r=1,2,...,R\}} = \sum_{S_n=0}^{2^R-1} Pr\left(\hat{x}_n \neq x_n|S_n\right).Pr(S_n), \tag{2.29}$$

where $Pr(S_n)$ follows (2.24) and

$$Pr\left(\hat{x}_n \neq x_n|S_n\right) = \Psi\left(\gamma_{0n|S_n}\right) \tag{2.30}$$

with $\gamma_{0n|S_n}$ following (2.25). By averaging (2.29) with respect to the exponential random variables $\{|h_{0n}|^2, |h_{0r}|^2,\ r = 1, 2, ..., R\}$, the exact SER in detecting x_n at

U_0 can be given by [45]

$$SER_n = \sum_{S_n=0}^{2^R-1} F\left(\left(1+\frac{bP_{nn}\sigma_{0n}^2}{N_0\sin^2\theta}\right)\prod_{r=1}^{R}\left(1+\frac{bP_{rn}\beta_{rn}\sigma_{0r}^2}{N_0\varepsilon_n\sin^2\theta}\right)\right)\prod_{r=1}^{R}G\left(\beta_{rn}\right), \quad (2.31)$$

where $G(.)$ and $F(.)$ follows (2.23) and (2.28), respectively.

For AF protocol, the conditional SER is

$$SER_{n|\{h_{uv}\}} = \Psi\left(\gamma_n\right), \quad (2.32)$$

where $\Psi(.)$ is defined in (2.26) and γ_n follows (2.22).

For P2M-WNCR, the information flows from the base node U_0 to the user nodes $U_1, U_2, ..., U_N$ through the relay nodes $R_1, R_2, ..., R_R$. The exact SER expression for detecting x_n at U_n for the DF protocol in P2M-WNCR can be shown as

$$SER_n = \sum_{S_n=0}^{2^R-1} F\left(\left(1+\frac{bP_{nn}\sigma_{n0}^2}{N_0\sin^2\theta}\right)\prod_{r=1}^{R}\left(1+\frac{bP_{rn}\beta_{rn}\sigma_{nr}^2}{N_0\varepsilon_n\sin^2\theta}\right)\right)\prod_{r=1}^{R}G\left(\beta_{rn}\right), \quad (2.33)$$

where $G(\beta_{rn})$ follows (2.23) with the SER in (2.27), where σ_{rn}^2 is replaced by σ_{r0}^2.

For M2P-WNC and P2M-WNC as described in Section 2.1.3, the $(N-1)$ user nodes act as relays to help the other user node. The exact SER expressions are

$$SER_n = \sum_{S_n=0}^{2^{(N-1)}-1} F\left(\left(1+\frac{bP_{nn}\sigma_{0n}^2}{N_0\sin^2\theta}\right)\prod_{\substack{r=1\\r\neq n}}^{N}\left(1+\frac{bP_{rn}\beta_{rn}\sigma_{0r}^2}{N_0\varepsilon_n\sin^2\theta}\right)\right)\prod_{\substack{r=1\\r\neq n}}^{N}G\left(\beta_{rn}\right) \quad (2.34)$$

and

$$SER_n = \sum_{S_n=0}^{2^{(N-1)}-1} F\left(\left(1+\frac{bP_{nn}\sigma_{n0}^2}{N_0\sin^2\theta}\right)\prod_{\substack{r=1\\r\neq n}}^{N}\left(1+\frac{bP_{rn}\beta_{rn}\sigma_{nr}^2}{N_0\varepsilon_n\sin^2\theta}\right)\right)\prod_{\substack{n=1\\r\neq n}}^{N}G\left(\beta_{rn}\right), \quad (2.35)$$

respectively.

2.3.2 Asymptotic SER Expressions

To obtain the asymptotic SER performance, i.e., performance at sufficiently high SNR, in detecting x_n at U_0 in M2P-WNCR, a number of approximations are needed. First, we expect that SER_{rn} at high SNR is sufficiently small compared to 1, and thus we can assume $(1 - SER_{rn}) \simeq 1$. Second, because of high SNR, we can ignore the 1's in the argument of $F(.)$. Hence we rewrite (2.31) as

$$SER_n \simeq \sum_{S_n=0}^{2^R-1} \underbrace{F\left(\left(\frac{bP_n\alpha_{nn}\sigma_{0n}^2}{N_0\sin^2\theta}\right)\prod_{r=1:\beta_{rn}=1}^{R}\left(\frac{bP_n\alpha_{rn}\sigma_{0r}^2}{N_0\varepsilon_n\sin^2\theta}\right)\right)}_{\mathcal{A}} \times \underbrace{\prod_{r=1:\beta_{rn}=0}^{R} F\left(\frac{bP_n\alpha_{nn}\sigma_{rn}^2}{N_0\sin^2\theta}\right)}_{\mathcal{B}}, \tag{2.36}$$

where $\alpha_{nn} = \frac{P_{nn}}{P_n}$ and $\alpha_{rn} = \frac{P_{rn}}{P_n}$ denote the fraction of power P_n allocated at the source node U_n and a relay node R_r.

Let Ω_{n0} and Ω_{n1} denote subsets of the indices of nodes that decode x_n erroneously and correctly, respectively. Then $\Omega_{n0} = \{r:\ \beta_{rn} = 0\}$ and $\Omega_{n1} = \{r:\ \beta_{rn} = 1\}$. Furthermore, $|\Omega_{n0}|$ and $|\Omega_{n1}| \in \{0, 1, ..., R\}$, and $|\Omega_{n0}| + |\Omega_{n1}| = R$ for any network detection state S_n. Hence in (2.36), we can show that

$$\mathcal{A} = \left(\frac{N_0}{bP_n}\right)^{1+|\Omega_{n1}|} \frac{g\left(1+|\Omega_{n1}|\right)}{\alpha_{nn}\sigma_{0n}^2\prod_{r\in\Omega_{n1}}\alpha_{rn}\left(\frac{\sigma_{0r}^2}{\varepsilon_n}\right)}, \tag{2.37}$$

$$\mathcal{B} = \left(\frac{N_0}{bP_n}\right)^{|\Omega_{n0}|} \frac{[g(1)]^{|\Omega_{n0}|}}{\alpha_{nn}^{|\Omega_{n0}|}\prod_{r\in\Omega_{n0}}\sigma_{rn}^2}, \tag{2.38}$$

where

$$g(x) = \frac{1}{\pi}\int_0^{(\mathcal{M}-1)\pi/\mathcal{M}} [\sin(\theta)]^{2x}\, d\theta. \tag{2.39}$$

Consequently, (2.36) can be rewritten as

$$SER_n \simeq \left(\frac{bP_n}{N_0}\right)^{-(R+1)} \frac{1}{\sigma_{0n}^2} \sum_{S_n=0}^{2^R-1} \frac{g\left(1+|\Omega_{n1}|\right)\left[g(1)\right]^{|\Omega_{n0}|}}{\alpha_{nn}^{1+|\Omega_{n0}|} \prod_{r\in\Omega_{n1}} \alpha_{rn} \left(\frac{\sigma_{0r}^2}{\varepsilon_n}\right) \prod_{r\in\Omega_{n0}} \sigma_{rn}^2}. \quad (2.40)$$

A similar derivation can be applied for the case of P2M-WNCR, M2P-WNC, and P2M-WNC, and the asymptotic SER expressions for these cases are

$$SER_n \simeq \left(\frac{bP_n}{N_0}\right)^{-(R+1)} \frac{1}{\sigma_{n0}^2} \sum_{S_n=0}^{2^R-1} \frac{g\left(1+|\Omega_{n1}|\right)\left[g(1)\right]^{|\Omega_{n0}|}}{\alpha_{nn}^{1+|\Omega_{n0}|} \prod_{r\in\Omega_{n1}} \alpha_{rn} \left(\frac{\sigma_{nr}^2}{\varepsilon_n}\right) \prod_{r\in\Omega_{n0}} \sigma_{r0}^2}, \quad (2.41)$$

$$SER_n \simeq \left(\frac{bP_n}{N_0}\right)^{-N} \frac{1}{\sigma_{0n}^2} \sum_{S_n=0}^{2^{(N-1)}-1} \frac{g\left(1+|\Omega_{n1}|\right)\left[g(1)\right]^{|\Omega_{n0}|}}{\alpha_{nn}^{1+|\Omega_{n0}|} \prod_{r\in\Omega_{n1}} \alpha_{rn} \left(\frac{\sigma_{0r}^2}{\varepsilon_n}\right) \prod_{r\in\Omega_{r0}} \sigma_{rn}^2}, \quad (2.42)$$

and

$$SER_n \simeq \left(\frac{bP_n}{N_0}\right)^{-N} \frac{1}{\sigma_{n0}^2} \sum_{S_n=0}^{2^{(N-1)}-1} \frac{g\left(1+|\Omega_{n1}|\right)\left[g(1)\right]^{|\Omega_{n0}|}}{\alpha_{nn}^{1+|\Omega_{n0}|} \prod_{r\in\Omega_{n1}} \alpha_{nr} \left(\frac{\sigma_{nr}^2}{\varepsilon_n}\right) \prod_{r\in\Omega_{n0}} \sigma_{r0}^2}, \quad (2.43)$$

respectively.

2.3.3 Diversity Order and Interference Impact on SNR

Diversity order of a communication scheme is defined as

$$\text{div} = -\lim_{\gamma\to\infty} \frac{\log SER(\gamma)}{\log \gamma}, \quad (2.44)$$

where $SER(\gamma)$ is the SER with the SNR $\gamma \triangleq P/N_0$. From (2.40), the interference impact ε_n does not affect the diversity gain, and x_n for all n is clearly received with a diversity order of $(R+1)$ at the base node U_0 in M2P-WNCR, as expected. In other words, the use of nonorthogonal codes with cross-correlations $\rho_{nm} \neq 0$, $n \neq m$, in WNCR schemes still guarantees full diversity.

To see the interference impact on the SNR due to the use of nonorthogonal code, we consider unique cross-correlations $\rho_{nm} = \rho$ for all $n \neq m$. In this case, we can write (2.15) as

$$\mathbf{R} = \begin{bmatrix} 1 & \rho & \cdots & \rho \\ \rho & 1 & \cdots & \rho \\ \vdots & \vdots & \ddots & \vdots \\ \rho & \rho & \cdots & 1 \end{bmatrix} = (1-\rho)\left(\mathbf{I} + \mathbf{c}\mathbf{d}^{\mathcal{T}}\right), \tag{2.45}$$

where $\mathbf{I}$ is an $N \times N$ identity matrix and $\mathbf{c} = \frac{\rho}{1-\rho}\,\mathbf{d}$ and $\mathbf{d} = [1, 1, ..., 1]^{\mathcal{T}}$ are $N \times 1$ vectors. Because $1 + \mathbf{d}^{\mathcal{T}}\mathbf{c} = 1 + \frac{N\rho}{1-\rho} \neq 0$, it can be shown that [47]

$$\mathbf{R}^{-1} = \frac{1}{1-\rho}\left(\mathbf{I} - \frac{\mathbf{c}\mathbf{d}^{\mathcal{T}}}{1 + \mathbf{d}^{\mathcal{T}}\mathbf{c}}\right), \tag{2.46}$$

and thus the diagonal elements of the inverse matrix are

$$\varepsilon_n = \frac{1 + (N-2)\rho}{(1-\rho)(1 + (N-1)\rho)} \triangleq \varepsilon, \tag{2.47}$$

the same for all n. Because $\varepsilon \geq 1$ and $|\Omega_{n1}| \leq R$, $\varepsilon^{|\Omega_{n1}|} \leq \varepsilon^R$. Hence we rewrite (2.40) as

$$SER_n \lesssim \left(\frac{bP_n}{N_0}\right)^{-(R+1)} \frac{\varepsilon^R}{\sigma_{0n}^2} \sum_{S_n=0}^{2^R-1} \frac{g\left(1 + |\Omega_{n1}|\right)\left[g(1)\right]^{|\Omega_{n0}|}}{\alpha_{nn}^{1+|\Omega_{n0}|} \prod_{r\in\Omega_{n1}} \alpha_{rn}\sigma_{0r}^2 \prod_{r\in\Omega_{n0}} \sigma_{rn}^2} \tag{2.48}$$

for M2P-WNCR. A similar result can be shown for P2M-WNCR. Based on (2.48), given the same required SER, the additional SNR in using unique nonorthogonal codes can be shown to be at most $\Delta\gamma = \frac{R}{R+1} 10 \log \varepsilon$ (dB), where ε follows (2.47). Furthermore,

$$\lim_{N\to\infty} \Delta\gamma = -\frac{R}{R+1} 10 \log(1-\rho) \ \text{(dB)}. \tag{2.49}$$

Equation (2.49) reveals the significance of WNCR schemes when using nonorthogonal codes. The use of such codes, which permit broader applications than orthogonal codes, still guarantees full diversity with the most SNR penalty in (2.49), regardless of the number of user nodes N. For instance, when using $\rho = 0.5$ and $R = 1$, the additional SNR is just at most 1.5 dB, relatively small compared to the gain provided by the achieved diversity, as seen in subsequent subsections.

2.3.4 SER Performance

We perform computer simulations to validate the performance analysis of WNCR schemes. For simulation setup, a network of ten user nodes ($N = 10$) and various numbers of relay nodes with binary phase-shift keying (BPSK) modulation are considered. In this setup, the relay nodes are placed with equal distance to the base node and the user nodes, and thus we assume $\sigma_{n0}^2 = \sigma_{0n}^2 = 1$, $\sigma_{nr}^2 = \sigma_{rn}^2 = \sigma_{r0}^2 = \sigma_{0r}^2 = 6$ for all n and r. The transmit power P_n corresponding to x_n is assumed the same for all n and thus denoted as P, and the equal power allocation [16] is used, where $P_{nn} = P/2$ and $P_{nr} = P/(2R)$. We also assume unit noise variance, i.e. $N_0 = 1$, and unique cross-correlations $\rho_{nm} = \rho$ for $n \neq m$, and we take $\rho = 0$ and $\rho = 0.5$ for orthogonal and nonorthogonal codes, respectively. With this setup, the performance is expected to be the same for all x_n, and hence we will present the performance associated with x_1.

Figure 2.5 presents the SER performance for DF and AF protocols of WNCR schemes; the SER performance of DTX is also displayed in the figure for a com-

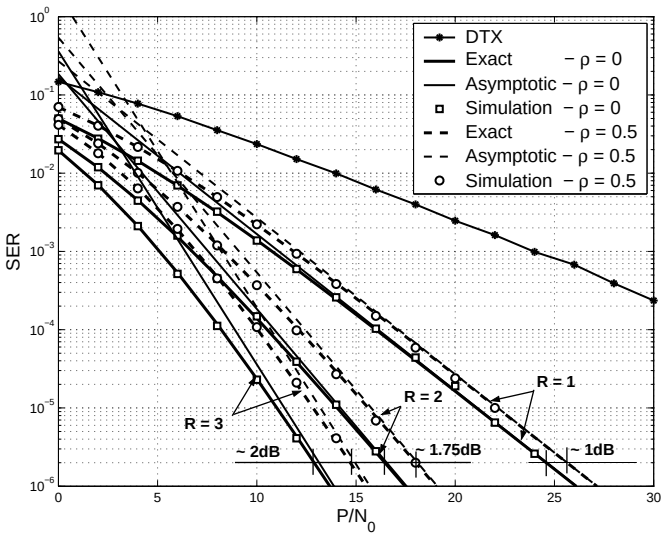

(a)

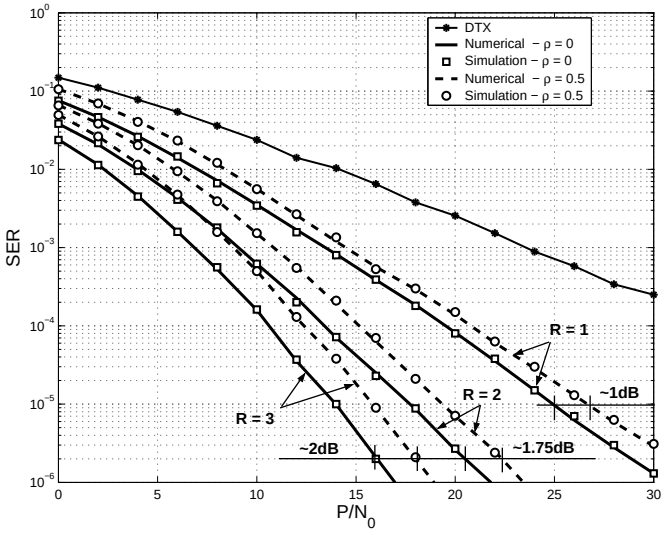

(b)

Figure 2.5: SER versus SNR performance for BPSK modulation in WNCR schemes with $N = 10$ and various numbers of relay nodes: (a) DF protocol and (b) AF protocol.

parison. In DTX, each user node transmits its symbol directly to the base node. Without any help from the relay nodes, the transmit power P is allocated entirely to the source node. In Figure 2.5, curves marked with Exact, Asymptotic, Numerical, and Simulation correspond to the exact, the asymptotic, the numerical, and the simulation performances. The Exact and Asymptotic curves are generated based on (2.31) and (2.40), respectively, for DF protocol while (2.32) is used in AF protocol to obtain the numerical curves.

From the figure, the Simulation curves in DF protocol match the corresponding Exact curves well. Likewise, the Simulation curves and the Numerical curves also match together in AF protocol. In addition, the Asymptotic curves are tight to the Exact curves at high SNR. These validate our performance analysis. The figure also shows that WNCR schemes clearly provide the expected diversity order of $(R+1)$ in both DF and AF. Moreover, the performance difference between the orthogonal and nonorthogonal codes is well confined even for $N = 10$ used in the figure. The gaps between the two performance curves are about 1, 1.75, and 2dB for $R = 1$, 2, and 3, respectively. Although additional SNR is required for transmitting a symbol when using nonorthogonal codes, the SNR gain over direct transmission by the spatial diversity greatly exceeds the loss in SNR, as revealed in the figure.

In Figure 2.6, the SER performance of the proposed WNCR schemes is compared with that of a traditional TDMA scheme. A similar simulation setup in Figure 2.5 with $\rho = 0$, $R = 1$ and 2, and DF protocol is used. For a fair comparison, a relay in the TDMA scheme detects a source symbol based solely on the source signal as in the proposed WNCR schemes. From the figure, the performance of the

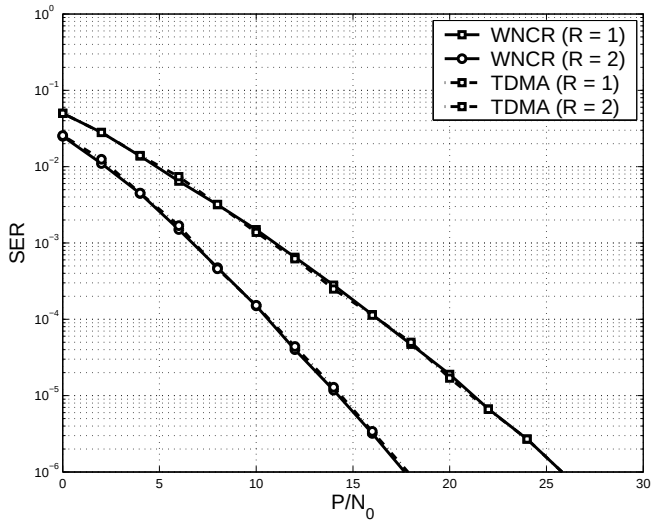

Figure 2.6: SER versus SNR performance of WNCR (solid curves) and traditional TDMA (dot-dash curves) schemes in DF protocol.

WNCR schemes is very comparable with that of the traditional TDMA scheme. Note that unlike the WNCR schemes, the traditional TDMA scheme suffers the long transmission delay as discussed in Chapter 1.

2.4 Performance Improvement by WNC in Clustering Setting

The STNCs of WNCR schemes provide general codings that can be applied in many wireless network settings. The most interesting setting is where a group of user nodes located in a close proximity to one another as in a cluster cooperate together to improve their performance. In this case, the user nodes also act as relays, helping one another in transmission between themselves and the distant base node. We refer this network setting as clustering setting, and its STNCs were discussed in Section 2.1.3. In this section, we study the performance of this network in terms

of SER performance, transmit power saving, range extension, and transmission rate improvement in comparison with DTX.

To see the benefits of using WNC schemes, the channel variances between any two user nodes are assumed the same and denoted as σ_{uu}^2. Likewise is for the channel variances between any user nodes and the base node, denoted as σ_{ub}^2. Since user nodes are in a cluster that is distant from the base node, it is assumed that $\sigma_{ub}^2 = 1$ and $\sigma_{uu}^2 = 30$. Equal power allocation is used in this study. In addition, BPSK modulation and the same cross-correlation $\rho = 0.5$ are used.

2.4.1 SER Performance of WNC Schemes

In clustering setting, the channel links among the user nodes are much stronger than the links between a user node and the base node. This could impact the performance of M2P-WNC and P2M-WNC differently although they share similar SER expressions.

Figure 2.7 reveals the performance of P2M-WNC (with the solid curves) and M2P-WNC (with the dot-dash curves) in a clustering setting for various N values. P2M-WNC clearly outperforms M2P-WNC greatly. The larger the number of nodes in the cluster, the larger the SNR gain given the same SER. For instance, a gain of 2dB for $N = 2$ increases to 9dB for $N = 5$ for the same SER of 10^{-6}. The reason relates to the strength of the source signal and the relaying signals. Both schemes have the same source signal strength since they share the same source power and source-destination channel variance. However, P2M-WNC has stronger

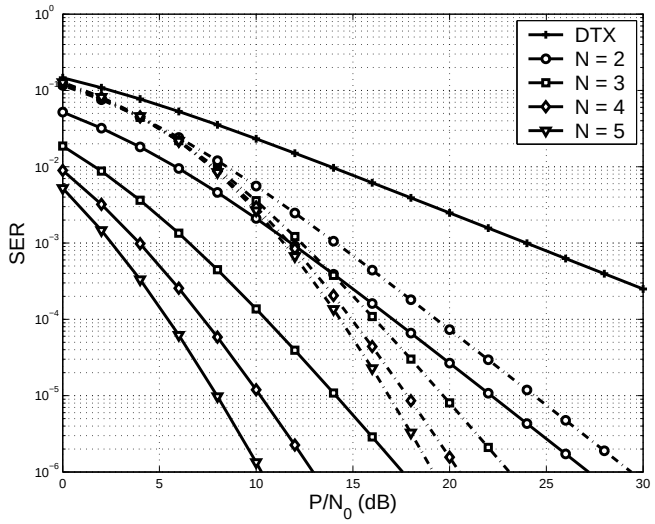

Figure 2.7: SER versus SNR performance of DF P2M-WNC (solid curves) and M2P-WNC (dot-dash curves): $\sigma_{ub}^2 = 1$, $\sigma_{uu}^2 = 30$, and $\rho = 0.5$.

relaying signals, due to the higher relay-destination channel variances. A strong relaying signal ensures a correctly-detected symbol to be forwarded with high quality. This behavior suggests that in applications to M2M transmissions as discussed in Section 2.1.3, P2M-WNC should be used. In other words, the cooperation in M2M transmissions should be imposed at the receiving cluster.

2.4.2 Power Saving

Given the same SER and transmission range as in DTX, we examine the power saving using WNC schemes over DTX in this subsection. The power saving of scheme 1 over scheme 2 is defined as the difference in transmit power between scheme 2 and scheme 1 to achieve the same SER. Figure 2.8 reveals the power saving for various SER with a fixed number of user nodes $N = 4$. From the figure, the lower the SER

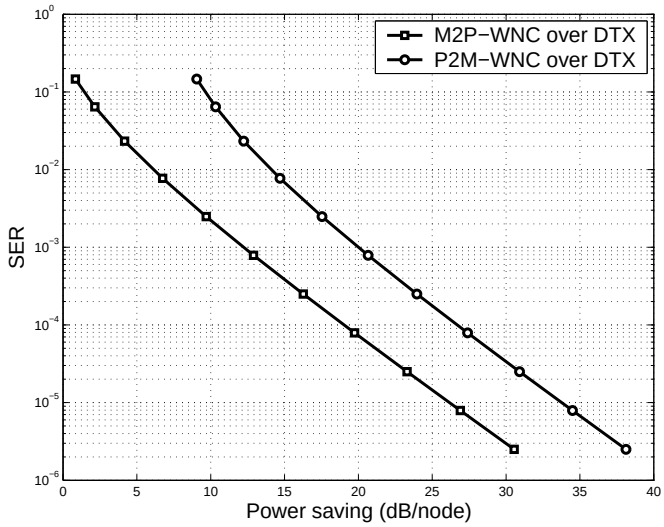

Figure 2.8: Power saving per transmitted symbol of WNC over DTX for various SER: $\sigma_{ub}^2 = 1$, $\sigma_{uu}^2 = 30$, $N = 4$, $\rho = 0.5$, and $\alpha = 2.5$.

is the higher the power saving over DTX. For instance, at $SER = 10^{-4}$, the saving associated with M2P-WNC and P2M-WNC are 19 and 27dB, respectively. The saving increases to 26 and 34dB, respectively, as SER of 10^{-5}. P2M-WNC achieves a better saving as expected due to its better performance in clustering setting over M2P-WNC, as discussed in Section 2.4.1.

In Figure 2.9, we study the power saving as the number of user nodes N varies. The SER is kept fixed at $SER = 10^{-6}$. From the figure, higher power saving is achieved by WNC schemes as N increases. This is due to the increment in the diversity order that the two schemes offer. However, the increment in power saving becomes saturate at high N values. The reason relates to the reduction of the marginal gain in power saving, defined as the difference in power saving between two consecutive numbers of user nodes. This suggests that we should not use WNC

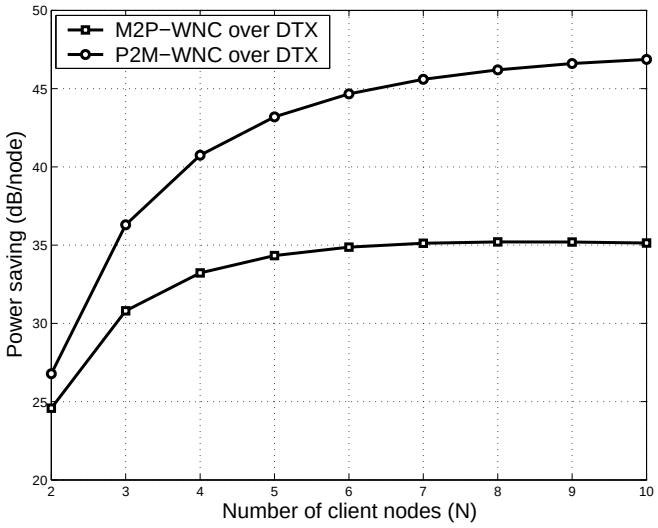

Figure 2.9: Power saving per transmitted symbol of WNC over DTX for various number of user nodes N: $\sigma_{ub}^2 = 1$, $\sigma_{uu}^2 = 30$, $\rho = 0.5$, and $SER = 10^{-6}$.

for large numbers of user nodes because the use does not provide much gain in power saving but would lead to a high system complexity. When the number of user nodes in a cluster is large, we can form sub-clusters with an appropriate value of N. WNC can be applied within each group to achieve the desired diversity order.

2.4.3 Range Extension

The diversity achieved by WNC schemes can be used to extend the transmission range between the user nodes and the base node in comparison with DTX. Given the same quality of service, represented by a required SER, and the same transmit power, the range extension of scheme 1 over scheme 2 is defined as the ratio of the distance between the user nodes and the base node in scheme 1 over that in scheme 2. Figure 2.10 shows the range extension for various SER with BPSK

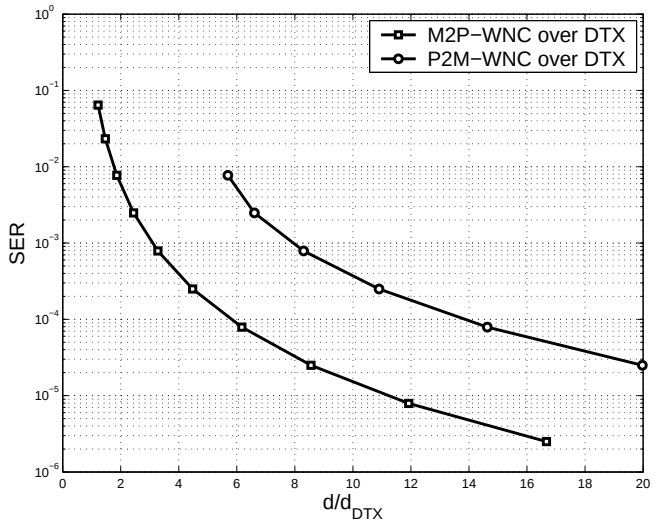

Figure 2.10: Range extension of WNC over DTX for various SER: $\sigma_{uu}^2 = 30$, $N = 4$, $\rho = 0.5$, and $\alpha = 2.5$.

modulation and a fixed number of user nodes $N = 4$. In the figure, we keep $\sigma_{uu}^2 = 30$ and vary σ_{ub}^2 to achieve the range extension with the assumption of the path loss exponent $\alpha = 2.5$. This scenario replicates a group of user nodes that move away from the base node. Similar trend as in Figure 2.8 can be seen here. From the figure, the lower the required SER is the larger the range extension for WNC over DTX. Moreover, the range extension is quite tremendous at low required SERs. For instance at $SER = 10^{-5}$, the range extension is 11 and 30 times for M2P-WNC and P2M-WNC, respectively. This is due to the higher power saving at lower SER as revealed in Figure 2.8 that can turn into extended transmission ranges. Again, P2M-WNC results in a better performance with the higher range extension.

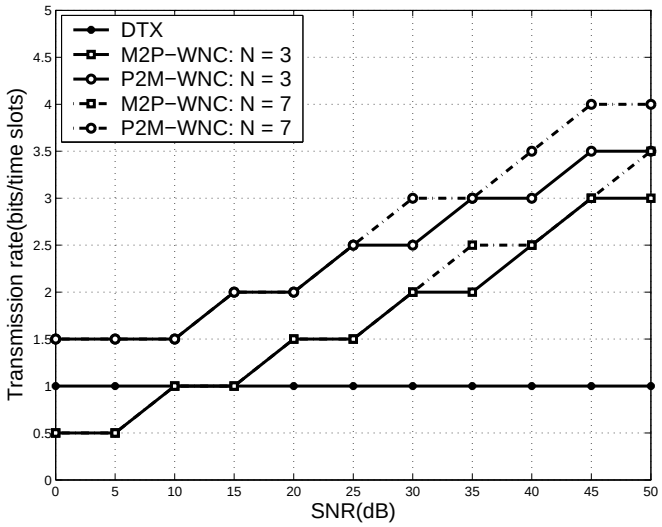

Figure 2.11: Transmission rate of WNC and DTX for various SNR: $\sigma_{ub}^2 = 1$, $\sigma_{uu}^2 = 30$, and $\rho = 0.5$.

2.4.4 Transmission Rate Improvement

Given the same quality of service and transmission range as in DTX, the power saving in WNC schemes can be used to transmit the signal with a larger constellation size and hence to increase the transmission rate. In this subsection, we study the transmission rate improvement over DTX by using WNC schemes. We assume transmission in DTX uses fixed modulation of BPSK and thus the transmission rate of DTX is always 1 bit per time slot (bpts) in this study. For WNC, we start with BPSK modulation and search for the maximum constellation size $\mathcal{M}$ such that the resulting SER does not exceed the SER in DTX, given that they all have the same transmit power. In this way, the SER performance of WNC scheme should be the same or better than that of DTX. For $\mathcal{M} = 2^m$, where m is the number of bits associated with the constellation size $\mathcal{M}$, the transmission rate in WNC is $m/2$

bpts since it requires $2N$ time slots to transmit N symbols.

Figure 2.11 shows the transmission rates that can be achieved by DTX and WNC for various SNR. From the figure, several points are worth noted. First, WNC schemes interestingly can provide higher transmission rates than DTX although they take more time to deliver a symbol. As seen in the figure, only M2P-WNC with $SNR < 10$dB results in a smaller transmission rate, compared to DTX. The reason relates to the power gaps in SER performance between these schemes and DTX that allows them to increase the constellation size of the $\mathcal{M}$-PSK modulation and thus the transmission rate. Secondly, the increase in the number of the user nodes does not lead to substantial increase in transmission rate at low and moderate SNR, as shown in the figure. This suggests that we should not use WNC for large numbers of user nodes. When the number of user nodes in a cluster is large, we can form sub-clusters and WNC is applied on each group.

2.5 Summary

In this chapter, we presented the novel WNC concept and proposed its associated STNCs to eliminate the issue of imperfect frequency and timing synchronization while achieving full spatial diversity with low transmission delays. Given a network of N user nodes and R relay nodes, signal model for the proposed STNCs was presented, signal detection was introduced, and SER performance was analyzed to confirm that a full diversity order of $(R + 1)$ was achieved for each transmitted symbol. The STNCs require only $(N + R)$ time slots, a reduction from $2N$ time

slots in traditional FDMA and CDMA cooperative communications given that N is usually greater than R and $N(R+1)$ time slots in traditional TDMA cooperative communications. We also applied WNCR schemes to M2P and P2M transmissions, where the user nodes acted as relays to help one another to improve their transmission performance. The performance in clustering setting was studied to reveal the improvement in power saving, range extension, and transmission rate.

Chapter 3

Location-Aware Cooperative Communications with Linear Network Coding

In conventional DTX protocol, where user nodes directly transmit their information to a common base node, distant user nodes require more transmit power to provide a comparable quality of service to that of the closer ones. Consequently, high aggregate transmit power, measured as the sum of all transmit power of individual user nodes, and uneven power distribution among them exist in the network. These two issues result in low network lifetime, which is defined as the time until the first user node dies. As we have seen in Chapter 2, spatial diversity achieved by cooperative communications can reduce the transmit power and thus can be used to improve network lifetime.

Much research in cooperative communication has considered symmetric problems, in which a pair of nodes help each other in their transmission to a common base node [48], [49], [50], [51], [52], or different source nodes in a network receive assistance from the same group of relays to achieve the same diversity order [20]. However, practical networks are asymmetric in nature. Node distances to a common base node vary based on node locations, and thus some nodes are disadvantageous in their transmission in comparison with others. Therefore, the node locations, which

can be obtained using network-aided position techniques [53], [54], should be taken into consideration to improve network performance.

In this chapter, we consider a number of location-aware cooperation-based schemes that achieve spatial diversity to reduce aggregate transmit power and achieve even power distribution in a network, where user nodes with known locations transmit their information to a common base node. The first proposed scheme, denoted as INC scheme, utilizes single-relay cooperative communication [55] in a network. In the INC scheme, each user node, except the closest node to the base node, is assigned a single relay, its immediate neighbor toward the base node, and thus a fixed diversity order of two is achieved. Consequently, the INC scheme achieves good reduction in aggregate transmit power with the expense of $(2N-1)$ time slots for a network of N user nodes. Nevertheless, distant users still require more power than the closer ones and power distribution is still uneven as in the DTX scheme.

The fundamental cause of high aggregate transmit power and uneven power distribution attributes to the dependency of transmit power on the distance between the source and the base node. Therefore, *incremental diversity*, a measure of diversity order of the user nodes that varies incrementally in terms of node location, should be leveraged in a network to provide high diversity orders for distant nodes to compensate the high required transmit power. The second proposed scheme, denoted as MAX scheme, provides incremental diversity to a network by means of cooperative communication. Multi-relay cooperative communication [16] is utilized in the MAX scheme, where each user node is assigned a group of user nodes locating

between itself and the base node as relays. Thus the more distant the user node, the higher diversity order to compensate the high required transmit power. Furthermore, the higher transmit power is shared and compensated by the larger group of relaying user nodes. Consequently, the MAX scheme with the incremental diversity achieves great reduction of aggregate transmit power and even power distribution.

The major drawback with the MAX scheme is the large transmission delay since each relay requires a time slot for its transmission. For a network of N user nodes, the MAX scheme incurs a delay of $N(N+1)/2$ time slots, which grows quadratically with the network size, defined as the number of user nodes N. Therefore, in this chapter we leverage the WNC concept in Chapter 2 to propose a location-aware WNC (denoted as WNC for convenient notation in this chapter) scheme to resolve the weaknesses of the INC and MAX schemes. Following the WNC concept, the combining of the overheard information from different sources, giving rise to the received signal at the base node, in the proposed WNC scheme happens within the relay nodes instead of through the air. As a result, the WNC scheme eliminates the issues of imperfect frequency and timing synchronization and achieves the incremental diversity of the MAX scheme with the low transmission delay of $(2N-1)$ time slots of the INC scheme. Both DF and AF protocols in cooperative communication are considered in the WNC scheme, where user nodes acting as relays form unique linearly-coded signals from a set of overheard symbols of different sources and transmit them to the base node. At the base node, a multiuser detection technique jointly detects the intended symbols from all received signals in the network. We derive the exact and the asymptotic SER expressions for general

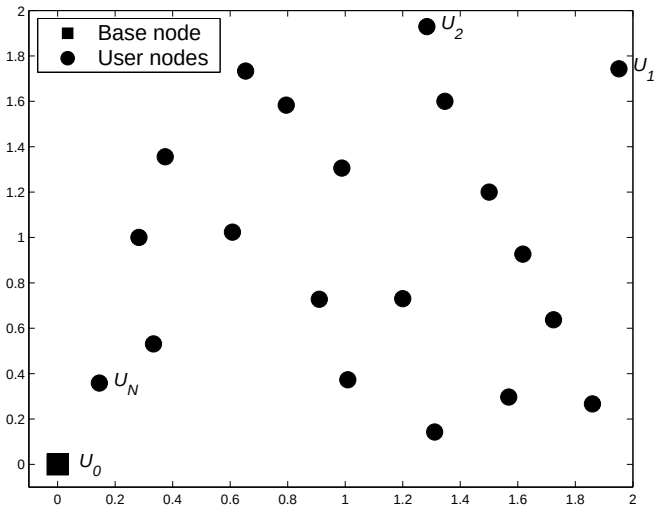

Figure 3.1: A uniformly distributed network with a base node U_0 and N user nodes $U_1, U_2..., U_N$ numbered in decreasing order of their distance to the base node.

$\mathcal{M}$-PSK modulation for DF WNC protocol. For AF WNC protocol, we offer the conditional SER expression given the channel knowledge. Performance evaluation in uniformly distributed networks shows that the INC, MAX, and WNC scheme outperform the DTX scheme greatly in terms of aggregate transmit power and power distribution. Furthermore, the WNC scheme achieves low aggregate transmit power and even power distribution of the MAX scheme with low transmission delay of the INC scheme.

3.1 System Model for WNC

We consider a wireless network consisting of a base node U_0 and N user nodes $U_1, U_2, ..., U_N$ as shown in Figure 3.1, where the user nodes have their own information that needs to be delivered to the base node. Without loss of generality, the

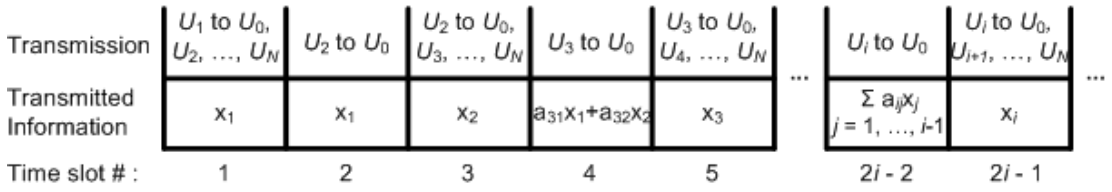

Figure 3.2: LA-WNC transmission structure.

transmitted information can be represented by symbols, denoted as $x_1, x_2, ..., x_N$. In this network, the user nodes are located within an area $\mathcal{A} \in \mathbb{R}_+^2$ at distances $d_1, d_2, ..., d_N$ to the base node while the base node is at $(0, 0)$. Without loss of generality, the user nodes are numbered in decreasing order of their distance to the base node. In this manner, U_1 and U_N are the farthest and the closest to U_0, respectively. The channels among the user nodes and the base node are modeled as narrow-band Rayleigh fading with AWGN. Let h_{uv} denote a generic channel coefficient representing the channel between any two nodes. Then h_{uv} is modeled as a zero-mean circular symmetric complex Gaussian random variable with variance $\sigma_{uv}^2 = d_{uv}^{-\alpha}$, where d_{uv} is the distance between the two nodes and α is the path loss exponent. The transmission from the user nodes is subject to TDMA, and we expect the same quality of service, which can be represented by a SER SER_0, in delivering $x_1, x_2, ..., x_N$ to U_0.

Figure 3.2 illustrates the transmission structure of the proposed WNC scheme, in which each user node U_i for $i = 2, 3, ..., N$ is allocated two time slots. In the first time slot, U_i acting as a relay node forms a unique linearly-coded signal from a set of the overheard symbols $x_1, ..., x_{i-1}$ and transmits it to U_0. U_i can either decode the

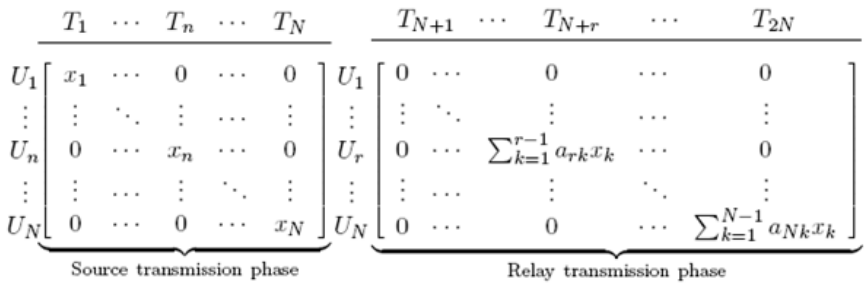

Figure 3.3: Space-time network code for LA-WNC.

overheard signals and re-encode the symbols, the so-called DF WNC protocol, or simply amplify the overheard signals, the so-called AF WNC protocol. In the second time slot, U_i acting as a source node transmits its own symbol x_i to $U_{i+1}, ..., U_N$ and U_0. U_1 has one time slot for its own transmission since it is not required to assist other nodes. The total time slots required to transmit a set of N symbols is $2N-1$, among which N time slots for source transmission and $N-1$ time slots for relay transmission. Since there is a single transmission at any given transmission time slot, the proposed WNC scheme eliminate the issues of imperfect frequency and timing synchronization. The transmit power P_j associated with symbol x_j is distributed among the source node and the corresponding relay nodes. We have $P_j = \sum_{i=j}^{N} P_{ij}$, where P_{ij} is the power from U_i in transmitting x_j. Because the base node detects symbol x_j based on $N-j+1$ copies of the symbol, we expect spatial diversity orders of $N, N-1, ..., 1$ for $x_1, x_2, ..., x_N$, respectively, which will be verified later in the paper. Note when separating the transmissions in the proposed location-aware WNC into source transmissions and relay transmissions, the transmission structure in Figure 3.2 can be expressed as in Figure 3.3, which is a special case of the STNC

for M2P-WNC shown in Figure 2.4(a).

To eliminate interference in the linearly coded version of the overheard symbols, each symbol x_j is protected by a complex signature waveform $s_j(t)$, where $\|s_j(t)\|^2 = 1$. The cross-correlation between $s_j(t)$ and $s_i(t)$ is $\rho_{ji} = < s_j(t), s_i(t) > \triangleq \frac{1}{T}\int_0^T s_j(t)s_i^*(t)dt$, the inner product between $s_j(t)$ and $s_i(t)$ with the symbol interval T and * representing the complex conjugate. We assume that each user node also knows the signature waveforms of others. In the sequel, we will present in detail the system model in DF and AF WNC protocols.

3.1.1 DF WNC Protocol

In DF WNC protocol, U_i in its first time slot decodes the overheard symbol and includes the symbol in its transmission only if the decoding is successful [55],[16]. The received signals at the base node from U_i in its first time slot is

$$y_{idr}^D(t) = h_{id}\sum_{j=1}^{i-1}\sqrt{\widetilde{P}_{ij}^D}x_j s_j(t) + n_{idr}^D(t), \tag{3.1}$$

for $i = 2, ..., N$ and $j = 1, ..., i-1$, where

$$\widetilde{P}_{ij}^D = \begin{cases} P_{ij} & \text{if } U_i \text{ decodes } x_j \text{ correctly} \\ 0 & \text{otherwise} \end{cases}. \tag{3.2}$$

We defer the discussion of detection at user nodes acting as relays and power allocation among cooperative nodes to Sections 3.2 and 3.3.2, respectively. The received signals at the base node from U_i in the second time slot is

$$y_{ido}^D(t) = \sqrt{P_{ii}}h_{id}x_i s_i(t) + n_{ido}^D(t). \tag{3.3}$$

In (3.1) and (3.3), $n_{idr}^{D}(t)$ and $n_{ido}^{D}(t)$ are modeled as independent and identically-distributed (i.i.d.) zero-mean AWGN with variance N_0. Note that the signal from U_1 follows (3.3) with $i = 1$ since it transmits its own symbol only. Note further that in the second time slot, other user nodes U_k for $k = i+1, ..., N$ also receive the signal from U_i as

$$y_{iko}(t) = \sqrt{P_{ii}} h_{ik} x_i s_i(t) + n_{iko}^{D}(t). \tag{3.4}$$

For notational convenience, we denote $a_{ij}^{D} = \sqrt{\widetilde{P}_{ij}^{D}} h_{id}$ and $a_{ii}^{D} = \sqrt{P_{ii}} h_{id}$ as signal coefficients and rewrite (3.1) and (3.3) as

$$y_{idr}^{D}(t) = \sum_{j=1}^{i-1} a_{ij}^{D} x_j s_j(t) + n_{idr}^{D}(t) \tag{3.5}$$

and

$$y_{ido}^{D}(t) = a_{ii}^{D} x_i s_i(t) + n_{ido}^{D}(t), \tag{3.6}$$

respectively.

3.1.2 AF WNC Protocol

The difference between AF and DF protocols is that U_i simply amplifies the overheard signals and forwards a linearly coded version of these signals to U_0 in its first time slot. In this time slot, the received signals at the base node is

$$y_{idr}^{A}(t) = h_{id} \sum_{j=1}^{i-1} \frac{\sqrt{P_{ij}}}{\sqrt{P_{jj}|h_{ji}|^2 + N_0}} y_{jio}(t) + n_{idr}^{A}(t), \tag{3.7}$$

where

$$y_{jio}^{A}(t) = \sqrt{P_{jj}} h_{ji} x_j s_j(t) + n_{jio}^{A}(t), \tag{3.8}$$

is the received signal at relay i corresponding to transmit symbol x_j for $i = 1, ..., N$ and $j = 1, ..., i-1$. The received signal at the base node from U_i in its second time

slot is

$$y_{ido}^{A}(t) = \sqrt{P_{ii}} h_{id} x_i s_i(t) + n_{ido}^{A}(t). \tag{3.9}$$

In (3.7)-(3.9), $n_{idr}^{A}(t)$, $n_{jio}^{A}(t)$, and $n_{ido}^{A}(t)$ are modeled as i.i.d. zero-mean AWGN with variance N_0. The signal from U_1 follows (3.9) with $i = 1$. As in the case of DF, other mobile units U_k for $k = i+1, ..., N$ also receive the signal from U_i in the second time slot as

$$y_{iko}(t) = \sqrt{P_{ii}} h_{ik} x_i s_i(t) + n_{iko}^{A}(t). \tag{3.10}$$

Substituting (3.8) into (3.7), we have

$$\begin{aligned} y_{idr}^{A}(t) &= h_{id} \sum_{j=1}^{i-1} \frac{\sqrt{P_{ij} P_{jj}} h_{ji}}{\sqrt{P_{jj}|h_{ji}|^2 + N_0}} \, x_j s_j(t) + \\ &\quad h_{id} \sum_{j=1}^{i-1} \frac{\sqrt{P_{ij}}}{\sqrt{P_{jj}|h_{ji}|^2 + N_0}} \, n_{jio}(t) + n_{idr}^{A}(t) \\ &= \sum_{j=1}^{i-1} a_{ij}^{A} x_j s_j(t) + \widetilde{n}_{idr}^{A}(t), \end{aligned} \tag{3.11}$$

where we denote $a_{ij}^{A} = \sqrt{\widetilde{P}_{ij}^{A}} h_{id}$, in which

$$\widetilde{P}_{ij}^{A} = \frac{P_{ij} P_{jj} |h_{ji}|^2}{P_{jj}|h_{ji}|^2 + N_0}, \tag{3.12}$$

as a signal coefficient from U_i in association with x_j. The resulting noise $\widetilde{n}_{idr}^{A}(t)$ has power spectral density $N_0 f_i$, where

$$f_i = \sum_{j=1}^{i-1} \frac{P_{ij}|h_{id}|^2}{P_{jj}|h_{ji}|^2 + N_0} + 1 \tag{3.13}$$

is a factor representing the noise amplification impact at U_i. Likewise, we denote $a_{ii}^{A} = \sqrt{P_{ii}} h_{id}$ and rewrite (3.9) as

$$y_{ido}^{A}(t) = a_{ii}^{A} x_i s_i(t) + n_{ido}^{A}(t). \tag{3.14}$$

3.1.3 A General System Model for WNC

We see that DF and AF WNC protocols share the same system model with different parameters. For notational convenience in subsequent analysis, we denote the transmit signals from U_i in the first and the second time slots as

$$y_{idr}(t) = \sum_{j=1}^{i-1} a_{ij} x_j s_j(t) + n_{idr}(t) \tag{3.15}$$

and

$$y_{ido}(t) = a_{ii} x_i s_i(t) + n_{ido}(t), \tag{3.16}$$

respectively, for $i = 1, ..., N$ and $j = 1, ..., i-1$. In the above equations, $a_{ii} = \sqrt{P_{ii}} h_{id}$, $a_{ij} = \sqrt{\widetilde{P}_{ij}} h_{id}$ where $\widetilde{P}_{ij}$ follows (3.2) and (3.12) for DF and AF, respectively, and the power spectral density of $n_{ido}(t)$ and $n_{idr}(t)$ is N_0 and $N_0 f_i$, respectively with

$$f_i = \begin{cases} 1 & \text{for DF} \\ \sum_{j=1}^{i-1} \frac{P_{ij}|h_{id}|^2}{P_{jj}|h_{ji}|^2 + N_0} + 1 & \text{for AF} \end{cases}. \tag{3.17}$$

3.2 Signal Detection in WNC

Since we assume each user node knows the signature waveforms of other user nodes, the detection of symbol x_j at user node U_i for $j = 1, ..., N$ and $i = j+1, ..., N$ in DF WNC protocol follows matched-filtering that is applied to the received signal $y^D_{jio}(t)$ as

$$\hat{x}_{ji} \triangleq < y^D_{jio}(t), s_j(t) > = \sqrt{P_{jj}} h_{ji} x_j + n_{ji}, \tag{3.18}$$

where $n_{ji} \sim \mathcal{N}(0, N_0)$. Here no multiuser detection is required at user nodes.

Signal detection at the base node in DF and AF WNC protocols is performed by first applying matched-filtering to the received signals with respect to signature waveforms. To achieve a tractable performance analysis, we then use a multiuser detection technique that includes a decorrelator and a maximum-ratio combining detector. Nevertheless, one can use MMSE detector, which is optimal among linear detectors. At high SNR, however, we expect that MMSE detector and our multiuser detector have comparable performance.

3.2.1 Matched Filtering

Given the system models in Section 4.1, the base node receives N direct transmissions in the odd time slots and $(N-1)$ relaying transmissions in the even ones. Matched-filtering with respect to signature waveforms is applied to the received signals to produce a total of $M = \frac{N(N+1)}{2}$ discrete-time signals of the forms

$$y_{idj} =< y_{idr}(t), s_j(t) > = a_{ij}x_j + \sum_{\substack{k=1 \\ k\neq j}}^{i-1} a_{ik}\rho_{jk}x_k + n_{idj} \tag{3.19}$$

and

$$y_{idi} =< y_{ido}(t), s_i(t) > = a_{ii}x_i + n_{idi} \tag{3.20}$$

for $i = 1, ..., N$ and $j = 1, ..., i-1$. In (3.19) and (3.20), $n_{idi} \sim \mathcal{N}(0, N_0)$ and $n_{idj} \sim \mathcal{N}(0, N_0 f_i)$ are the AWGN.

Let $\mathbf{y} = [y_{1d1}, y_{2d1}, y_{2d2}, ..., y_{id1}, ..., y_{idj}, ..., y_{idi}, ..., y_{Nd1}, ..., y_{NdN}]^T$, where ^{T} denotes transpose, be the $M \times 1$ received signal vector and $\mathbf{R}_i = < \mathbf{s}_i, \ \mathbf{s}_i^H >$ be the cross-correlation matrix where $\mathbf{s}_i = [s_1(t), s_2(t), ..., s_i(t)]^T$. We can write

$$\mathbf{y} = \mathbf{RAx} + \mathbf{n}, \tag{3.21}$$

where $\mathbf{x} = [x_1, x_2, ..., x_N]^T$ is the $N \times 1$ transmit symbol vector,

$$\mathbf{R} = \text{diag}\left\{1, \mathbf{R}_1, 1, \mathbf{R}_2, 1, ..., \mathbf{R}_{i-1}, 1, ..., \mathbf{R}_{N-1}, 1\right\}$$

is the $M \times M$ cross-correlation matrix, and

$$\mathbf{A} = \begin{bmatrix} \text{diag}(a_{11}) & \mathbf{0}_{1\times(N-1)} \\ \text{diag}(a_{21}, a_{22}) & \mathbf{0}_{2\times(N-2)} \\ \text{diag}(a_{31}, a_{32}, a_{33}) & \mathbf{0}_{3\times(N-3)} \\ \ddots & \vdots \\ \text{diag}(a_{i1}, ..., a_{ij}, ..., a_{ii}) & \mathbf{0}_{i\times(N-i)} \\ \ddots & \vdots \\ \text{diag}(a_{N1}, ..., a_{Nj}, ..., a_{NN}) & \end{bmatrix}$$

is the $M \times N$ signal coefficient matrix. In the above equations, $\text{diag}\{.\}$ and $\mathbf{0}_{u\times v}$ denote a diagonal matrix and a u-by-v matrix of zeros, respectively. Also in (3.21), $\mathbf{n} \sim \mathcal{N}(\mathbf{0}, N_0\widetilde{\mathbf{R}})$ where $\mathbf{0}$ is an $M \times 1$ vector of zeros and

$$\widetilde{\mathbf{R}} = \text{diag}\left\{1, \widetilde{\mathbf{R}}_1, 1, \widetilde{\mathbf{R}}_2, 1, ..., \widetilde{\mathbf{R}}_{i-1}, 1, ..., \widetilde{\mathbf{R}}_{N-1}, 1\right\}$$

with $\widetilde{\mathbf{R}}_{i-1} = f_i\mathbf{R}_{i-1}$. Let us define

$$\mathbf{F} \triangleq \text{diag}\left\{1, f_2, 1, f_3, f_3, 1, ..., \underbrace{f_i, ..., f_i}_{\text{(i}-1\text{) times}}, 1, ..., \underbrace{f_N, ..., f_N}_{\text{(N}-1\text{) times}}, 1\right\},$$

then $\widetilde{\mathbf{R}} = \mathbf{FR}$ and $\mathbf{n} \sim \mathcal{N}(\mathbf{0}, N_0\mathbf{FR})$.

3.2.2 Multiuser Detection

Assume $\mathbf{R}_i$ is invertible with the invert matrix $\mathbf{R}_i^{-1}$. Then the inverse of $\mathbf{R}$ exists with $\mathbf{R}^{-1} = \text{diag}\left\{1, \mathbf{R}_1^{-1}, 1, \mathbf{R}_2^{-1}, 1, ..., \mathbf{R}_{i-1}^{-1}, 1, ..., \mathbf{R}_{N-1}^{-1}, 1\right\}$. Multiuser detec-

tion is applied to the received signal vector in two steps. First the vector $\mathbf{y}$ is pre-multiplied with the inverse $\mathbf{R}^{-1}$ to obtain

$$\widetilde{\mathbf{y}} = \mathbf{R}^{-1}\mathbf{y} = \mathbf{A}\mathbf{x} + \widetilde{\mathbf{n}}, \tag{3.22}$$

where $\widetilde{\mathbf{n}} \sim \mathcal{N}(\mathbf{0}, N_0\mathbf{R}^{-1}\mathbf{F})$. Then $\widetilde{\mathbf{y}}$ is grouped into $(N-j+1)\times 1$ signal vectors in association with the desired symbols x_j as

$$\mathbf{y}_j = \mathbf{a}_j x_j + \mathbf{n}_j, \tag{3.23}$$

where $\mathbf{a}_j = [a_{jj}, ..., a_{ij}, ..., a_{Nj}]^T$ for $j = 1, ..., N$ and $i = j, ..., N$ and $\mathbf{n}_j \sim \mathcal{N}(\mathbf{0}, \mathbf{K}_j)$. We have $\mathbf{K}_j = \text{diag}\left\{\sigma_{jj}^2, ..., \sigma_{ij}^2, ..., \sigma_{Nj}^2\right\}$, where

$$\sigma_{ij}^2 = N_0 \begin{cases} 1 & \text{if } i = j \\ f_i r_{ij} & \text{if } j < i \leq N \end{cases}. \tag{3.24}$$

In (3.24), f_i follows (3.17) and $r_{ij} \triangleq \left(\mathbf{R}_{i-1}^{-1}\right)_{jj}$ represents the interference impact on the symbol x_j in the linearly-coded signal of overheard symbols from U_i. For the case of $\rho_{ji} = \rho$ for all $i \neq j$, it can be shown [47] that

$$r_{ij} = \frac{1 + (i-3)\rho}{(1-\rho)(1+(i-2)\rho)} \triangleq r_i, \tag{3.25}$$

independent of j. Now let us define

$$\mathbf{b}_j \triangleq \left[\frac{a_{jj}}{\sigma_{jj}^2}, ..., \frac{a_{ij}}{\sigma_{ij}^2}, ..., \frac{a_{Nj}}{\sigma_{Nj}^2}\right]^T. \tag{3.26}$$

Then the desired symbol is detected based on

$$\hat{x}_j \triangleq \mathbf{b}_j^H \mathbf{y}_j = a_j x_j + n_j, \tag{3.27}$$

where $a_j \triangleq \mathbf{b}_j^H \mathbf{a}_j = \sum_{i=j}^N \frac{|a_{ij}|^2}{\sigma_{ij}^2}$, and $n_j \triangleq \mathbf{b}_j^H \mathbf{n}_j \sim \mathcal{N}\left(0, \sigma_j^2\right)$ with $\sigma_j^2 = \sum_{i=j}^N \frac{|a_{ij}|^2}{\sigma_{ij}^2}$.

3.3 Performance Analysis of WNC

The detection in (3.27) provides the maximal conditional SINR γ_j corresponding to the desired symbol x_j as

$$\gamma_j = \frac{a_j^2}{\sigma_j^2} = \sum_{i=j}^{N} \frac{|a_{ij}|^2}{\sigma_{ij}^2} = \frac{P_{jj}|h_{jd}|^2}{N_0} + \sum_{i=j+1}^{N} \frac{\widetilde{P}_{ij}|h_{id}|^2}{f_i r_{ij} N_0}. \tag{3.28}$$

In the sequel, we derive the exact and the asymptotic SER expressions for the use of M-PSK modulation in DF WNC protocol; a similar approach can be used to obtain SER expressions for the case of $\mathcal{M}$-QAM modulation. We also provide simulations to validate the SER performance of both DF and AF WNC protocols.

3.3.1 SER Expression

For DF WNC protocol, let $\beta_{ij} \in \{0, 1\}$ for $j = 1, ..., (N-1)$ and $i = j+1, ..., N$ represent a success or a failure in detection of x_j at U_i. Because U_i forwards x_j only if it has successfully detected the symbol, $\widetilde{P}_{ij} = P_{ij}\beta_{ij}$. All β_{ij}'s form a decimal number $S_j = \sum_{i=j+1}^{N} \beta_{ij}\ 2^{N-i}$, which represents one of $2^{(N-j)}$ detection states of $(N-j)$ user nodes $U_{j+1}, ..., U_N$ acting as relays in association with x_j. Because the detection is independent from one user node to the other, β_{ij}'s are independent Bernoulli random variables with a distribution

$$G(\beta_{ij}) = \begin{cases} 1 - SER_{ji} & \text{if } \beta_{ij} = 1 \\ SER_{ji} & \text{if } \beta_{ij} = 0 \end{cases}, \tag{3.29}$$

where SER_{ji} is the SER in detection of x_j at U_i. Hence the probability of detecting x_j in state S_j is

$$Pr(S_j) = \prod_{i=j+1}^{N} G(\beta_{ij}). \tag{3.30}$$

Given a detection state S_j, we rewrite the conditional SINR in (3.28) for DF WNC protocol as

$$\gamma^D_{j|S_j} = \frac{P_{jj}|h_{jd}|^2}{N_0} + \sum_{i=j+1}^{N} \frac{P_{ij}\beta_{ij}|h_{id}|^2}{r_{ij}N_0}, \tag{3.31}$$

where we have used $f_i = 1$ for DF WNC protocol.

In general, the conditional SER for $\mathcal{M}$-PSK modulation with conditional SNR γ for a generic set of channel coefficients $\{h_{uv}\}$ is given by [45]

$$SER_{\,|\{h_{uv}\}} = \Psi(\gamma) \triangleq \frac{1}{\pi}\int_0^{(\mathcal{M}-1)\pi/\mathcal{M}} \exp\left(-\frac{b\gamma}{\sin^2\theta}\right) d\theta, \tag{3.32}$$

where $b = \sin^2(\pi/\mathcal{M})$. Based on (3.18), the SNR, in detection of x_j at U_i, given the channel gain is $\gamma_{ji} = P_{jj}|h_{ji}|^2/N_0$. By averaging (3.32) with respect to the exponential random variable $|h_{ji}|^2$, the SER in detecting x_j at U_i can be shown as [45]

$$SER_{ji} = F\left(1 + \frac{bP_{jj}\sigma^2_{ji}}{N_0 \sin^2\theta}\right), \tag{3.33}$$

where

$$F\left(x(\theta)\right) = \frac{1}{\pi}\int_0^{(\mathcal{M}-1)\pi/\mathcal{M}} \frac{1}{x(\theta)} d\theta. \tag{3.34}$$

Given a detection state S_j, which can take $2^{(N-j)}$ values, the conditional SER in detecting x_j at the base node can be calculated using the law of total probability [46] as

$$SER^D_{j|\{h_{id}\}_{i=j}^N} = \sum_{S_j=0}^{2^{(N-j)}-1} Pr\left(\hat{x}_j \neq x_j|S_j\right).Pr(S_j), \tag{3.35}$$

where $Pr(S_j)$ follows (3.30) and

$$Pr\left(\hat{x}_j \neq x_j|S_j\right) = \Psi\left(\gamma^D_{j|S_j}\right) \tag{3.36}$$

with $\gamma^D_{j|S_j}$ following (3.31). By averaging (3.35) with respect to the exponential random variables $\{|h_{id}|^2\}_{i=j}^N$, the exact SER in detecting x_j at the base node can be given by [16]

$$SER_j^D = \sum_{S_j=0}^{2^{(N-j)}-1} F\left(\left(1+\frac{bP_{jj}\sigma_{jd}^2}{N_0\sin^2\theta}\right)\prod_{i=j+1}^{N}\left(1+\frac{bP_{ij}\beta_{ij}\sigma_{id}^2}{r_{ij}N_0\sin^2\theta}\right)\right)\times \prod_{i=j+1}^{N} G\left(\beta_{ij}\right), \qquad (3.37)$$

where $G(.)$ and $F(.)$ follow (3.29) and (3.34), respectively.

Our next objective is to obtain the asymptotic SER performance, i.e., performance at high SNR, in detecting x_j at the base node. A number of approximations are needed. First, we expect that SER_{ji} is sufficiently small compared to 1 at high SNR. Thus we assume that $(1-SER_{ji}) \simeq 1$ and rewrite (3.37) as

$$SER_j^D \simeq \sum_{S_j=0}^{2^{(N-j)}-1} \underbrace{F\left(\left(1+\frac{bP_j\alpha_{jj}\sigma_{jd}^2}{N_0\sin^2\theta}\right)\prod_{\substack{i=j+1\\ \beta_{ij}=1}}^{N}\left(1+\frac{bP_j\alpha_{ij}\sigma_{id}^2}{r_{ij}N_0\sin^2\theta}\right)\right)}_{\mathcal{A}} \underbrace{\prod_{\substack{i=j+1\\ \beta_{ij}=0}}^{N} F\left(1+\frac{bP_j\alpha_{jj}\sigma_{ji}^2}{N_0\sin^2\theta}\right)}_{\mathcal{B}}, \qquad (3.38)$$

where $\alpha_{ij} = \frac{P_{ij}}{P_j}$ denotes the fraction of power P_j allocated at U_i in forwarding x_j. Secondly, because of high SNR, we can ignore the 1's in the argument of $F(.)$. Let Ω_{j0} and Ω_{j1} denote subsets of the indices of user nodes that decode x_j erroneously and correctly, respectively. Then $\Omega_{j0} = \{i:\ \beta_{ij}=0\}$ and $\Omega_{j1} = \{i:\ \beta_{ij}=1\}$. Furthermore, $|\Omega_{j0}|$ and $|\Omega_{j1}| \in \{0,1,...,(N-j)\}$, and $|\Omega_{j0}|+|\Omega_{j1}| = N-j$ for any detection state S_j, where $|.|$ denotes the size of a set. Hence in (3.38), we can show

that

$$\mathcal{A} \simeq \left(\frac{N_0}{bP_j}\right)^{1+|\Omega_{j1}|} \frac{g\left(1+|\Omega_{j1}|\right)}{\alpha_{jj}\sigma_{jd}^2 \prod_{i\in\Omega_{j1}} \alpha_{ij} \frac{\sigma_{id}^2}{r_{ij}}}, \tag{3.39}$$

$$\mathcal{B} \simeq \left(\frac{N_0}{bP_j}\right)^{|\Omega_{j0}|} \frac{[g(1)]^{|\Omega_{j0}|}}{\alpha_{jj}^{|\Omega_{j0}|} \prod_{i\in\Omega_{j0}} \sigma_{ji}^2}, \tag{3.40}$$

where

$$g(x) = \frac{1}{\pi} \int_0^{(M-1)\pi/M} [\sin(\theta)]^{2x}\, d\theta. \tag{3.41}$$

Consequently, (3.38) can be rewritten as

$$SER_j^D \simeq \left(\frac{bP_j}{N_0}\right)^{-(N-j+1)} \frac{1}{\sigma_{jd}^2} \sum_{S_j=0}^{2^{(N-j)}-1} \frac{g\left(1+|\Omega_{j1}|\right)[g(1)]^{|\Omega_{j0}|}}{\alpha_{jj}^{1+|\Omega_{j0}|} \prod_{i\in\Omega_{j1}} \alpha_{ij} \left(\frac{\sigma_{id}^2}{r_{ij}}\right) \prod_{i\in\Omega_{j0}} \sigma_{ji}^2}. \tag{3.42}$$

The diversity order of a communication scheme is defined as

$$div = -\lim_{\gamma\to\infty} \frac{\log SER(\gamma)}{\log \gamma}, \tag{3.43}$$

where $SER(\gamma)$ is the SER associated with the SNR $\gamma \triangleq P_j/N_0$. From (3.42) and (3.43), the interference impact r_{ij} does not affect the diversity gain, and it is clear that x_j achieves full spatial diversity with an order of $N-j+1$. Hence DF WNC protocol provides the incremental diversity to the network, as expected.

Now when $j = N$, because x_N is directly transmitted to U_0, the exact and the asymptotic SER can be given by

$$SER_N^D = F\left(1 + \frac{bP_N\sigma_{Nd}^2}{N_0 \sin^2\theta}\right), \tag{3.44}$$

and

$$SER_N^D \simeq \left(\frac{bP_N}{N_0}\right)^{-1} \frac{g(1)}{\sigma_{Nd}^2}, \tag{3.45}$$

respectively, where $F(.)$ and $g(.)$ follow (3.34) and (3.41), respectively.

For AF WNC protocol, the conditional SER is

$$SER_{j\ |\{h_{id},\ h_{ji}\}}^{A} = \Psi\left(\gamma_j^A\right), \tag{3.46}$$

where $\Psi(.)$ is defined in (3.32) and γ_j^A follows (3.28) with f_i in (3.17) for AF protocol.

3.3.2 Performance Validation

In this subsection, we perform computer simulations to validate the SER performance analysis for both DF and AF WNC protocols. The exact and asymptotic SER expressions in (3.37) and (3.42) are used for analytical results in DF WNC protocol. For AF WNC protocol, (3.46) is used to provide numerical results.

For simulation setup, BPSK modulation is used. The number of mobile units is $N = 4$, and the variance of the noise is $N_0 = 1$. We assume unit channel variances, i.e., $\sigma_{jd}^2 = \sigma_{ji}^2 = 1$ for $j = 1, ..., N$ and $i = j + 1, ...N$ and transmit power $P_j = \sum_{i=j}^{N} P_{ij}$ corresponding to x_j is the same for all j. Furthermore, we assume equal power allocation [16] for x_j for $j = 1, ..., N-1$, i.e.

$$P_{ij} = \begin{cases} \frac{P_j}{2} & \text{if } i = j \\ \frac{P_j}{2(N-j)} & \text{if } j < i \leq N \end{cases} \tag{3.47}$$

since this strategy is optimal in the case of lacking channel state information at transmitters. For x_N, $P_{NN} = P_N$ since it is transmitted directly to the base node. We also assume that the cross-correlation $\rho_{ji} = \rho$ for all $i \neq j$, and we use $\rho = 0$ and $\rho = 0.5$ in our simulations. The user nodes are numbered in the decreasing order of their distance to the base node; therefore, we expect a diversity order of 4, 3, 2, and 1 for x_1, x_2, x_3, and x_4, respectively.

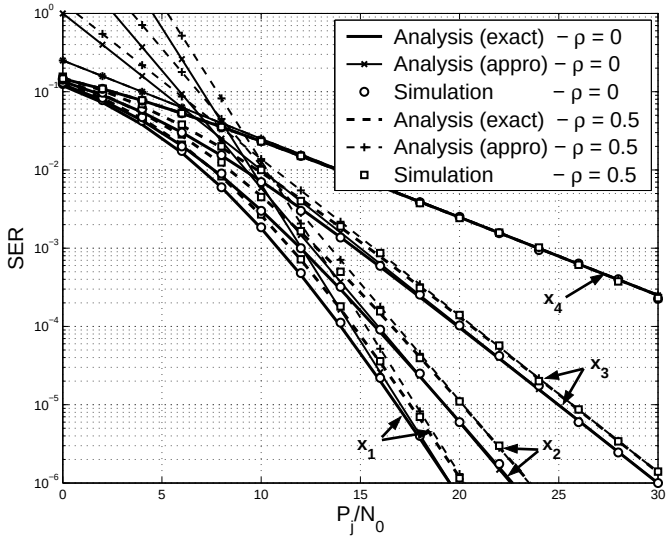

(a)

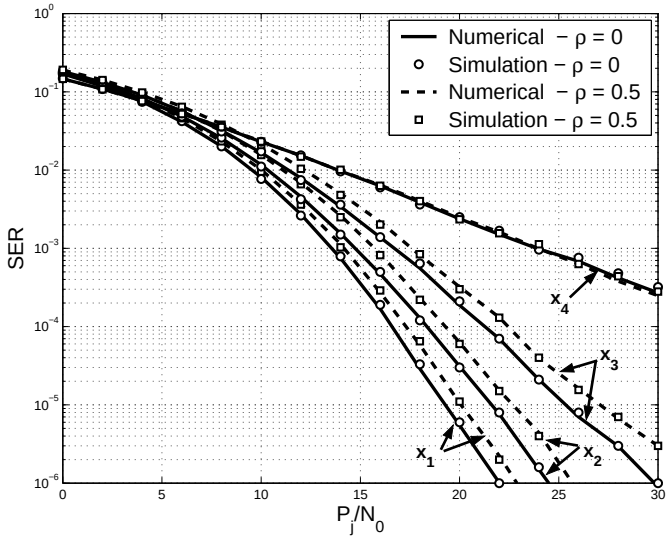

(b)

Figure 3.4: SER versus SNR performance for BPSK modulation in (a) DF WNC and (b) AF WNC protocols.

Figure 3.4 presents the SER performance for DF and AF WNC protocols. In each figure, SER versus SNR (P_j/N_0) for each information x_j is presented. It is clear from the figures that WNC provides the expected diversity orders in both DF and AF protocols. In other words, using nonorthogonal code, WNC still achieves full diversity as shown in (3.42) for the case of DF protocol. In addition, the figures show that for the case of $\rho = 0.5$, the gap at high SNR between orthogonal and nonorthogonal code is about 1dB, given the same SER.

3.4 Aggregate Transmit Power, Power Distribution, and Delay

In this section, we derive the expressions of aggregate transmit power and power distribution in a network at high SNR for the four considered schemes: DTX, INC, MAX, and WNC. We also provide the transmission delay for each scheme. These expressions are used to provide performance evaluation of the INC, MAX, and WNC schemes in the next section.

We consider a network consisting of N user nodes and a base node as described in Section 4.1, where transmissions from user nodes to a common base node are subject to TDMA and the same quality of service represented by a SER, denoted as SER_0. BPSK modulation is assumed for the demonstration purpose. For cooperation-based INC, MAX, and WNC schemes, we consider DF protocol with equal power distribution strategy. Power P_j to transmit x_j is equally distributed between U_j and U_{j+1} in the INC scheme. For the MAX and WNC schemes, power P_j distributed among $U_j, U_{j+1}, ..., U_N$ follows (3.47).

3.4.1 DTX

In the DTX scheme, each user node U_j directly transmits its information to U_0. The asymptotic SER expression for BPSK modulation can be given by [56]

$$SER_j \simeq \frac{N_0}{4\sigma_{j0}^2 P_j}, \tag{3.48}$$

where N_0 is the variance of AWGN, P_j is the transmit power, and $\sigma_{j0}^2 = d_j^{-\alpha}$ is the variance of channel fading between U_j and U_0 with the path loss exponent α. Consequently, given SER SER_0, transmit power associated with mobile unit U_j is

$$P_j \simeq \frac{N_0}{4\sigma_{j0}^2 SER_0}, \tag{3.49}$$

and aggregate transmit power for the DTX scheme is

$$P_{DTX} = \sum_{j=1}^{N} P_j. \tag{3.50}$$

Because transmission from each user node requires one time slot, transmission delay in the DTX scheme is N time slots for a network of N user nodes.

3.4.2 INC and MAX

The INC and MAX schemes apply single-relay cooperative communication [55] and multi-relay cooperative communication [16] in a network, respectively. Note that single-relay cooperative communication is a specific case of multi-relay cooperative communication [16]. Multi-relay cooperative communication considers a problem of single source s transmitting its information to a destination d with the assistance of $\mathcal{N}$ relays $u_1, u_2, ..., u_{\mathcal{N}}$. The asymptotic SER for $\mathcal{M}$-PSK modulation

can be expressed as [16]

$$SER \simeq \left(\frac{N_0}{bP}\right)^{\mathcal{N}+1} \frac{1}{\sigma_{sd}^2} \sum_{n=1}^{\mathcal{N}+1} \frac{g(\mathcal{N}-n+2)\left[g(1)\right]^{(n-1)}}{\alpha_s^n \prod_{l=n}^{\mathcal{N}} \alpha_{u_l} \sigma_{u_l d}^2 \prod_{k=1}^{n-1} \sigma_{su_k}^2}, \tag{3.51}$$

where b and $g(.)$ are defined in Section 3.3.1, N_0 is the variance of AWGN, P is the transmit power, α_s and α_{u_n} are the fraction of transmit power P allocated at source s and relay u_n, respectively, and σ_{uv}^2 for generic nodes u and v is the channel variance of the link between u and v.

For BPSK modulation ($M = 2$), we can show that $b = 1$ and $g(x) = \frac{1}{2\sqrt{\pi}} \cdot \frac{\Gamma\left(\frac{1}{2}+x\right)}{\Gamma(1+x)}$, where $\Gamma(.)$ is the Gamma-function. Because x takes integer values in (3.51), we can further show that $\Gamma\left(\frac{1}{2}+x\right) = \sqrt{\pi} . \frac{(2x-1)!!}{2^x}$ and $\Gamma(1+x) = x!$, where $(.)!$ and $(.)!!$ are single factorial and double factorial operations, respectively. If we consider equal power allocation strategy, then the SER for detecting the source information is given by

$$SER \simeq \left(\frac{N_0}{P}\right)^{\mathcal{N}+1} \frac{1}{\sigma_{sd,\text{eff}}^2}, \tag{3.52}$$

where

$$\sigma_{sd,\text{eff}}^2 = \frac{\sigma_{sd}^2}{\sum_{n=1}^{\mathcal{N}+1} \frac{(2(\mathcal{N}-n+2)-1)!!}{(\mathcal{N}-n+2)!} \cdot \frac{\mathcal{N}^{\mathcal{N}-n+1}}{2^n \prod_{l=n}^{\mathcal{N}} \sigma_{u_l d}^2 \prod_{k=1}^{n-1} \sigma_{su_k}^2}} \tag{3.53}$$

is the effective channel variance between the source and the base node in $\mathcal{N}$-relay multi-relay cooperative communication. From (3.52), the transmit power for a given SER_0 at high SNR is

$$P \simeq N_0 \left(SER_0 \sigma_{sd,\text{eff}}^2\right)^{-\frac{1}{\mathcal{N}+1}}. \tag{3.54}$$

For single-relay cooperative communication, (3.52)-(3.54) can be applied di-

rectly with $\mathcal{N} = 1$. It can also be shown that

$$\sigma^2_{sd,\text{eff}} = 4\sigma^2_{sd}\left(\frac{1}{\sigma^2_{su}} + \frac{3}{\sigma^2_{ud}}\right)^{-1}, \tag{3.55}$$

where u denotes the relay node.

Given the network in Section 4.1 that consists of N user nodes $U_1, U_2, ..., U_N$ transmitting their information $x_1, x_2, ..., x_N$, respectively, to a common base node, multi-relay cooperative communication is applied in the MAX scheme as follows. The MAX scheme comprises of $(N-1)$ multi-relay cooperative communication stages and a direct transmission stage. The jth cooperation stage involves a source node U_j and $\mathcal{N} = N-j$ relays, which are user nodes $U_{j+1}, ..., U_N$ located between U_j and U_0. Thus diversity orders of $N, (N-1), ..., 2$ are expected for $U_1, ..., U_{N-1}$, respectively. The effective channel variance between U_j and U_0, $\sigma^2_{j0,\text{eff}}$, can be directly determined using (3.53) with $\mathcal{N} = N - j$. Consequently, given SER_0, transmit power P_j associated with x_j follows (3.54) with $\sigma^2_{sd,\text{eff}} = \sigma^2_{j0,\text{eff}}$ and $\mathcal{N} = N - j$. The power P_j is distributed among $U_j, U_{j+1}, ..., U_N$ following the equal power distribution strategy in (3.47). User node U_N operates in direct transmission mode with diversity order of one and transmit power $P_{NN} = P_N$ following (3.49). Because U_i for $i = 1, ..., N$ forwards $x_1, x_2, ..., x_{i-1}$ and transmits its own x_i to the base node, transmit power required at U_i is

$$P_i^{MAX} = \sum_{j=1}^{i} P_{ij}. \tag{3.56}$$

Thus aggregate transmit power for the MAX scheme is

$$P_{MAX} = \sum_{i=1}^{N} P_i^{MAX} = \sum_{i=1}^{N}\sum_{j=1}^{i} P_{ij}. \tag{3.57}$$

Similarly, the INC scheme consists of $(N-1)$ single-relay cooperative communication stages for $U_1, ..., U_{N-1}$ and one direct transmission stage for U_N. The effective channel variance between U_j and U_0, $\sigma^2_{j0,\text{eff}}$, for $j = 1, ..., (N-1)$ can be determined based on (3.55). From that, given SER_0, transmit power P_j associated with x_j is determined by (3.54) where $\mathcal{N} = 1$. The power P_j is divided equally between U_j and U_{j+1}. U_N operates in direct transmission mode with transmit power $P_{NN} = P_N$ following (3.49). Because U_i forwards x_{i-1} and transmits its own x_i, transmit power at U_i is

$$P_i^{INC} = \frac{\left(P_{(i-1)} + P_i\right)}{2}. \tag{3.58}$$

Thus aggregate transmit power for the INC scheme is

$$P_{INC} = \sum_{i=1}^{N} P_i^{INC} = \sum_{i=1}^{N} \frac{\left(P_{(i-1)} + P_i\right)}{2}. \tag{3.59}$$

In the INC and MAX schemes, each relay requires one time slot for its transmission. Thus transmission delay in the INC and MAX schemes is $(2N-1)$ and $N(N+1)/2$ time slots, respectively. The transmission delay in the INC scheme grows linearly with the network size while that in the MAX scheme grows quadratically.

3.4.3 WNC

From (3.42), following the same procedure in Section 3.4.2 for BPSK modulation, we are able to show that

$$SER_j^D \simeq \left(\frac{N_0}{P_j}\right)^{N-j+1} \frac{1}{\sigma^2_{j0,\text{eff}}} \tag{3.60}$$

for $j = 1, ..., (N-1)$, where

$$\sigma^2_{j0,\text{eff}} = \frac{\sigma^2_{j0}}{\sum_{S_j=0}^{2^{(N-j)}-1} \frac{(2|\Omega_{j1}|+1)!!}{(1+|\Omega_{j1}|)!} . \frac{(N-j)^{|\Omega_{j1}|}}{2^{1+|\Omega_{j0}|} \prod_{i\in\Omega_{j1}} \frac{\sigma^2_{i0}}{r_{ij}} \prod_{i\in\Omega_{j0}} \sigma^2_{ji}}} \tag{3.61}$$

is the effective channel variance between U_j and U_0. From (3.60), given SER SER_0, transmit power associated with x_j is

$$P_j \simeq N_0 \left(SER_0 \sigma^2_{j0,\text{eff}}\right)^{-\frac{1}{N-j+1}} . \tag{3.62}$$

Equal power distribution strategy is also used in the WNC scheme where P_j is distributed following (3.47). User node U_N operates in direct transmission mode with transmit power $P_{NN} = P_N$ following (3.49). Because U_i for $i = 1, ..., N$ forwards $x_1, x_2, ..., x_{i-1}$ and transmits its own x_i to the base node, transmit power at U_i is

$$P_i^{WNC} = \sum_{j=1}^{i} P_{ij}. \tag{3.63}$$

Thus aggregate transmit power for the WNC scheme is

$$P_{WNC} = \sum_{i=1}^{N} P_i^{WNC} = \sum_{i=1}^{N} \sum_{j=1}^{i} P_{ij}. \tag{3.64}$$

Based on the WNC transmission structure in Section 4.1, transmission delay in the WNC scheme is $(2N-1)$ time slots.

3.5 Performance Simulation and Validation

In this section, we perform computer simulations to evaluate and validate the performance of the INC, MAX, and WNC schemes. We aim to verify that these schemes result in substantial reduction of aggregate transmit power over the DTX

scheme and to confirm that the WNC scheme achieves low aggregate transmit power and even power distribution with low transmission delay. To show power reduction of scheme 2 over scheme 1, we define

$$\text{Power reduction} = \frac{P_{scheme1} - P_{scheme2}}{P_{scheme1}} \times 100(\%). \tag{3.65}$$

For simulation setup, we assume a network whose N user nodes are uniformly distributed in an area $\mathcal{A} = [0, 2]^2$ and the base node locates at $(0, 0)$ as shown in Figure 3.1. We consider the path loss exponent $\alpha = 3$, the SER $SER_0 = 5 \times 10^{-4}$, and the noise variance $N_0 = 10^{-2}$. The results are obtained over 1000 network realizations. For each network realization, we compute channel variances between any two nodes u and v as $\sigma_{uv}^2 = d_{uv}^{-\alpha}$ where d_{uv} is the distance between the two nodes.

3.5.1 Validation of INC, MAX, and WNC Improvement over DTX

Figure 3.5 presents the reduction in aggregate transmit power using the INC, MAX, and WNC schemes over the DTX scheme for various network sizes. For the WNC scheme, we take the cross-correlation $\rho = 0.5$. It is clear from the figure that great reduction in aggregate transmit power can be achieved using the INC, MAX, and WNC scheme over the DTX scheme, especially for large network sizes. The power reduction of 69% at a network size of two increases rapidly as the network size increases and achieves more than 90% for network sizes larger than five user nodes. The reason for the INC, MAX, and WNC schemes to achieve substantial power reduction is the spatial diversity used to compensate the large path loss. User

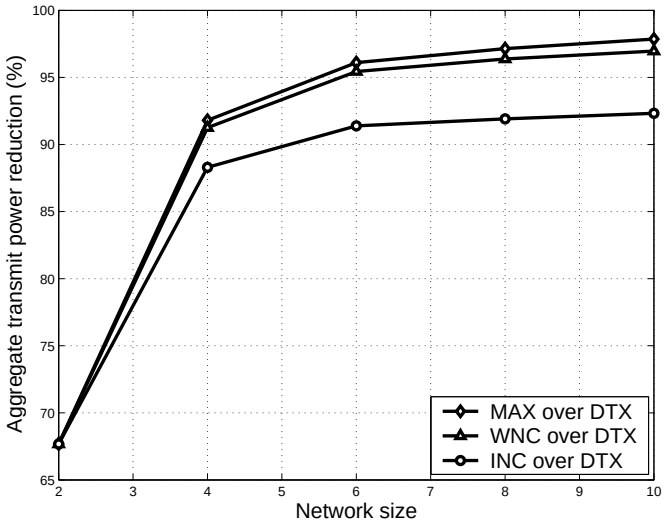

Figure 3.5: Reduction in aggregate transmit power of INC, MAX, and WNC ($\rho = 0.5$) over DTX versus network size.

nodes other than U_N in the INC scheme receive a diversity order of two for their transmission while those in the MAX and WNC schemes receive diversity order incrementally based on their locations. The spatial diversity results in substantial reduction of the aggregate transmit power in our schemes over the DTX scheme.

Figure 3.6 presents the distribution of aggregate transmit power in a 10-unit network for the four considered schemes; nevertheless, the finding is unique to other network sizes. Note that user nodes are numbered in the decreasing order of their distance to the base node. Clearly from the figure, the DTX scheme leads to substantial power burden on user nodes away from the base node. This is due to large transmit powers required in association with large distances. The power burden reduction in the INC scheme is due to diversity order of two for each user node and transmit power shared by two consecutive units, a half of power for each. High

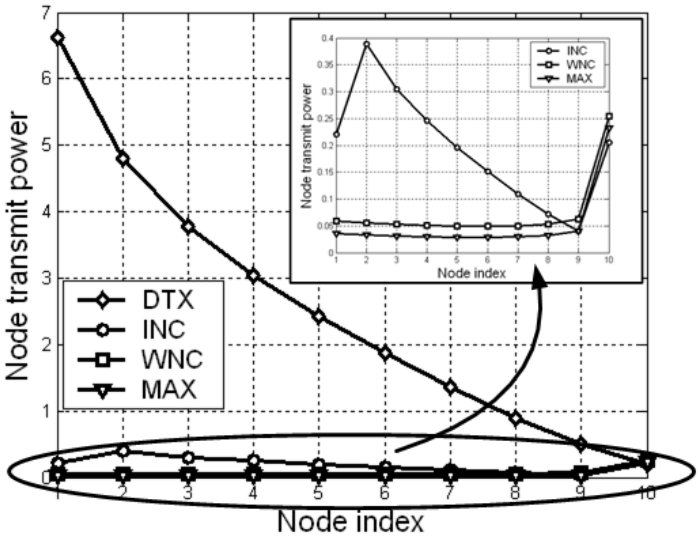

Figure 3.6: Distribution of transmit power in DTX, INC, MAX, and WNC ($\rho = 0.5$) for a 10-unit network.

transmit power for distant units, however, still remains. Nevertheless, power distribution is much better than that in the DTX scheme as shown in the figure. The best power distribution is found in the MAX and WNC schemes. In these schemes, incremental diversity provides higher diversity order to user nodes with larger distances to compensate the high required transmit power. Furthermore, the higher transmit power is shared by the larger group of user nodes. Consequently, the MAX and WNC schemes achieve the best power distribution as shown in the figure.

3.5.2 Validation of WNC over INC and MAX

It is clear from Figures 3.5 and 3.6 that the WNC scheme for the case of $\rho = 0.5$ results in a comparable performance with the MAX scheme. In particular, Figure 3.5 shows that power reduction of the WNC scheme over the DTX scheme

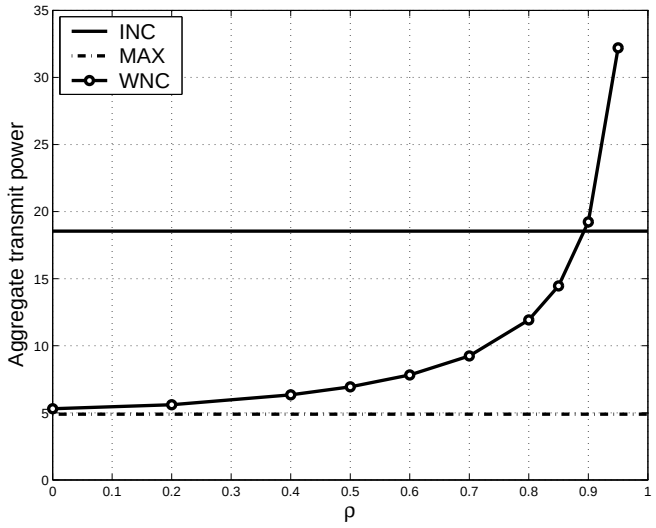

Figure 3.7: Aggregate transmit power in INC, MAX, and WNC versus ρ for a 10-unit network.

is less than 1% lower than that of the MAX scheme while Figure 3.6 reveals that the WNC and MAX schemes have the same power distribution profile.

Now let us take a close look at the performance of the INC, MAX, and WNC schemes. Figure 3.7 illustrates the aggregate transmit power using the INC, MAX, and WNC schemes in a 10-unit network for various values of the cross correlation ρ; nevertheless, the finding is unique for other network sizes. As shown in the figure, when ρ is chosen appropriately, for example $\rho \in [0, 0.6]$ in this setup, aggregate transmit power in the WNC and MAX schemes is not much different. It is also clear from the figure that the WNC scheme outperforms the INC scheme in terms of aggregate transmit power for a wide range of ρ values ($\rho \in [0, 0.85]$ in this setup) and the WNC scheme performance becomes no longer better than the INC scheme only for very high values of ρ ($\rho > 0.85$ in this setup). Here high values of the cross

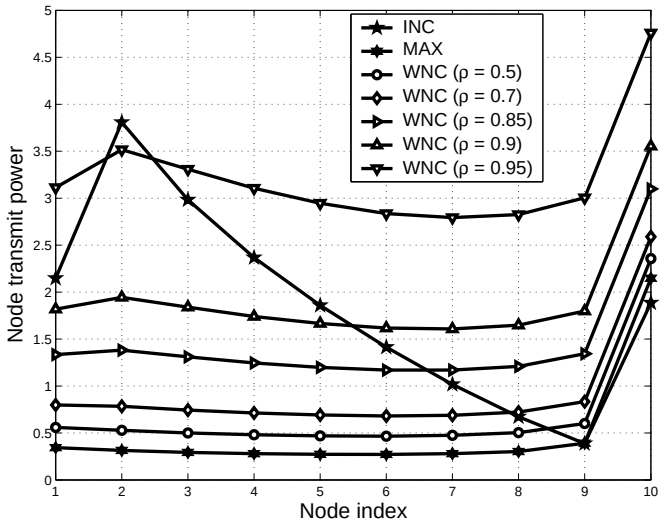

Figure 3.8: Power distribution in INC, MAX, and WNC (for various ρ values) for a 10-unit network.

correlation ρ associate with high interference, caused by the linear combination of overheard symbols at relay, that overcomes the benefit of incremental diversity and causes high aggregate transmit power in the WNC scheme.

Lastly, Figure 3.8 provides the power distribution among user nodes using the INC, MAX, and WNC schemes for various values of ρ for the same network in Figure 3.7. We see that the WNC scheme provides the same power distribution profile as in the MAX scheme for any $\rho \leq 0.9$. Moreover, the WNC scheme outperforms the INC scheme in terms of power distribution for a wide range of ρ values. Even for $\rho = 0.95$, the power distribution profile of the WNC scheme is still better than that of the INC scheme (the node power varies within 2 units in WNC while that is about 3.5 in INC) although the WNC scheme with this ρ value results in much higher aggregate transmit power as shown in Figure 3.7. Incremental diversity

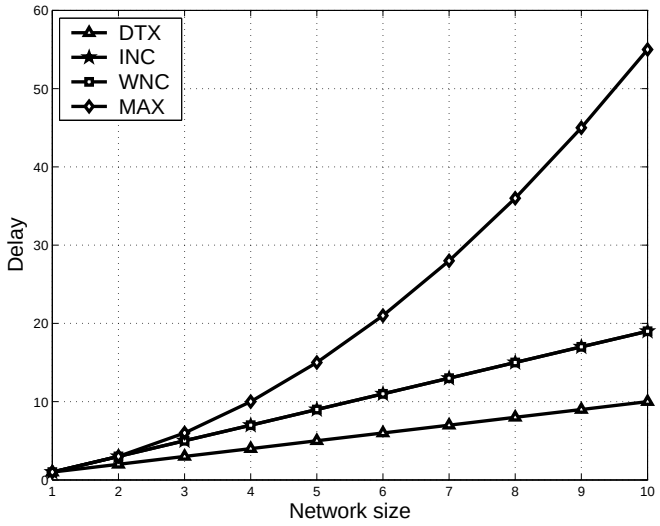

Figure 3.9: Transmission delay in DTX, INC, MAX, and WNC.

provided in the WNC scheme, where higher diversity order are allocated for more distant user nodes to reduce the high transmit power, provides the balance in power distribution. Furthermore, transmit power is shared among many user nodes by cooperative communication, where higher transmit power is shared by a larger group of relays, providing further balance in power distribution.

3.5.3 Remarks

From the performance evaluation presented in this section, a number of remarks are noteworthy. First, the jump in transmit power at U_N, the closest user node to the base node, in the INC, MAX, and WNC schemes in Figures 3.6 and 3.8 is due to the fact that this unit does not receive assistance from others and the transmission of its own information is in direct mode. Also the most distant unit U_1 may require less transmit power than others in the INC and WNC schemes since

it is not required to assist any unit. Second, as we have seen, the INC, MAX, and WNC schemes outperform the DTX scheme greatly in terms of aggregate transmit power and power distribution. Higher gain in power reduction and even power distribution of the INC, MAX, and WNC schemes over the DTX scheme is expected when higher quality of service, equivalently lower SER, is desired. A similar notice is given for the case of using the MAX and WNC schemes over the INC scheme. Third, the MAX scheme achieves the lowest power aggregation and the best power distribution, as shown in Figures 3.5 - 3.8. However, the transmission delay in the MAX scheme is very high, compared to the WNC and INC schemes, as illustrated in Figure 3.9. For a network of N user nodes, the MAX scheme incurs a delay of $N(N+1)/2$ time slots while both the WNC and INC schemes have the same transmission delay of $(2N-1)$ time slots. On the other hand, although the INC scheme incurs a low transmission delay, it requires much higher transmit power and the power is distributed unevenly, as revealed in Figures 3.6 and 3.8. Clearly, the WNC scheme achieves the advantages of both MAX and INC schemes, which are characterized by low transmit power, even power distribution, and low transmission delay. Lastly, the WNC scheme requires no multiuser detection at user nodes while it employs a simple multiuser detection method at the base node, as shown in Section 3.2. These characteristics make the WNC scheme be the best candidate to improve network performance.

3.6 Summary

In this chapter, we considered a number of location-aware cooperation-based schemes, denoted as INC, MAX, and WNC that achieve spatial diversity to reduce aggregate transmit power and achieve even power distribution in a network. The INC scheme utilizes single-relay cooperative communication in a network, resulting in good reduction of aggregate transmit power; however, the issue of uneven power distribution still remains. For the MAX scheme, multi-relay cooperative communication is leveraged to provide incremental diversity to solve the uneven power distribution and achieves substantial reduction in aggregate transmit power. However, transmission delay in the MAX scheme grows quadratically with the network size. For a network of N mobile units, the transmission delays in the INC and MAX schemes are $(2N-1)$ and $N(N+1)/2$ time slots, respectively. The novel WNC scheme resolves the weaknesses of both the INC and MAX schemes. In particular, the proposed INC, MAX, and WNC schemes can result in more than 90% reduction in aggregate transmit power over DTX scheme. Moreover, the WNC scheme can achieve low aggregate transmit power and even power distribution of the MAX scheme with low transmission delays of the INC scheme.

Chapter 4

Transform-based Space-Time Network Coding

In MIMO communications, space-time block coding is a technique to transmit redundant signals across a number of antennas and time slots to improve the reliability of the transmitted data. The first space-time block code (STBC) was invented by Alamouti [5], and thus called Alamouti's STBC, to provide full spatial diversity for two-transmit-antenna MIMO systems. Like single-antenna systems, Alamouti's STBC is a rate-1 code, i.e. that it takes two time slots to transmit two symbols, resulting in one transmitted symbol per time slot. In [6], orthogonal STBCs for MIMO systems with more than two transmit antennas were proposed. These codes provide full spatial diversity; however, they cannot achieve full rate. What makes orthogonal STBCs attractive is that maximum-likelihood (ML) decoding can be achieved at the receiver with only linear processing [57].

Distributed space-time block coding is the application of space-time block coding to cooperative communications to achieve higher spectral efficiency over traditional FDMA and CDMA schemes in cooperative communications. In [19], outage performance of DSTBCs for DF protocol was analyzed. Bit-error-rate (BER) performance for DF and AF protocols for distributed Alamouti's STBC is provided in [58], [59] with the assumption of perfect timing synchronization. Unlike MIMO

systems, which always achieve full diversity when using Alamouti's STBC, the inter-user channel variances affect the performance of distributed Alamouti's STBC in cooperative communications. When the inter-user channel variances are not high enough, the distributed Alamouti schemes incur an error-floor behavior of their BER performance even under perfect timing synchronization [58], [59].

In Chapter 2, STNCs based on FDMA-like and CDMA-like techniques are utilized to combine the signals at relay nodes. Although these STNCs help reducing the transmission delays, they do not achieve better spectral efficiency over the traditional TDMA scheme in cooperative communications. In this chapter, a STNC based on transform-based coding [40], [41], whose coding matrices take a form of Hadamard or Vandermonde matrices and compose a set of parameters that are optimized for conventional signal constellations, is proposed to improve the spectral efficiency of the combining signals at relay nodes while while overcoming the issues of imperfect synchronization and maintaining the full spatial diversity over DSTBC schemes. We analyze the PEP performance of the proposed STNC scheme and derive the design criteria of the network coding matrix to achieve full diversity even under finite inter-user channel variances. We also perform simulations to validate the performance of the proposed STNC. In addition, performance comparison between the proposed STNC and a DSTBC scheme [19] employing Alamouti's code [5] under timing synchronization errors is investigated through simulations.

Notation: Lower and upper case bold symbols denote column vectors and matrices, respectively. *, $^{\mathcal{T}}$, and $^{\mathcal{H}}$ denote complex conjugate, transpose, and Hermitian transpose, respectively. $\mathsf{E}\{.\}$, $\mathrm{diag}\{.\}$, and $|.|$ represent the expectation, a

diagonal matrix, the size of a set, respectively. $\mathcal{CN}(0, \sigma^2)$ is the circular symmetric complex Gaussian random variable with zero mean and variance σ^2. r refers to the index of a relay node, and n denotes the index of a transmitted symbol of interest and also the index of a user node.

4.1 System Model and Signal Detection

We consider a multi-source wireless network as shown in Figure 4.1, where $U_1, U_2, ..., U_N$ are the N user nodes transmitting their information to the common base node U_0. Without loss of generality, the transmitted information can be represented by symbols, denoted as $x_1, x_2, ..., x_N$. Nevertheless, the user nodes in practice transmit the information in packets that contains a large number of symbols. We assume that the base node has M antennas while the user nodes are single-antenna devices. The channels are modeled as narrow-band Rayleigh fading with AWGN. We assume that the antenna separations at the base node are at least a half of wavelengths apart and thus the channels are spatially uncorrelated. The channel coefficient between an arbitrary receiver u and transmitter v is defined as $h_{uv} \sim \mathcal{CN}(0, \sigma_{uv}^2)$, where σ_{uv}^2 is the channel variance.

4.1.1 System Model

The system model comprises a source transmission phase and a relay transmission phase. Each transmission phase consists of N time slots, and the network requires $2N$ time slots for transmissions of the N symbols to U_0. In the source

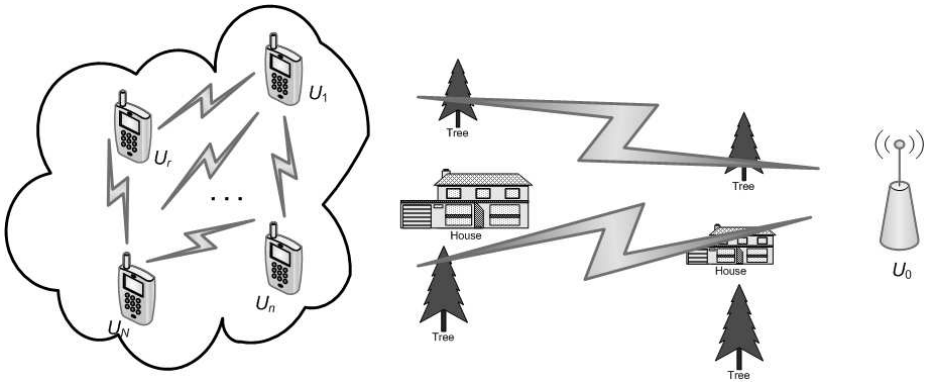

Figure 4.1: A multi-source wireless network.

transmission phase, each user node U_n for $n = 1, 2, ..., N$ is assigned a time slot, denoted T_n, to broadcast its symbol x_n to other user nodes U_r, $r \neq n$, where x_n is from an $\mathcal{M}$-QAM constellation $\mathbb{X}$. At the end of this phase, each user node U_r for $r = 1, 2, ..., N$ possesses a set of N symbols $x_1, x_2, ..., x_N$, comprising its own symbol x_r. In the relay transmission phase, U_r forms a single linearly-coded signal, a linear combination of the overheard symbols and its own one, and transmits the signal to the base node in its dedicated time slot T_{N+r}. U_r detects the symbol x_n based on the source signal and re-encode the symbol in its linearly-coded signal if the decoding is successful, the so called DF protocol. A detection state, a success or a failure in detecting a symbol, can be determined based on the amplitude of the estimated channel coefficient [14] or the received signal-to-noise ratio (SNR) [16]. Notice that this DF scheme is also called the selective-relaying protocol in literature [14].

Figure 4.2 illustrates the transmissions in the source transmission and relay transmission phases of the WNC network. As shown in the figure, the STNC requires $2N$ time slots to complete the transmission in the network and guarantees a single

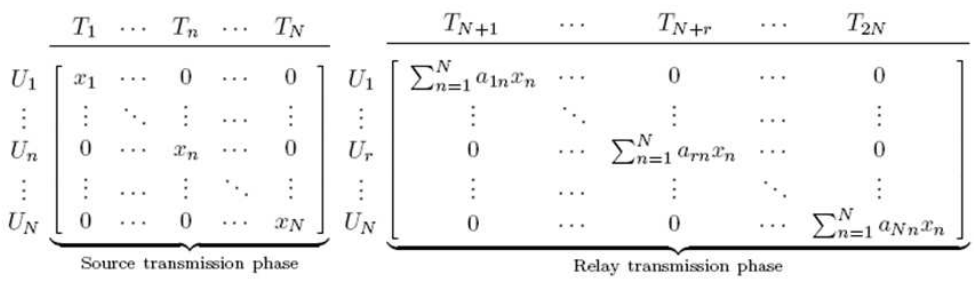

Figure 4.2: Transform-based space-time network coding.

transmission in the network at any given time slot to eliminate the issue of imperfect frequency and timing synchronization in traditional cooperative communications. In the source transmission phase, the signal received at U_r from U_n is

$$y_{rn} = h_{rn}\sqrt{P_n}x_n + w_{rn}, \tag{4.1}$$

where P_n is the transmit power at U_n in the source transmission phase and $w_{rn} \sim \mathcal{CN}(0, N_0)$ is the AWGN. In the relay transmission phase, the signal received at the mth antenna, $m = 1, 2, ..., M$, of the base node U_0 from U_r is

$$y_{mr} = h_{mr}\sqrt{P_r}s_r + w_{mr}, \tag{4.2}$$

where P_r is the transmit power in the relay transmission phase, $w_{mr} \sim \mathcal{CN}(0, N_0)$ is the AWGN, and

$$s_r = \sum_{n=1}^{N} a_{rn}\beta_{rn}x_n = \mathbf{a}_r^{\mathcal{T}}\mathbf{B}_r\mathbf{x} \tag{4.3}$$

is the linearly-coded symbol at U_r. In (4.3), $\mathbf{a}_r = [a_{r1}, ..., a_{rn}, \ ..., a_{rN}]^{\mathcal{T}}$, where $\mathbf{a}_r^{\mathcal{T}}\mathbf{a}_r = 1$ to normalize the transmitted signal, is the code vector at U_r with a_{rn} being the code coefficient at U_r associated with x_n, $\mathbf{x} = [x_1, x_2, ..., x_N]^{\mathcal{T}}$ is the transmitted

symbol vector, and $\mathbf{B}_r = \text{diag}\{\beta_{r1}, ..., \beta_{rn}, \ ..., \beta_{rN}\}$ is a matrix representing the detection state at U_r with β_{rn} being detection state associated with x_n. We have $\beta_{rr} = 1$ always since U_r has its own symbol x_r and for $n \neq r$,

$$\beta_{rn} = \begin{cases} 1 & \text{if } U_r \text{ decodes } x_n \text{ correctly} \\ 0 & \text{otherwise} \end{cases} . \tag{4.4}$$

The received signals at U_0 can be expressed in a matrix form as

$$\mathbf{Y} = \mathbf{HS} + \mathbf{W}, \tag{4.5}$$

where $\mathbf{Y}$, $\mathbf{H}$, and $\mathbf{W}$ are $M \times N$ matrices comprising the received signals, the channel coefficients, and the AWGN's, and $\mathbf{S} = \text{diag}\left\{\sqrt{P_1}s_1, ..., \sqrt{P_r}s_r, ..., \sqrt{P_N}s_N\right\}$ is the $N \times N$ code matrix. Note that a relay node uses a bandwidth of $1/N$ times of that used in relay nodes in the FDMA-like and CDMA-like STNCs to transmit the unique symbol in (4.3). Thus the proposed STNC is more spectrally efficient than the FDMA-like and CDMA-like STNCs.

4.1.2 Signal Detection

To detect the transmitted symbols, we assume that receivers have a full knowledge of the channel state information, which can be acquired using a preamble in the transmitted signal as usually done in systems such as 802.11 [43]. We also assume that the base node knows the detection states at the relay nodes. This can be done by using an N-bit indicator in the relaying signal. Notice that in practice, information is transmitted in packets [43] that contain a large number of symbols. Each packet is detected as a whole, and a cyclic redundancy check [44] is sufficient

to determine the detection state of the packet. Thus one bit per packet results in a minimal overhead.

To derive code criteria in the next section, ML detectors, which is a minimum distance rule, are used. The detected symbol vector at the base node U_0 is

$$\widehat{\mathbf{x}} = \underset{\mathbf{x}\in\mathbb{X}^N}{\operatorname{argmin}} \left\{ \| \mathbf{Y} - \mathbf{HS} \|_{\mathcal{F}}^2 \right\}, \tag{4.6}$$

where $\| \, . \, \|_{\mathcal{F}}$ denotes the Frobenius norm. As shown in (4.6), detecting $\mathbf{x}$ requires testing $|\mathbb{X}|^N$ possible vectors $\mathbf{x}$, which is computationally prohibitive as N and/or $|\mathbb{X}|$ are large. In that case, sphere decoder [60], which results in suboptimal decoding, can be used. The detection of x_n at user node U_r in the source transmission phase follows

$$\widehat{x}_n = \underset{x\in\mathbb{X}}{\operatorname{argmin}} \left\{ |y_{rn} - h_{rn}\sqrt{P_n}x|^2 \right\}. \tag{4.7}$$

4.2 Performance Analysis and Code Design

In this section, we analyze the performance of the proposed transform-based STNC and derive the PEP. Based on the PEP analysis, we derive two design criteria for the network coding matrix, namely the diversity criterion and the product criterion.

4.2.1 Performance Analysis of Transform-based STNC

Let us define $\mathbf{y} = \text{vec}(\mathbf{Y})$, $\mathbf{h} = \text{vec}(\mathbf{H})$, and $\mathbf{w} = \text{vec}(\mathbf{W})$, where vec(.) denotes the vectorization of a matrix by stacking the columns of the matrix on the top of

one another. Then the signal matrix in (4.5) can be rewritten in vector form as

$$\mathbf{y} = \mathbf{D}\mathbf{h} + \mathbf{w}, \tag{4.8}$$

where $\mathbf{D} = \mathbf{S} \otimes \mathbf{I}_M$ with $\otimes$ denoting the Kronecker product [61] and $\mathbf{I}_M$ being an identity matrix of size M. Suppose that $\mathbf{D}$ and $\widetilde{\mathbf{D}}$ are two different matrices related to two different code matrices $\mathbf{S}$ and $\widetilde{\mathbf{S}}$. The base node applies the ML detector in (4.6), and thus the conditional PEP is given by

$$\begin{aligned} &Pr\left(\mathbf{S} \to \widetilde{\mathbf{S}} \mid \{\mathbf{B}_r\}, \mathbf{h}\right) = \\ &Pr\left(\| \mathbf{y} - \mathbf{D}\mathbf{h} \|^2 > \| \mathbf{y} - \widetilde{\mathbf{D}}\mathbf{h} \|^2 \mid \{\mathbf{B}_r\}, \mathbf{h}, \mathbf{S} \text{ transmitted}\right). \end{aligned} \tag{4.9}$$

In a quadratic form of a complex Gaussian random variable, the PEP can be expressed as

$$Pr\left(\mathbf{S} \to \widetilde{\mathbf{S}} \mid \{\mathbf{B}_r\}, \mathbf{h}\right) = Pr(Q < 0 \mid \{\mathbf{B}_r\}, \mathbf{h}), \tag{4.10}$$

where

$$Q = \begin{bmatrix} \mathbf{z}_1^{\mathcal{H}} & \mathbf{z}_2^{\mathcal{H}} \end{bmatrix} \begin{bmatrix} \mathbf{I}_{MN} & \mathbf{0} \\ \mathbf{0} & \mathbf{I}_{MN} \end{bmatrix} \begin{bmatrix} \mathbf{z}_1 \\ \mathbf{z}_2 \end{bmatrix}, \tag{4.11}$$

in which $\mathbf{0}$ represents a zero matrix, $\mathbf{I}_{MN}$ is an identity matrix of size MN, $\mathbf{z}_1 = (\mathbf{D} - \widetilde{\mathbf{D}})\mathbf{h} + \mathbf{w}$, and $\mathbf{z}_2 = \mathbf{w}$. Because $\mathbf{h}$ and $\mathbf{w}$ are mutually independent random vectors, the conditional PEP can be averaged over the channel realization $\mathbf{h}$. At high SNR, the conditional PEP between $\mathbf{S}$ and $\widetilde{\mathbf{S}}$ can be upper-bounded as [62]

$$Pr\left(\mathbf{S} \to \widetilde{\mathbf{S}} \mid \{\mathbf{B}_r\}\right) \leq \begin{pmatrix} 2\nu - 1 \\ \nu - 1 \end{pmatrix} N_0^{\nu} \prod_{i=1}^{\nu} \gamma_i^{-1}, \tag{4.12}$$

where $\binom{a}{b}$ represents the *a choose b* operation, ν and γ_i is the rank and the ith non-zero eigenvalue of the matrix $\left(\mathbf{D}-\widetilde{\mathbf{D}}\right)\mathbf{R_h}\left(\mathbf{D}-\widetilde{\mathbf{D}}\right)^{\mathcal{H}}$ with $\mathbf{R_h} \triangleq \mathsf{E}\left\{\mathbf{h}\mathbf{h}^{\mathcal{H}}\right\} = \text{diag}\left\{\sigma_{11}^2,...,\sigma_{M1}^2,\sigma_{12}^2,...,\sigma_{M2}^2,...,\ \sigma_{1N}^2,...,\sigma_{MN}^2\right\}$ being the correlation matrix of the channel vector $\mathbf{h}$. Based on the relationship between $\mathbf{D}$ and $\mathbf{S}$ in (4.8) and the fact that $\mathbf{D}$, $\widetilde{\mathbf{D}}$, and $\mathbf{R_h}$ are all diagonal matrices, we have [61]

$$\left(\mathbf{D}-\widetilde{\mathbf{D}}\right)\mathbf{R_h}\left(\mathbf{D}-\widetilde{\mathbf{D}}\right)^{\mathcal{H}} = \left(\mathbf{\Delta_S}\otimes\mathbf{I}_M\right)\mathbf{R_h}, \tag{4.13}$$

where we define

$$\begin{aligned}\mathbf{\Delta_S} &\triangleq \left(\mathbf{S}-\widetilde{\mathbf{S}}\right)\left(\mathbf{S}-\widetilde{\mathbf{S}}\right)^{\mathcal{H}} \\ &= \text{diag}\left\{P_1|\mathbf{a}_1^{\mathcal{T}}\mathbf{B}_1\Delta\mathbf{x}|^2,...,P_r|\mathbf{a}_r^{\mathcal{T}}\mathbf{B}_r\Delta\mathbf{x}|^2,...,P_N|\mathbf{a}_N^{\mathcal{T}}\mathbf{B}_N\Delta\mathbf{x}|^2\right\},\end{aligned} \tag{4.14}$$

in which $\Delta\mathbf{x} = \mathbf{x}-\widetilde{\mathbf{x}}$ with two distinct transmitted symbol vectors $\mathbf{x}$ and $\widetilde{\mathbf{x}}$. Given that $\text{rank}\left(\mathbf{R_h}\right) = MN$, we have $\nu = M\nu_{\mathbf{S}}$, where $\nu_{\mathbf{S}} \triangleq \text{rank}(\mathbf{\Delta_S})$. In (4.14), the maximum rank of $\mathbf{\Delta_S}$ is N. We should design the coding vectors $\mathbf{a}_r$'s to achieve this rank and the design criteria will be derived later in this section. In that case, the N eigenvalues of $\mathbf{\Delta_S}$ are $\lambda_r = P_r|\mathbf{a}_r^{\mathcal{T}}\mathbf{B}_r\Delta\mathbf{x}|^2$ for $r = 1,2,...,N$, and we can express (4.12) as

$$\begin{aligned}Pr\left(\mathbf{S}\rightarrow\widetilde{\mathbf{S}}\mid\ \{\mathbf{B}_r\}\right) \leq \begin{pmatrix}2MN-1\\ MN-1\end{pmatrix} N_0^{MN}\left(\prod_{m=1}^{M}\prod_{r=1}^{N}\frac{1}{\sigma_{mr}^2}\right)\times \\ \left(\prod_{r=1}^{N}\left(P_r|\mathbf{a}_r^{\mathcal{T}}\mathbf{B}_r\Delta\mathbf{x}|^2\right)^{-M}\right).\end{aligned} \tag{4.15}$$

Averaging with respect to the detection state matrices $\{\mathbf{B}_r\}$ with a notice that the detection state matrices are mutually independent because the detection at each

user node is independent from one another, the PEP can be rewritten as

$$Pr\left(\mathbf{S}\rightarrow\widetilde{\mathbf{S}}\right)\leq\left(\begin{array}{c}2MN-1\\ \\ MN-1\end{array}\right)N_0^{MN}\left(\prod_{m=1}^{M}\prod_{r=1}^{N}\frac{1}{\sigma_{mr}^2}\right)\times \left(\underbrace{\prod_{r=1}^{N}\mathsf{E}\left\{\left(P_r\left|\sum_{n=1}^{N}a_{rn}\beta_{rn}\Delta x_n\right|^2\right)^{-M}\right\}}_{\mathcal{A}}\right), \tag{4.16}$$

where $\Delta x_n = x_n - \widetilde{x}_n$.

Let $S_r \triangleq [\beta_{r1},...,\beta_{rn},...,\beta_{rN}]_2$ for $n \neq r$, where $[.]_2$ denotes a base-2 number. S_r is a decimal number representing one of 2^{N-1} detection states at U_r. Because symbols at a user node are independently detected, β_{rn}'s are independent Bernoulli random variables with a distribution

$$G(\beta_{rn})=\begin{cases}1-SER_{rn} & \text{if } \beta_{rn}=1\\ \\ SER_{rn} & \text{if } \beta_{rn}=0\end{cases}, \tag{4.17}$$

where SER_{rn} is the SER for detecting x_n at U_r. For $\mathcal{M}$-QAM modulation, it can be shown that [16]

$$SER_{rn}=F\left(1+\frac{b\sigma_{rn}^2P_n}{N_0\sin^2(\theta)}\right), \tag{4.18}$$

where $b=\frac{3}{2(\mathcal{M}-1)}$ and

$$F(x(\theta))=\frac{4C}{b\pi}\int_0^{\frac{\pi}{2}}\frac{1}{x(\theta)}d\theta-\frac{4C^2}{b\pi}\int_0^{\frac{\pi}{4}}\frac{1}{x(\theta)}d\theta, \tag{4.19}$$

in which $C=1-\frac{1}{\sqrt{\mathcal{M}}}$ and $x(\theta)$ denotes a function of θ. At high SNR, we can ignore the one in (4.18) and obtain

$$SER_{rn}\simeq\mathcal{K}\frac{N_0}{\sigma_{rn}^2P_n}, \tag{4.20}$$

where

$$\mathcal{K} = \frac{4C}{b\pi}\int_0^{\frac{\pi}{2}} \sin^2\theta d\theta - \frac{4C^2}{b\pi}\int_0^{\frac{\pi}{4}} \sin^2\theta d\theta. \tag{4.21}$$

Hence the probability of detection state at U_r in state S_r is

$$Pr(S_r) = \prod_{n=1;n\neq r}^{N} G(\beta_{rn}) = \prod_{n=1;\beta_{rn}=1}^{N} (1 - SER_{rn}) \prod_{n=1;\beta_{rn}=0}^{N} SER_{rn}. \tag{4.22}$$

Given a detection state S_r, which can take 2^{N-1} values,

$$\begin{aligned}
\mathcal{A} &= \prod_{r=1}^{N} \sum_{S_r=0}^{2^{N-1}-1} Pr\left(\mathbf{x} \rightarrow \widetilde{\mathbf{x}} \mid S_r\right).Pr(S_r) \\
&= \prod_{r=1}^{N} \sum_{S_r=0}^{2^{N-1}-1} \left(\frac{1}{P_r \left| \sum_{n=1;\beta_{rn}=1}^{N} a_{rn}\Delta x_n \right|^2} \right)^M \times \\
&\quad \prod_{n=1;\beta_{rn}=1}^{N} (1 - SER_{rn}) \prod_{n=1;\beta_{rn}=0}^{N} SER_{rn}.
\end{aligned} \tag{4.23}$$

Examining (4.23), we have

$$\begin{aligned}
\mathcal{A} &= \prod_{r=1}^{N} \left[\left(\frac{1}{P_r \left| \mathbf{a}_r^{\mathcal{T}} \mathbf{\Delta x} \right|^2} \right)^M \prod_{n=1;n\neq r}^{N} (1 - SER_{rn}) \right. \\
&\quad + \sum_{l=1;l\neq r}^{N} \left(\frac{1}{P_r \left| \sum_{n=1;n\neq l}^{N} a_{rn}\Delta x_n \right|^2} \right)^M \prod_{n=1;n\neq l}^{N} (1 - SER_{rn}) SER_{rl} \\
&\quad \left. + \cdots + \left(\frac{1}{P_r \left| a_{rr}\Delta x_r \right|^2} \right)^M \prod_{n=1;n\neq r}^{N} SER_{rn} \right],
\end{aligned} \tag{4.24}$$

where the first term corresponds to the case the relay U_r correctly detects all overheard symbols, the second term is associated the case the relay U_r correctly detects all overheard symbols but one, the x_l, and the last term is the case where U_r erroneously detects all the overheard symbols. At high SNR, the SERs are small and their high-order terms can be ignored. Considering the first two terms,

$$\mathcal{A} \lesssim \prod_{r=1}^{N} \left[\left(\frac{1}{P_r \left| \mathbf{a}_r^{\mathcal{T}} \mathbf{\Delta x} \right|^2} \right)^M + \sum_{l=1;l\neq r}^{N} SER_{rl} \right], \tag{4.25}$$

where we used the approximation $1 - SER_{rn} \simeq 1$. Substituting (4.20) into (4.25), we can show that

$$\mathcal{A} \lesssim P^{-MN} \prod_{r=1}^{N} \left(\frac{1}{\left| \mathbf{a}_r^{\mathcal{T}} \mathbf{\Delta x} \right|^2} \right)^M \left(\frac{1}{\alpha_r^M} + \sum_{n=1; n \neq r}^{N} \frac{\mathcal{K} N_0 \left(d_{\max}^2 \right)^M}{\alpha_n \sigma_{rn}^2} \right), \tag{4.26}$$

where $d_{\max}$ is the maximum Euclidean distance of $\mathbb{X}$ and $\alpha_r = P_r/P$ and $\alpha_n = P_n/P$ are fractions of the total transmit power P allocated in the source and relay transmission phases, respectively. Substituting (4.26) into (4.16), the PEP is

$$\begin{aligned} Pr\left(\mathbf{S} \to \widetilde{\mathbf{S}} \right) \;\; \leq \;\; & \binom{2MN-1}{MN-1} \prod_{m=1}^{M} \prod_{r=1}^{N} \left(\frac{1}{\sigma_{mr}^2 \left| \mathbf{a}_r^{\mathcal{T}} \mathbf{\Delta x} \right|^2} \times \right. \\ & \left. \left(\frac{1}{\alpha_r^M} + \sum_{n=1; n \neq r}^{N} \frac{\mathcal{K} N_0 \left(d_{\max}^2 \right)^M}{\alpha_n \sigma_{rn}^2} \right) \right) \left(\frac{P}{N_0} \right)^{-MN}. \end{aligned} \tag{4.27}$$

4.2.2 Code Design Criteria

From (4.27), the design criteria for the coding vectors $\mathbf{a}_r$'s are as follows.

Diversity criterion: The system provides full diversity with order MN if $\left| \mathbf{a}_r^{\mathcal{T}} \mathbf{\Delta x} \right| \neq 0$, $\forall r \in [1, N]$, $\forall \mathbf{x}, \widetilde{\mathbf{x}} \in \mathbb{X}$.

Product criterion: The minimum value of the product $\prod_{r=1}^{N} \mathbf{a}_r^{\mathcal{T}} \mathbf{\Delta x}$ over all pairs of distinct symbol vectors $\mathbf{x}$ and $\widetilde{\mathbf{x}}$ should be as large as possible. The product criterion is of secondary importance and should be optimized if full diversity is achieved.

Let $\mathbf{A} \triangleq [\mathbf{a}_1, ..., \mathbf{a}_r, ..., \mathbf{a}_N]$ be the coding matrix. With the above design criteria, $\mathbf{A}$ has been proposed in a number of previous work [40], [41], [42], where Hadamard and Vandermonde matrices were used to construct $\mathbf{A}$. Note that the coding matrices based on Vandermonde matrices result in larger minimum prod-

uct values than those using Hadamard matrices. Thus we will use Vandermonde matrices for our STNC scheme. In that case,

$$\mathbf{A} = \frac{1}{\sqrt{N}} \begin{bmatrix} 1 & \cdots & 1 & \cdots & 1 \\ \theta_1 & \cdots & \theta_r & \cdots & \theta_N \\ \vdots & \vdots & \vdots & \vdots & \vdots \\ \theta_1^{N-1} & \cdots & \theta_r^{N-1} & \cdots & \theta_N^{N-1} \end{bmatrix}, \tag{4.28}$$

where θ_r depends on N and the construction methods [40], [41], [42]. In the following are some of good code coefficients.

- If $N = 2^k$ for $k \geq 1$, the optimum $\theta_r = e^{j\frac{4r-3}{2N}\pi}$ for $r = 1, 2, ..., N$ and $j = \sqrt{-1}$.
- If $N = 3 \times 2^k$ for $k \geq 0$, the optimum $\theta_r = e^{j\frac{6r-3}{3N}\pi}$ for $r = 1, 2, ..., N$ and $j = \sqrt{-1}$.
- If $N = 2^k \times 3^l$ for $k \geq 1$ and $l \geq 1$, (not optimum) $\theta_r = e^{j\frac{6r-5}{3N}\pi}$ for $r = 1, 2, ..., N$ and $j = \sqrt{-1}$.
- For any value of N, the code matrix in (4.28) can be constructed as $\mathbf{A} = \text{diag}\left\{1, \alpha, ..., \alpha^{N-1}\right\} \mathbf{F}_N$, where $\mathbf{F}_N$ is the normalized $N \times N$ discrete Fourier transform matrix and $\alpha \triangleq e^{j2\pi/J}$ with the choice of J discussed in [42].

4.3 Impact of Synchronization Errors on DSTBC

The source transmission phase of schemes using DSTBC is the same with that of the STNC scheme, i.e., that the N user nodes take turn to exchange their transmit symbols among themselves. Thus the signal model for this phase follows (4.1). After

the source transmission phase, a STBC matrix is formed from the overheard symbol vector $\mathbf{x}$ as

$$\mathbf{S}(l) = \begin{bmatrix} s_{01}(l) & \cdots & s_{0r}(l) & \cdots & s_{0N}(l) \\ \vdots & \ddots & \vdots & \cdots & \vdots \\ s_{k1}(l) & \cdots & s_{kr}(l) & \cdots & s_{kN}(l) \\ \vdots & \cdots & \vdots & \ddots & \vdots \\ s_{(K-1)1}(l) & \cdots & s_{(K-1)r}(l) & \cdots & s_{(K-1)N}(l) \end{bmatrix}, \tag{4.29}$$

where l denotes the code matrix at frame l, which consists of K time slots required to transmit the code matrix, and $s_{kr}(l)$ is the code symbol transmitted at time slot k and through user node U_r. For example, the code matrix for two cooperative user nodes is the well-known Alamouti STBC [5]

$$\begin{bmatrix} x_1(l) & x_2(l) \\ -x_2^*(l) & x_1^*(l) \end{bmatrix}. \tag{4.30}$$

Note that if a symbol is erroneously decoded at a user node, the associated code symbols at that node are set to zero and the node remains silent during that time slot [19]. Note further that for orthogonal STBCs [4], which provide full spatial diversity in traditional MIMO systems, $K \geq N$ with the equality for only the case of $N = 2$. Therefore, transmitting N symbols from N user nodes in the relay transmission phase using DSTBCs requires more than N time slots and thus the use of DSTBC schemes results in less bandwidth efficiency than the use of the proposed STNC scheme.

In the relay transmission phase, the symbols in the kth row of the code matrix (4.29) for $k = 0, 1, ..., K-1$ are simultaneously transmitted through the N user

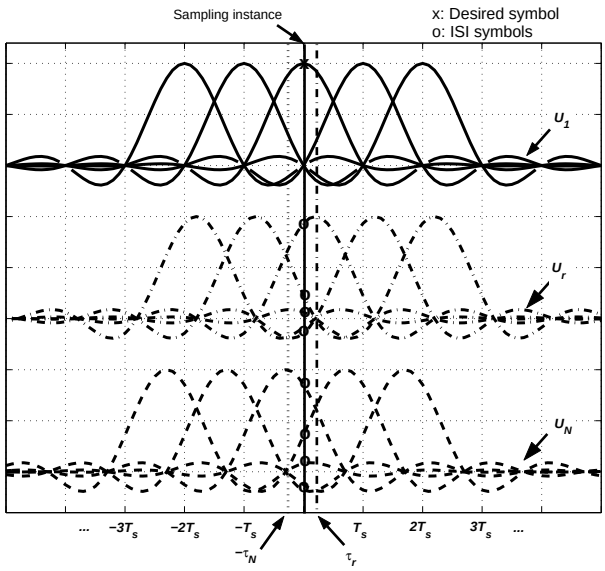

Figure 4.3: Impact of timing synchronization errors on DSTBC.

nodes, each acting as a respective antenna of a traditional MIMO system. Here we assume that nodes in the source and relay transmission phases transmit information in packets that comprise a large number of symbols as usually done in practice such as in 802.11 systems [43]. This transmission manner is to achieve efficiency by reducing the number of interframe spacings and the amount of channel estimation. In this way, the received signal at antenna m and time slot k of frame l due to the time synchronization errors is

$$\begin{aligned} y_m^k(l) &= \sqrt{\frac{P_r}{K}} \sum_{r=1}^{N} h_{mr}(l) \sum_{q=-q_0}^{q_0} s_{(\mathrm{mod}(k+q,K))r} \left(l + \left\lfloor \frac{k+q}{K} \right\rfloor \right) \times \\ & \quad p((q-l)T_s - \tau_r) + w_{mk}(l), \end{aligned} \tag{4.31}$$

where mod and $\lfloor . \rfloor$ denote the modulo and floor operations, respectively, $w_{mk}(l) \sim \mathcal{CN}(0, N_0)$ is the AWGN,

$$p(t) = \frac{\sin(\pi t/T_s)}{\pi t/T_s} \frac{\cos(\pi \beta t T_s)}{1 - 4\beta^2 t^2 T_s^2} \tag{4.32}$$

is the raised cosine pulse shape with a symbol period T_s and the roll-off factor β [56], q_0 is the number of nearest neighbor symbols from each side (left or right) that cause the ISI on the symbol of interest, and τ_r is the timing error associated with the signal from U_r. Figure 4.3 illustrates the ISI effect on the desired symbol, caused by timing synchronization errors.

Because the base node assumes perfect timing synchronization, it applies the detection techniques in [57]. For example in the case of $N = 2$ and Alamouti's code is used,

$$\widehat{x}_1(l) = \underset{x_1 \in |\mathbb{X}|}{\operatorname{argmin}} \left\{ \left| \left[\sum_{m=1}^{M} \left(y_m^0(l) \sqrt{\frac{P_1}{2}} h_{m1}^*(l) + (y_m^1(l))^* \sqrt{\frac{P_2}{2}} h_{m2}(l) \right) \right] - x_1 \right|^2 + \left(-1 + \sum_{m=1}^{M} \sum_{r=1}^{2} \frac{P_r}{2} |h_{mr}(l)|^2 \right) |x_1|^2 \right\} \quad (4.33)$$

$$\widehat{x}_2(l) = \underset{x_2 \in |\mathbb{X}|}{\operatorname{argmin}} \left\{ \left| \left[\sum_{m=1}^{M} \left(y_m^0(l) \sqrt{\frac{P_2}{2}} h_{m2}^*(l) - (y_m^1(l))^* \sqrt{\frac{P_1}{2}} h_{m1}(l) \right) \right] - x_2 \right|^2 + \left(-1 + \sum_{m=1}^{M} \sum_{r=1}^{2} \frac{P_r}{2} |h_{mr}(l)|^2 \right) |x_2|^2 \right\}. \quad (4.34)$$

This detection inherits the ISI effect in (4.31) and thus degrades the performance as we will see in the next section.

4.4 Simulations

We perform computer simulations to verify our proposed STNC scheme and to compare the performance of our scheme with a scheme that employs DSTBC. Both perfect and imperfect timing synchronization is considered in the DSTBC scheme. In these simulations, we assume that the N user nodes are in a cluster and the

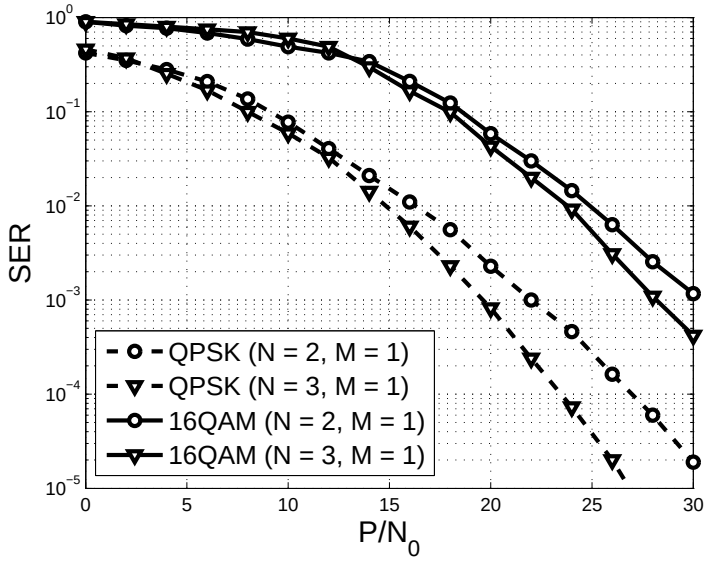

(a)

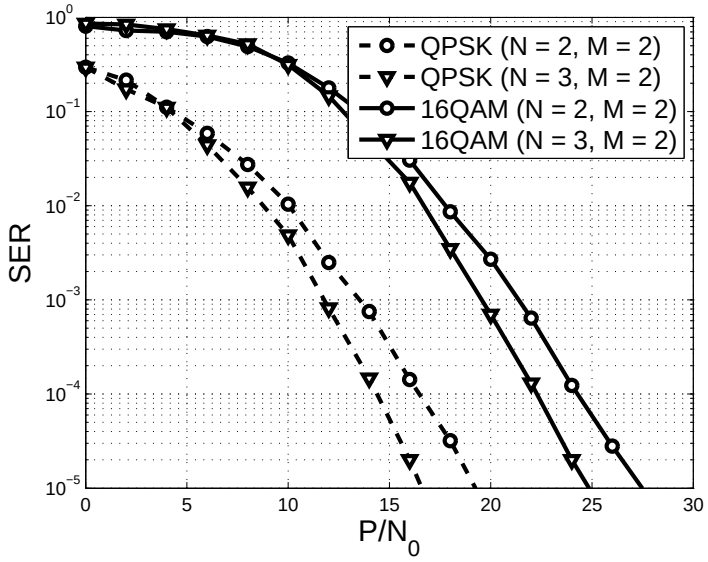

(b)

Figure 4.4: SER versus SNR performance of the transformed-based STNC for different numbers of user nodes ($N = 2$ and $N = 3$), QPSK and 16-QAM modulation, and (a) ($M = 1$) and (b) ($M = 2$) .

channel variances between a pair of user nodes are $\sigma_{rn}^2 = 30$, the same for all pairs. The cluster is faraway from the base node, and thus the channel variance between the base node and a user node is $\sigma_{0n}^2 = 1$, the same for all user nodes. Also we assume the noise variance $N_0 = 1$. Equal power allocation is assumed, where a total transmit power P associated with transmitted symbol is divided equally among the transmissions. In this case, $P_n = P/(N+1)$ and $P_r = PN/(N+1)$ for STNC scheme and $P_n = P/(K+1)$ and $P_r = PK/(K+1)$ for DSTBC scheme that requires K time slots for transmitting the space-time block-code matrix. Given the simulation setup, all transmitted symbols have the same performance and thus the performance associated with x_1 is presented.

Figure 4.4 presents the SER versus SNR performance of the proposed STNC. In these figures, we consider the number of user nodes $N = 2$ and 3 and the number of receive antennas $M = 1$ and 2. For modulations, we use quadrature phase-shift keying (QPSK) and 16-QAM. The coding coefficients in (4.28) for $N = 2$ are $\theta_r = e^{j\frac{4r-3}{4}\pi}$ with $r = 1, 2$ and for $N = 3$ are $\theta_r = e^{j\left(\frac{1}{9}+\frac{2(r-1)}{3}\right)\pi}$ with $r = 1, 2, 3$. From the figures, the proposed STNC clearly provides the expected diversity orders, i.e., that symbols x_n are received with diversity order MN for N user nodes and M receive antennas.

Figures 4.5 and 4.6 provide performance comparison between the proposed STNC scheme and a DSTBC scheme employing Alamouti's code for two user nodes ($N = 2$) cooperating with each other. In these simulations, QPSK and 16-QAM modulations are used, and numbers of receive antennas $M = 1, 2$ are considered. Various synchronization error ranges, denoted as ΔT_s, of $0T_s$, $0.3T_s$, and $0.5T_s$

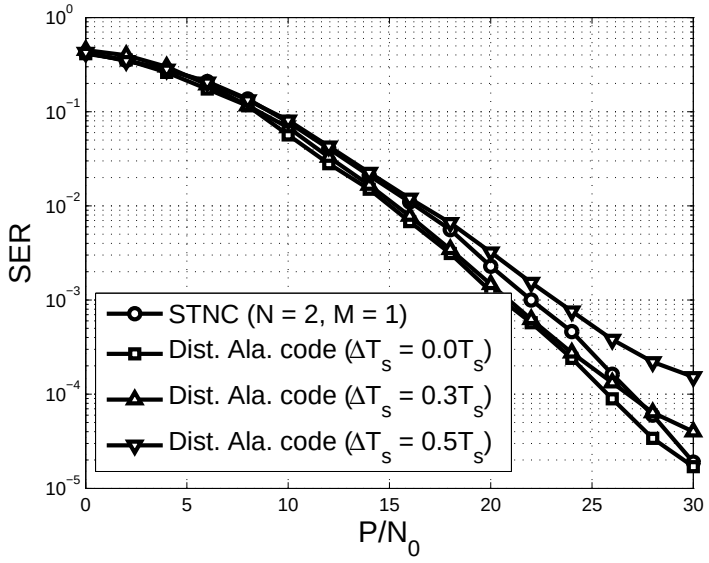

(a)

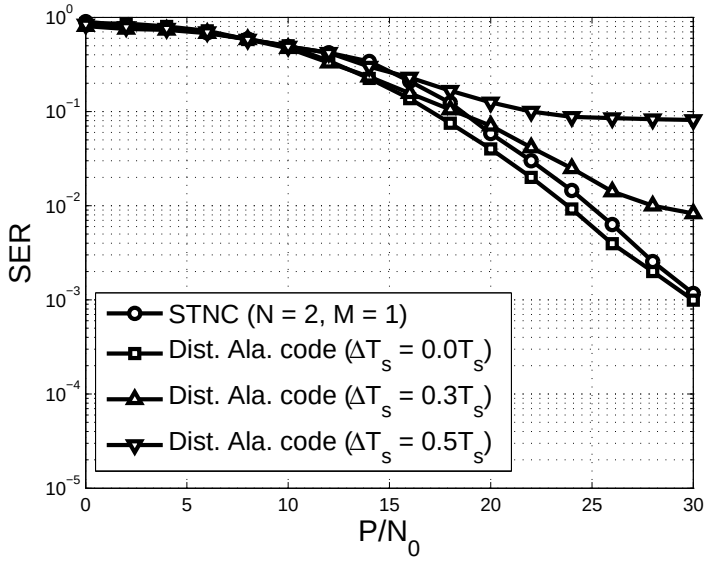

(b)

Figure 4.5: Performance comparison between the proposed STNC scheme and a scheme employing distributed Alamouti code for N = 2 and M = 1, (a) QPSK and (b) 16-QAM modulations.

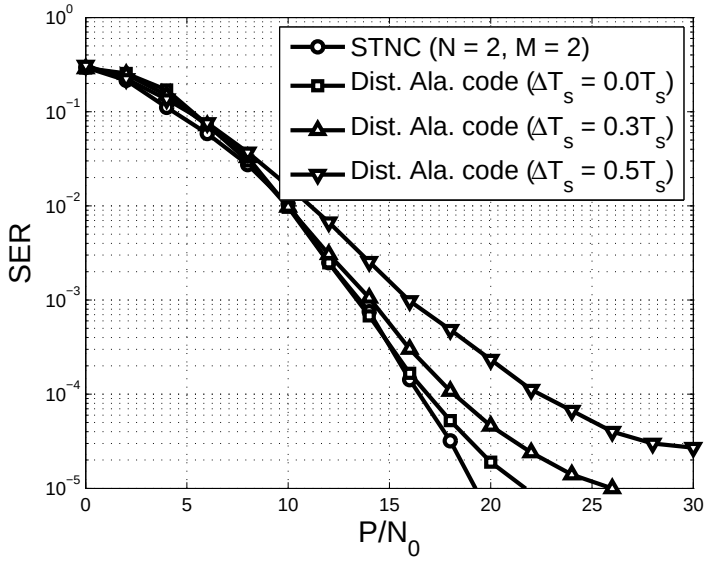

(a)

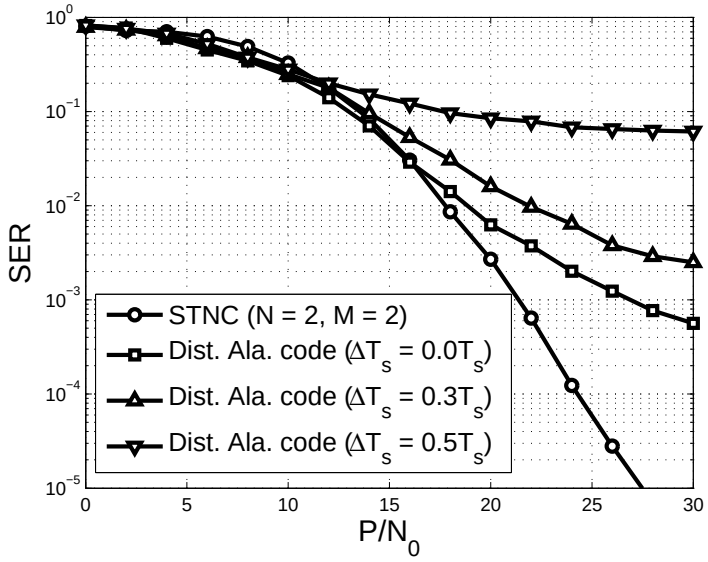

(b)

Figure 4.6: Performance comparison between the proposed STNC scheme and a scheme employing distributed Alamouti code for N = 2 and M = 2, (a) QPSK and (b) 16-QAM modulations.

are assumed, and the timing errors τ_r for $r = 1, 2$ is uniformly distributed in $[-\Delta T_s/2, \Delta T_s/2]$. Several points are worth noting from the figures. First, they clearly show that the proposed STNC scheme outperforms the distributed Alamouti scheme in most of the considered cases. Only the distributed Alamouti scheme with a single receive antenna ($M = 1$) and perfect synchronization ($\Delta T_s = 0T_s$) provides about 1dB advantage over the STNC scheme at moderate SNRs. Secondly, in contrast with the STNC scheme, which provides full diversity for all the considered cases, the distributed Alamouti scheme shows an error-floor behavior as high SNR regime, even under perfect synchronization (i.e. $\Delta T_s = 0T_s$). The error-floor behavior of the distributed Alamouti scheme under perfect synchronization is due to the dependency of the diversity order on the inter-user SNR and was reported in a number of previous work, both for DF and AF protocols in cooperative communications [58], [59]. Clearly, the proposed STNC is advantageous over the distributed Alamouti scheme with and without the occurrence of timing synchronization errors.

4.5 Summary

In this chapter, we proposed a STNC scheme that utilizing transform-based coding to achieve spatial diversity with low transmission delay and eliminate the issue of imperfect frequency and timing synchronization. The scheme is applied to M2P-WNC network with an arbitrary number of user nodes N to provide a diversity order of N for each transmitted symbol. The PEP was analyzed and the code design criteria were derived to ensure achieving full diversity order. Simulations

are conducted to verify the performance of the proposed scheme and to show its advantage over a DSTBC scheme under timing synchronization errors.

Chapter 5

Coalition Formation Games for Energy Efficient Wireless Network Cocast

In the previous chapters, we have seen that WNC and its associated STNCs provide spatial diversity to combat channel fading and thus dramatically reduce the required transmit power in comparison with DTX. However, due to the additional processing power in receiving and retransmitting each other's information, not all nodes and WNC networks result in energy efficiency.

In this chapter, we first examine the power consumption of WNC networks and compare the power consumption with that of DTX networks for a given quality of service represented by a required SER. The network setting follows the M2P-WNC protocol in Chapter 2; however, this work can be easily extended to cover other WNC network settings. The power consumption model considers the processing power at the transmitter and receiver RF components and the required transmit power, which accounts for power amplifier (PA) energy efficiency and the peak-to-average-power ratio (PAPR), to convey the information over the medium between the transmitter and the receiver. Since user nodes are randomly distributed around the network, there is a need for a distributed algorithm that allows them to form cooperative groups and ensures network power saving without causing additional

power consumption to individual members. Thus in this chapter, we utilize coalition formation games to derive such an algorithm.

Coalition formation games have been applied in economics and political science. Recently, they are also used to analyze performance of communication networks [63]. For example, the authors in [64] consider a network of single antenna user nodes that send data in the uplink TDMA system to a base node with multiple antennas. The user nodes can transmit directly to the base node or they can form cooperative groups that employ MIMO to improve their capacity. To cooperate, the user nodes must exchange data, and thus the exchange of information incurs a cost in terms of power. Given a limited transmit power each node can be used to transmit, there is a tradeoff between the transmit power used to exchange and used to transmit to the base node. The tradeoff prevents the network from forming grand coalition, a coalition that comprises all user nodes in the network. The problem is to find the optimal coalition structure. To form cooperative groups, the authors employ the merge-and-split rules [65], which are proved to converge to a unique solution with arbitrary merge and split iterations.

In this chapter, each user node in WNC networks is treated as a player, who seeks partners to form a cooperative group to achieve power saving for itself and for the whole group. There is a tradeoff in power consumption when forming cooperative groups. Each user node when joining a cooperative group achieves transmit power saving through spatial diversity while incurs additional processing power due to the reception and retransmission of overheard information. The tradeoff represents the gain and the cost in cooperation. As the size of the cooperative group increases,

both the gain and the cost also increase. The additional processing power linearly increases with the size of the cooperative group. However, the transmit power saving in cooperation gradually diminishes due to the nature of incremental diversity that causes the relative transmit power saving[1] to reduce, as discussed in Chapter 3. In such a case, user nodes at some point can no longer be added to the cooperative group since the extra gain of involving the nodes is smaller than the additional cost. This prevents WNC networks from forming a grand coalition. Unlike [64], where the authors assume channel information is available at user nodes, we realize that information exchange also require certain medium access control and thus offer a TDMA-based merge process to orderly and efficiently form the cooperative groups in WNC networks. In addition, the complexity of exchanging information in wireless networks is too high, especially with large numbers of user nodes, we propose a heuristic approach in forming cooperative groups. The condition for a merge is that the merge only leads to power saving for the group without causing additional power burden to the individual members. Simulation is provided to corroborate the energy efficient WNC networks. From the simulation, there is a substantial reduction in network power consumption when using the proposed merge process. In addition, the merge process also improves the network lifetime.

[1] A relative power saving is defined as the difference in savings over direct transmission of two consecutive diversity orders.

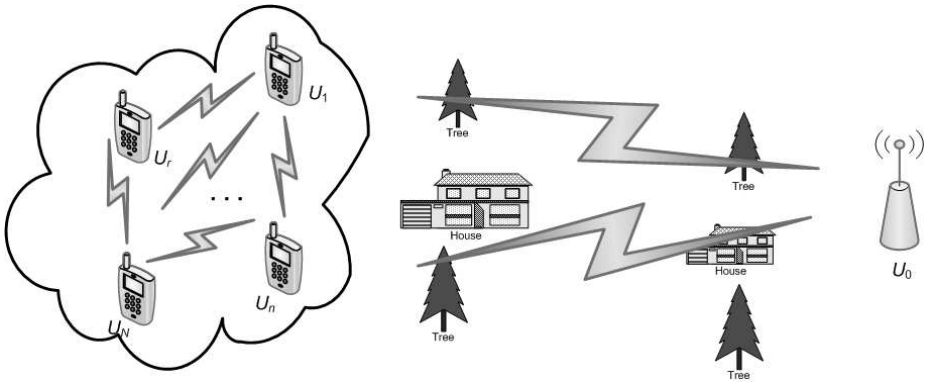

Figure 5.1: A multi-source wireless network.

5.1 Power Consumption in WNC and DTX Networks

5.1.1 System Model

We consider a network consisting of N user nodes denoted as $U_1, U_2, ..., U_N$ having their own information that need to be delivered to a common base node U_0 as shown in Figure 5.1. All nodes in the network are assumed to have a single antenna. The channels are modeled as narrow-band Rayleigh fading with additive white Gaussian noise (AWGN). The channel variance between arbitrary nodes U_u and U_v is $\sigma_{uv}^2 = \kappa d_{uv}^{-\alpha}$, where d_{uv}, κ, α are the distance between U_u and U_v, the pathloss constant, and the pathloss exponent, respectively. The pathloss constant can be modeled as

$$\kappa = \left(\frac{\lambda}{4\pi}\right)^2 \frac{G_t G_r}{N_f}, \tag{5.1}$$

where λ is the carrier wavelength, G_t and G_r are, respectively, the transmit and receive antenna gains, and N_f is the noise figure.

Two transmission protocols, namely DTX and WNC, are considered for the

network. Each user node in DTX directly transmit its own information to the base node while in WNC, the N user nodes cooperate with each other following the M2P-WNC scheme in Chapter 2, where the relay nodes utilize FDMA-like and CDMA-like techniques to combine the overheard information. The SER for transmitting information from U_n to U_0 in DTX using PSK modulation can be expressed as [56]

$$SER_n^{DTX} = F\left(1 + \frac{bE_{s,n}^{DTX}\sigma_{0n}^2}{N_0 \sin^2\theta}\right), \tag{5.2}$$

where $b = \sin^2(\pi/\mathcal{M})$ is a coefficient associated with $\mathcal{M}$-PSK modulation, N_0 is the thermal noise power spectral density (PSD), $E_{s,n}^{DTX}$ is the energy per symbol, and

$$F\left(x(\theta)\right) = \frac{1}{\pi}\int_0^{(\mathcal{M}-1)\pi/\mathcal{M}} \frac{1}{x(\theta)} d\theta. \tag{5.3}$$

When the SNR is high, the SER can be approximated as

$$SER_n^{DTX} \simeq \left(\frac{bE_{s,n}^{DTX}}{N_0}\right)^{-1} \frac{g(1)}{\sigma_{0n}^2}, \tag{5.4}$$

where $g(x) = \frac{1}{\pi}\int_0^{(\mathcal{M}-1)\pi/\mathcal{M}} [\sin(\theta)]^2 d\theta$.

As discussed in Chapter 2, the WNC network encompasses two phases, the source transmission phase and the relay transmission phase. In the first phase, each user node takes turn to transmit its own information to the base node. Due to the broadcast nature of wireless communications, other user nodes overhear the information and help relaying it to the base node in the later phase. In the relay transmission phase, each user node acting as a relay node constructs a unique signal in FDMA-like or CDMA-like manners. The signal is a combination of the overheard information previously received from the $(N-1)$ source nodes in the source transmission phase. The base node U_0 jointly detects the transmitted information from

the received signals in both source transmission phase and relay transmission phase.

We assume DF protocol in cooperation, where a relay node decodes the overheard information and then re-encodes and transmits it to the base node if the decoding is correct. From Chapter 2, the exact SER expression associated with information from U_n for $\mathcal{M}$-PSK modulation is

$$SER_n^{WNC} = \sum_{S_n=0}^{2^{(N-1)}-1} F\left(\left(1+\frac{bE_{s,nn}^{WNC}\sigma_{0n}^2}{N_0\sin^2\theta}\right)\prod_{\substack{r=1\\r\neq n}}^{N}\left(1+\frac{bE_{s,rn}^{WNC}\sigma_{0r}^2\beta_{rn}}{N_0\epsilon_n\sin^2\theta}\right)\right)\times \prod_{\substack{r=1\\r\neq n}}^{N} G\left(\beta_{rn}\right), \quad (5.5)$$

where $E_{s,nn}^{WNC}$ and $E_{s,rn}^{WNC}$ (for $r \neq n$) are, respectively, the energy per symbol allocated at the source node U_n and at the relay node U_r, ϵ_n is the interference impact due to the cross-correlations in forming the unique signal at a relay node, and $\beta_{rn} \in \{0,1\}$ for $r \neq n$ represents a detection state at U_r. When U_r detects U_n's information correctly, $\beta_{rn} = 1$; otherwise, $\beta_{rn} = 0$. All β_{rn}'s form the decimal number S_n in (5.5), i.e., $S_n = [\beta_{1n}...\beta_{rn}...\beta_{Nn}]_2$ that represents one of 2^{N-1} network detection states associated with information from U_n. In (5.5), we also have

$$G\left(\beta_{rn}\right) = \begin{cases} 1 - SER_{rn} & \text{if } \beta_{rn} = 1 \\ SER_{rn} & \text{if } \beta_{rn} = 0 \end{cases}, \quad (5.6)$$

where

$$SER_{rn} = F\left(1+\frac{bE_{s,nn}^{WNC}\sigma_{rn}^2}{N_0\sin^2\theta}\right) \quad (5.7)$$

is the SER in detecting U_n's information at U_r. Note that the total symbol energy associated with U_n's information is $E_{s,n}^{WNC} = E_{s,nn}^{WNC} + E_{s,rn}^{WNC}$. When the SNR is

high, the approximate SER can be expressed as

$$SER_n^{WNC} \simeq \left(\frac{bE_{s,n}^{WNC}}{N_0}\right)^{-N} \frac{1}{\sigma_{0n}^2} \sum_{S_n=0}^{2^{(N-1)}-1} \frac{g(1+|\Omega_{n1}|)[g(1)]^{|\Omega_{n0}|}}{\alpha_{nn}^{1+|\Omega_{n0}|} \prod_{r\in\Omega_{n1}} \alpha_{rn} \left(\frac{\sigma_{0r}^2}{\epsilon_n}\right) \prod_{r\in\Omega_{n0}} \sigma_{r0}^2}, \quad (5.8)$$

where α_{nn} and α_{rn} are, respectively, the fractions of the energy per symbol $E_{s,n}^{WNC}$ allocated at U_n and U_r, and Ω_{n0} and Ω_{n1} denote, respectively, subsets of indexes of relay nodes that decode U_n's information erroneously and correctly.

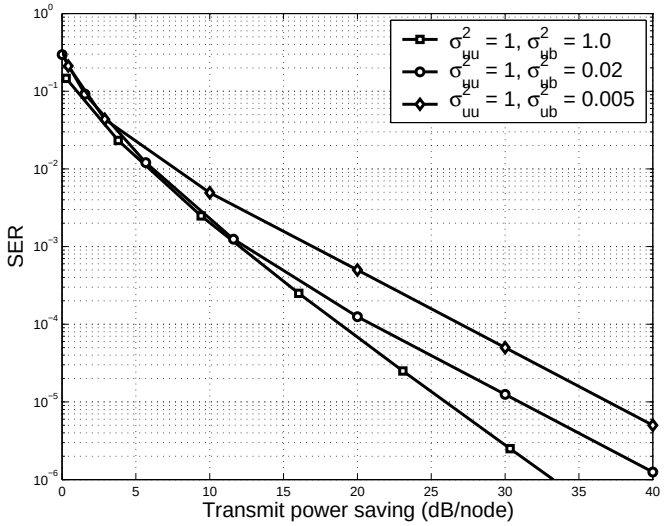

Figure 5.2: Transmit power saving of WNC over DTX for $N = 4$.

The transmit power for a given bit rate R_b and a constellation size $\mathcal{M}$ is

$$P_{s,n} = E_{s,n}\left(R_b/\log_2(\mathcal{M})\right), \quad (5.9)$$

where $E_{s,n}$ is the symbol energy in (5.2) and (5.5) for DTX and WNC, respectively. As shown in (5.8) and (5.4), WNC provides a spatial diversity order of N for transmissions to the base node U_0 while DTX results in a diversity order of one. The spatial diversity in WNC is the source of transmit power saving over DTX. Figure 5.2 illustrates the power saving of WNC over DTX, defined as a ratio between the

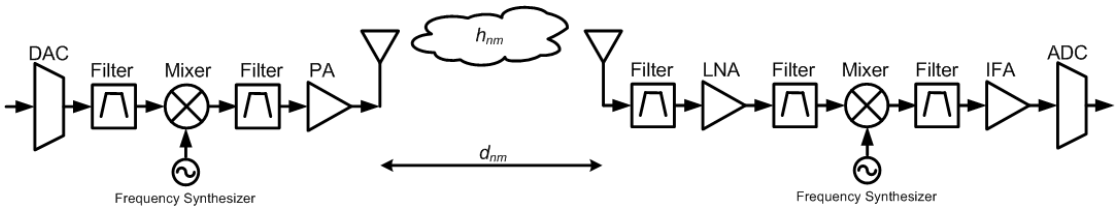

Figure 5.3: Transmitter and receiver chains.

required transmit power in DTX over that in WNC and expressed in dB. In the figure, σ_{uu}^2 and σ_{ub}^2 represents the channel variances among the user nodes and between the user nodes and the base nodes. σ_{uu}^2 is kept the same in the simulation, assuming the user nodes staying in the same cluster area and equidistant to each other, while σ_{ub}^2 varies, representing different distances between the user nodes and the base node. From the figure, we can see that two factors affect the transmit power saving. For the same channel variance, equivalently the same distance between the base nodes and the user nodes, the lower the required SER is the more transmit power saving. For the same required SER, the smaller the channel variance, equivalently the larger the distance between the base node and the user nodes, is the larger the power saving. When the saving exceed the additional processing power in relaying information, energy efficiency is achieved for WNC network.

5.1.2 Power Consumption in DTX Networks

Figure 5.3 illustrates the transmitter and receiver chains of single-antenna systems. As modeled in [66], [67], power consumption includes two major parts, the power consumption by the PA and the power consumption of other RF components.

In this work, we neglect the power consumption of the baseband signal processing blocks such as those to perform forward error correction and modulation. Nevertheless, the power consumption for these blocks can be incorporated into the model in future work [68].

In DTX networks, a user node U_n only transmits its own information. Thus its PA power consumption is

$$P_{PA,n}^{DTX} = \frac{\xi}{\eta} P_{s,n}^{DTX}, \tag{5.10}$$

where ξ is the PAPR, η is the PA efficiency, and $P_{s,n}^{DTX}$ is the required transmit power in DTX to convey the information over the transmission medium and is computed following (5.9). U_n also incurs the transmitter processing power due to the power consumption at the transmitter RF components. The transmitter power consumption can be given as

$$P_{TP,n}^{DTX} \approx P_{DAC} + P_{filt} + P_{mix} + P_{syn}, \tag{5.11}$$

where P_{DAC}, P_{filt}, P_{mix}, and P_{syn} are the power consumption at the digital-to-analog converter (DAC), the transmit filters, the mixer, and the frequency synthesizer, respectively. P_{filt}, P_{mix}, and P_{syn} can be modeled as constants [66] while P_{DAC} can be approximated as [66]

$$P_{DAC} \approx \left(\frac{1}{2} V_{dd} I_0 \left(2^{n_1} - 1\right) + n_1 C_p \left(2B + f_{cor}\right) V_{dd}^2 \right), \tag{5.12}$$

where V_{dd} and I_0 are the voltage and current supplies, C_p is the parasitic capacitance, n_1 is the number of bits in the DAC, $B = R_b / \log_2(\mathcal{M})$ is the symbol bandwidth,

and f_{cor} is the corner frequency. The total power consumption for U_n in DTX is

$$P_n^{DTX} = P_{PA,n}^{DTX} + P_{TP,n}^{DTX}. \tag{5.13}$$

The base node U_0's function is only receiving signals from the user nodes. Thus the power consumption at U_0 is also the receiver processing power consumption and can be given as

$$P_0^{DTX} \approx N(P_{LNA} + P_{filr} + P_{mix} + P_{IFA} + P_{ADC} + P_{syn}), \tag{5.14}$$

where P_{LNA}, P_{filr}, P_{mix}, P_{syn}, P_{IFA}, and P_{ADC} are the power consumption at low-noise amplifier (LNA), the receive filters, the mixer, the frequency synthesizer, the intermediate-frequency amplifier (IFA), and the analog-to-digital converter (ADC), respectively. The factor of N in (5.14) is due to the fact that U_0 receives N times in DTX networks. Like the transmitter RF chain, P_{LNA}, P_{filr}, P_{mix}, P_{syn}, and P_{IFA} can be modeled as constants [66] while P_{ADC} can be approximated as [66]

$$P_{ADC} \approx \frac{3V_{dd}^2 L_{min}\,(2B + f_{cor})}{10^{-0.1525n_2+4.838}}, \tag{5.15}$$

where L_{min} is the minimum channel length in the complementary metal-oxide-semiconductor (CMOS) technology and n_2 is the number of bits in the ADC.

5.1.3 Power Consumption in WNC Networks

Since all nodes in WNC networks are assumed to have a single antenna, the transmitter and receiver chain follows Figure 5.3. In WNC networks, user node U_n transmits its own information in the source transmission phase and relays other

nodes' information in the relay transmission phase. We assume equal power consumption strategy, which allocates one half of the required transmit power at the source node and equally divides the other half at the $(N-1)$ relay nodes. Thus the PA power consumption of user node U_n is

$$P_{PA,n}^{WNC} = \frac{\xi}{\eta}\left(\frac{1}{2}P_{s,n}^{WNC} + \sum_{\substack{r=1 \\ r\neq n}}^{N} \frac{1}{2(N-1)} P_{s,r}^{WNC}\right), \tag{5.16}$$

where ξ is the PAPR, η is the PA efficiency, and $P_{s,n}^{WNC}$ and $P_{s,r}^{WNC}$ follow (5.9). In addition, U_n incurs transmitter processing power consumption, which can be given as

$$P_{TP,n}^{WNC} = P_{TP,STP}^{WNC} + P_{TP,STP}^{WNC}, \tag{5.17}$$

where $P_{TP,STP}^{WNC}$ and $P_{TP,RTP}^{WNC}$ are the power consumption at the transmitter RF components in the source transmission phase and the relay transmission phase, respectively. $P_{TP,STP}^{WNC}$ and $P_{TP,RTP}^{WNC}$ follows (5.11), in which P_{DAC} takes the form of (5.12) in the source transmission phase and

$$P_{DAC} \approx \left(\frac{1}{2}V_{dd}I_0\left(2^{n_1}-1\right) + n_1 C_p\left(2(N-1)B + f_{cor}\right)V_{dd}^2\right) \tag{5.18}$$

in the relay transmission phase. Note that the factor of $(N-1)$ in (5.18) is due to use of FDMA-like or CDMA-like techniques to relay overheard information in WNC. In the source transmission phase, U_n also consumes power in reception of signals from other user nodes. The power consumption can be expressed as

$$P_{RP,n}^{WNC} \approx (N-1)(P_{LNA} + P_{filr} + P_{mix} + P_{IFA} + P_{ADC} + P_{syn}), \tag{5.19}$$

where P_{ADC} follows (5.15) and the power consumption of the remaining components can be modeled as constants. Note that the factor of $(N-1)$ in (5.19) accounts

for the $(N-1)$ receptions at U_n in the source transmission phase. In summary, the power consumption at user node U_n in WNC is

$$P_n^{WNC} = P_{PA,n}^{WNC} + P_{TP,n}^{WNC} + P_{RP,n}^{WNC}. \tag{5.20}$$

The base node U_0 in WNC receives signals in both phases. The receiver processing power consumption can be expressed as

$$P_0^{WNC} = P_{RP,STP}^{WNC} + P_{RP,RTP}^{WNC}, \tag{5.21}$$

where $P_{RP,STP}^{WNC}$ and $P_{RP,RTP}^{WNC}$ are the receiver power consumption in the source transmission phase and the relay transmission phase, respectively. $P_{RP,STP}^{WNC}$ and $P_{RP,RTP}^{WNC}$ follow (5.14), in which P_{ADC} takes the form of (5.15) for the source transmission phase and

$$P_{ADC} \approx \frac{3V_{dd}^2 L_{min}\,(2(N-1)B + f_{cor})}{10^{-0.1525n_2+4.838}} \tag{5.22}$$

in the relay transmission phase. Again, the factor of $(N-1)$ is due to the use of FDMA-like or CDMA-like techniques in the relaying signals in WNC.

5.1.4 Simulations

We perform computer simulations of the power consumption in DTX and WNC networks to realize the power saving of WNC over DTX. In this work, a power saving is defined as a ratio of the power consumption in DTX over that in WNC. We consider two power savings: network power saving, denoted as S_{net}, and

Table 5.1: Simulation parameters

Transmission parameters	RF parameters [66]	Parameters to compute P_{DAC} and P_{ADC} [66]
$f_c = 400$MHz	$\xi = 4$dB (QPSK)	$V_{dd} = 3$V
$\alpha = 3$	$\eta = 0.35$	$I_0 = 10\mu$A
$G_t = G_r = 3$dBi	$N_f = 7$	$C_p = 1$pF
N_0 = -174dBm/Hz	$P_{mix} = 30.0$mW	$L_{min} = 0.5\mu$m
$R_b = 10$Kbps	$P_{filt} = P_{filr} = 2.5$mW	$f_{cor} = 1MHz$
$\mathcal{M} = 4$ (QPSK)	$P_{LNA} = 20$mW	$n_1 = 16$ (16-bit DAC)
SER_0 =2e-3	$P_{IFA} = 3$mW	$n_2 = 14$ (14-bit ADC)
(equivalently BER_0 =1e-3)	$P_{syn} = 50.0$mW	

individual power saving, denoted as S_{ind}. We define

$$S_{net} \triangleq \frac{\sum_{n=0}^{N} P_n^{DTX}}{\sum_{n=0}^{N} P_n^{WNC}} \text{ (times)}, \tag{5.23}$$

$$S_{ind} \triangleq \frac{P_n^{DTX}}{P_n^{WNC}} \text{ (times)}. \tag{5.24}$$

Table 5.1 lists the parameters used in this simulation. We consider corner networks, in which the base node locates at $(0, 0)$ and N user nodes are uniformly distributed in a square area $\mathcal{A} = [0, D]^2$, where D measured in meters denotes the network dimension. Without loss of generality, the user nodes are numbered in decreasing order of their distance to the base node. In this manner, U_1 and U_N are the farthest and the closest to U_0, respectively. The number of user nodes is fixed with $N = 7$ while the network dimension takes different values. For each network

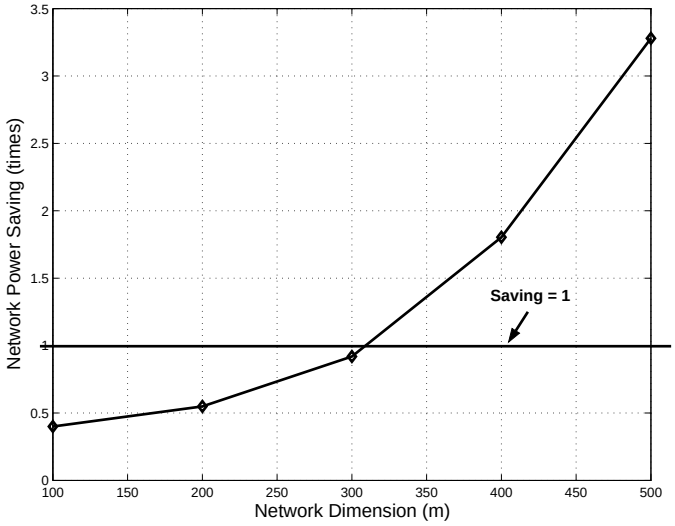

Figure 5.4: Average network power saving of WNC over DTX for $N = 7$.

dimension, fifty network realizations were generated.

Figure 5.4 presents the average network power saving of WNC over DTX for various network dimensions. As shown in the figure, the larger the network dimension is the larger the saving in network power consumption of WNC over DTX. For the given simulation setup, network power savings of 0.4, 0.6, 0.9, 1.8, and 3.3 are respectively realized for network dimensions of 100, 200, 300, 400, and 500m. However, WNC does not always lead to network power saving over DTX; the power saving is only realized for large network dimensions with $D > 300$m. From the previous section, the power consumption includes the transmit power accounting for the PA energy efficiency and PAPR and the processing power. The cooperation among nodes in WNC leads to transmit power saving as shown in Figure 5.2; the larger the transmission distance is the larger the transmit power saving of WNC over DTX. Nevertheless, the cooperation also incurs additional processing power due to

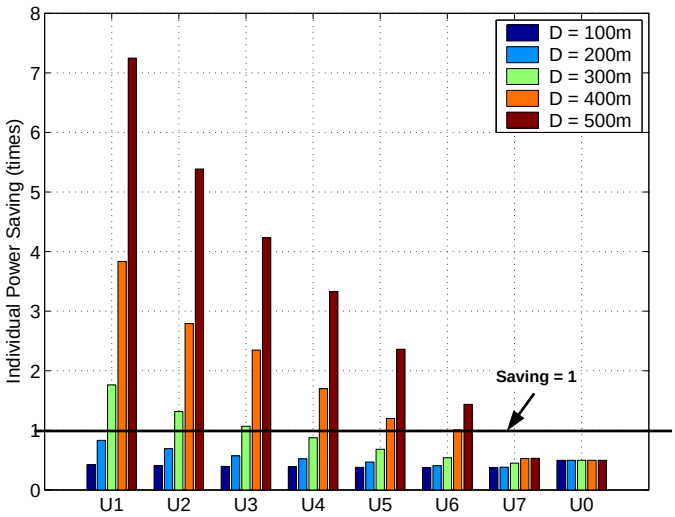

Figure 5.5: Average individual power saving of WNC over DTX for $N = 7$.

the reception and retransmission at the relay nodes. For small network dimensions, the saving in transmit power cannot compensate the additional processing power needed for cooperation. As a result, WNC consumes more power than DTX for these network dimensions.

Figure 5.5 presents the average power saving of individual nodes when participating in WNC over that in DTX for networks generated in Figure 5.4. An interesting observation is that for network dimensions associated with network power saving of WNC over DTX, not all user nodes have individual power saving. For example, U_6 and U_7 in WNC incur more power consumption over DTX for $D =$ 400m and 500m. They are the closest nodes to the base node and thus require much less transmit power in DTX. When participating in WNC, they do not have large transmit power saving that can compensate the additional processing power required in cooperation. As a result, they consume more power in WNC than in

DTX.

5.2 Coalition Formation Games for Energy Efficient WNC

5.2.1 Motivation

The simulation results presented in Subsection 5.1.4 show that there is no guarantee for arbitrary cooperative groups to achieve network power saving when using WNC over DTX. In addition, for cooperative groups that have network power saving, not all user nodes achieve individual power saving when cooperating together. Since user nodes are randomly distributed around the network, there is a need for a distributed algorithm that allows them to form cooperative groups and ensures power saving to the groups without causing additional power consumption to individual members. In this section, we utilize coalition formation games to derive such an algorithm for WNC networks.

Coalition formation games have been applied in economics and political science. Recently, they are also used to analyze performance of communication networks [63]. Fundamentally, a coalition formation game consists of a three-tuple $(\mathcal{N}, v, \mathbf{x})$ [63], where $\mathcal{N} = \{1, 2, ..., N\}$ is a set of players who seek to form cooperative groups (or coalitions) to improve their positions in the games, v is a utility function that defines how the game would play, and $\mathbf{x}$ is a vector representing the payoffs the members would receive from the value v.

In this work, each user node is treated as a player, who seeks partners to form a cooperative group to achieve power saving for itself and for the whole group. There is

a tradeoff in power consumption of WNC networks when forming cooperative groups. Each user node in a cooperative group achieves transmit power saving through spatial diversity while incurs additional processing power due to the reception and retransmission of overheard information. As a result, we define the utility function and individual payoff for WNC networks as

$$v(C) = \sum_{U_n \in C} \left(P_{PA,n}^{DTX} - P_{PA,n}^{WNC}\right) - \sum_{U_n \in C} \left(\left(P_{TP,n}^{WNC} + P_{RP,n}^{WNC}\right) - P_{TP,n}^{DTX}\right), \quad (5.25)$$

and

$$x_n(C) = \left(P_{PA,n}^{DTX} - P_{PA,n}^{WNC}\right) - \left(\left(P_{TP,n}^{WNC} + P_{RP,n}^{WNC}\right) - P_{TP,n}^{DTX}\right), \quad (5.26)$$

respectively, where C denotes a cooperative group with members U_n's. Note when $C = \{U_n\}$, a single-member coalition, the power terms associated with WNC converge to those associated with DTX. In that case $v(C) = x_n(C) = 0$. In (5.25), the first summation is the transmission power saving while the second summation is the additional processing power. They represent the gain and the cost, respectively, in cooperation. As the size of the cooperative group increases, both the gain and the cost also increase. The additional processing power linearly increases with the size of the cooperative group. However, the transmit power saving in cooperation gradually diminishes due to the nature of incremental diversity that causes the relative transmit power saving to reduce. At some point, user nodes can no longer be added to the cooperative group. This prevents WNC networks from forming a grand coalition [63]. The problem now is to find the optimal coalition structures. In [65], merge and split rules are proposed to form cooperative groups and proved to converge to a unique solution with arbitrary merge and split iterations. However,

the complexity of exchanging information in wireless networks is too high, especially with large numbers of user nodes N. To make the problem traceable, we propose in the next subsection a heuristic approach to form the cooperative groups in WNC.

5.2.2 Merge Process for WNC Networks

As proposed in [65], a merge between two cooperative groups C_1 and C_2 happens if it increases the value of the utility function, i.e.

$$v(C_1 \cup C_2) > v(C_1) + v(C_2) \text{ for } C_1 \cap C_2 = \emptyset. \tag{5.27}$$

This condition is to ensure that the network power saving of the merged group would be achieved. To avoid additional power burden to individual nodes when cooperating together, we impose the second condition as

$$x_n(C_1 \cup C_2) \geq x_n(C_i) \ \forall n, \tag{5.28}$$

for $i = 1$ or 2, the index of the cooperative group that U_n belongs to before merging C_1 and C_2 together.

Given the merge conditions in (5.27) and (5.28), we propose three phases for energy efficient WNC networks, including transmission request, merge process, and WNC transmission. Since the merge requires the computation of each member's transmit power, which needs the knowledge of the inter-user and user-base channel variances for all members in the group, we propose a TDMA-based merge process that ensures the information exchange among the members occur orderly and efficiently.

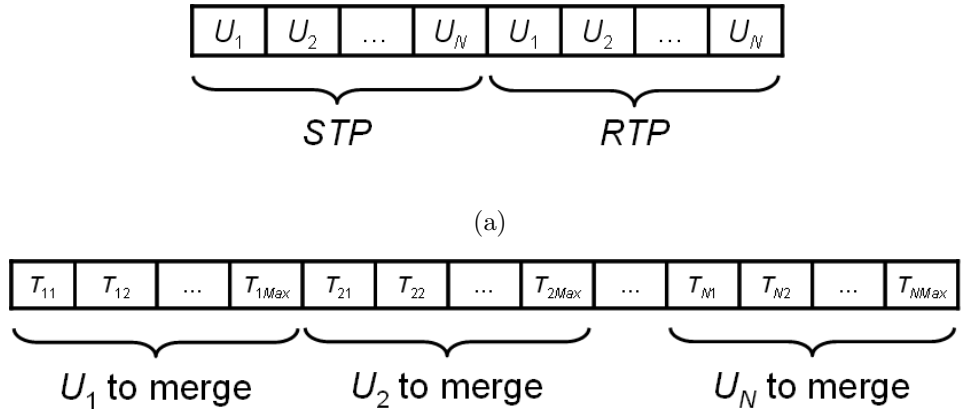

Figure 5.6: (a) WNC transmission schedule and (b) Merge schedule.

In the first phase, the N user nodes send a request-to-send (RTS) signal to the base node U_0. The user nodes are set to use a maximum transmission power so that other user nodes can estimate the inter-user channel variances. After receiving the RTS, U_0 broadcasts a WNC transmission schedule as shown in Figure 5.6(a), which includes $2N$ time slots for the source transmission phase and the relay transmission phase of WNC transmissions. Based on the broadcasting signal from U_0, the user nodes can also estimate the user-base channel variances. This information will be used later in the merge process. The WNC transmission schedule also indicates the transmission order, starting from the farthest to the closest user nodes. Without loss of generality, we can number the user nodes in decreasing order of their distance to the base node. In this manner, U_1 and U_N are the farthest and the closest to U_0, respectively.

Based on the order in the WNC transmission schedule, starting from U_1 down to U_N, the merge process takes place to form cooperative groups. In this manner,

disadvantageous nodes in terms of transmit power consumption will receive more assistance to lower their power burden. In the merge process, each node is allowed a maximum number of attempts, denoted as Max, which is used to control the overhead in forming cooperative groups. The merge schedule for the merge process is shown in Figure 5.6(b), which is TDMA-based. Note that the time slots in the merge schedule are much shorter than those in the WNC transmission schedule. Assume at present that we attempt to merge at user node U_n. If U_n already belongs to some cooperative groups due to previous merges at other user nodes, then U_n remains silent during its assigned $T_{n1}, T_{n2}, ..., T_{nMax}$ time slots. Otherwise, U_n begins to merge with other remaining nodes in the network. In this case, U_n is called the coalition head and its index n is used for the coalition index.

The merge at U_n happens as the following. At the beginning, U_n broadcasts its user-base channel variance to its neighbors. Assume at present that U_n attempts to merge with U_r, its closest non-member neighbor. U_n first sends the indexes of its members to U_r and requests for a merge. U_r agrees to merge if the following three conditions are satisfied. Firstly, U_r does not belong to any cooperative groups. Secondly, it has inter-user and user-base channel variances for all coalition members. This condition is to ensure full diversity for all user nodes in the cooperative group. Note that U_r obtains the inter-user channel variances during the transmission request phase and the user-base channel variances in the broadcasting signals from other members who already join the cooperative group. Lastly, conditions in (5.27) and (5.28), computed by U_r, are satisfied. When U_r agrees to merge, it acknowledges the merge back to the coalition members, sends the transmit power requirements for

each nodes in the cooperative group, and broadcasts its user-base channel variance. User nodes in range of U_r's transmission can record U_r's user-base channel variance for later computation when it is requested to merge. U_n then repeats its attempts to the next closest non-member node until there is no node available to merge or when U_n expires all its attempts.

After the cooperative groups have formed, WNC transmissions take place. Each user node takes turn to transmit based on U_0's WNC transmission schedule in Figure 5.6(a). A user node only decodes and relays information for its members. The base node detects information of user nodes based on the cooperative groups formed by the merge process. Table 5.2 summarizes the three phases of the energy efficient WNC networks.

5.2.3 Simulations

We perform computer simulations to validate the proposed merge process for WNC networks. The performance metrics of network power saving and individual power saving defined in (5.23) and (5.24) are used. For the simulation setup, the simulation parameters are listed in Table 5.1. We consider center networks, in which the base node locates at (0,0) and N user nodes are uniformly distributed in a square area $\mathcal{A} = [-500m, 500m]^2$. The user nodes are numbered in decreasing order of their distance to the base node with U_1 and U_N being the farthest and the closest to U_0, respectively.

In the first simulation, we examine the performance of the proposed merge

Table 5.2: Three phases for energy efficient WNC networks

Transmission request phase:

1. Each user node sends a RTS to the base node.
   1.1. Other user nodes estimate the inter-user channel variances.
2. Base node broadcasts WNC schedule with transmission orders.
3. User nodes estimate inter-user channel variances.

Merge process phase: For $n = 1, 2, ..., N$

1. U_n remains silent during $T_{n1}, T_{n2}, ..., T_{nMax}$ if it is already merged.
2. Otherwise, U_n starts the merge process with Max attempts.
   2.1. U_n follows the merge process in 5.2.2.

WNC transmission phase:

1. Each user node takes turn to transmit based on WNC schedule.
   1.1. A node decodes and relays only for its cooperative members.
2. Base node detects information based on the cooperative groups.

process with various numbers of attempts Max. As discussed in Subsection 5.2.2, Max affects the overhead in forming the cooperative groups; larger Max values associate with larger overhead. However, the maximum coalition sizes are governed by the conditions in (5.27) and (5.28). When these conditions fail, no node can be added into the cooperative group and further attempts are not helpful in improving power saving. Thus there is a need to obtain an optimal Max value for each WNC network.

Figure 5.7 presents the average network power saving versus various Max

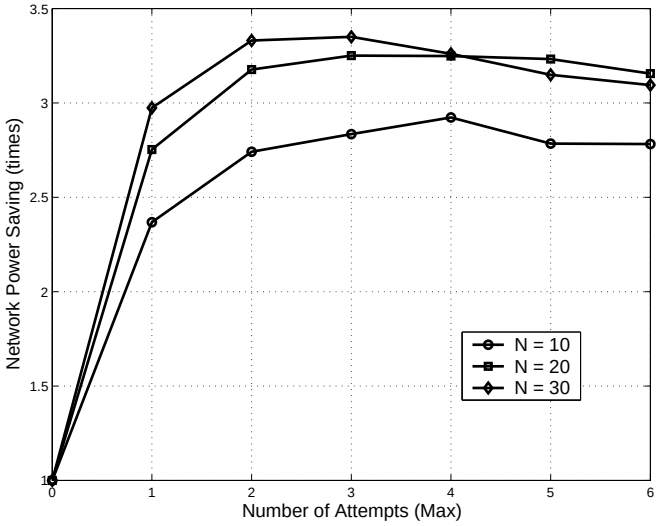

Figure 5.7: Average network power saving versus various numbers of attempts (Max).

values for different numbers of user nodes N. Fifty network realizations were used in the simulation. In the figure, $Max = 0$ associates with the use of DTX protocol and thus the network power saving takes a value of one. From the figure, as Max increases, the network power saving first also increases but then gradually reduces and tends to be stable for large values of Max. The increment in network power saving for the first few of Max values is due to the large gain in transmit power saving of WNC over DTX. As Max continues increasing, more processing power is needed while the relative gain in transmit power reduces, and that causes the reduction in network power saving. For large values of Max, the cooperative groups are no longer able to accept new members due to the failure of conditions (5.27) and (5.28). As a result, the network power saving tends to be stable for large values of Max and further attempts are no longer necessary. In this particular setup, Max

= 4, 3, and 2 are optimal for $N = 10$, 20, and 30, respectively.

Next, we examine the coalition structures generated by the proposed merge process for different Max values. In this simulation, the same WNC network with $N = 30$ user nodes is used for $Max = 1$, 2, and 3. Note that for a Max value, the maximum size of a cooperative group is $Max + 1$. In Figure 5.8, the generated coalition structures are shape and color coded. From the figure, different values of Max result in different coalition structures, as expected. A common point among the coalition structures is that some of user nodes stand by itself, creating single-member coalitions, for example $\{U_{25}\}, \{U_{26}\}, \{U_{27}\}, \{U_{28}\}, \{U_{29}\}$, and $\{U_{30}\}$. These nodes are usually in locations close to the base node and do not have large transmit power saving to offset the additional processing power when cooperating with other nodes. The figure also shows that some cooperative groups, for example $\{U_9, U_{13}\}$ and $\{U_{11}, U_{17}\}$ in Figures 5.8(b) and 5.8(c), do not have the full coalition size (i.e. $Max + 1$). Although these cooperative groups welcome additional members since that would help reducing their power consumption, other nodes may not find the benefits to join due to the additional power burden to themselves, and thus larger cooperative groups could not be formed.

For the generated coalition structures, the associated network power savings are 3.09, 3.40, and 3.39 times for $Max = 1$, 2, and 3, respectively. Clearly on one hand, the merge process with $Max = 1$ does not exploit the full potential of cooperation. On the other hand, $Max = 3$ does not provide more network power saving over $Max = 2$. This again emphasizes the importance of choosing the right value for Max in WNC networks. A small value of Max does not exploit the full

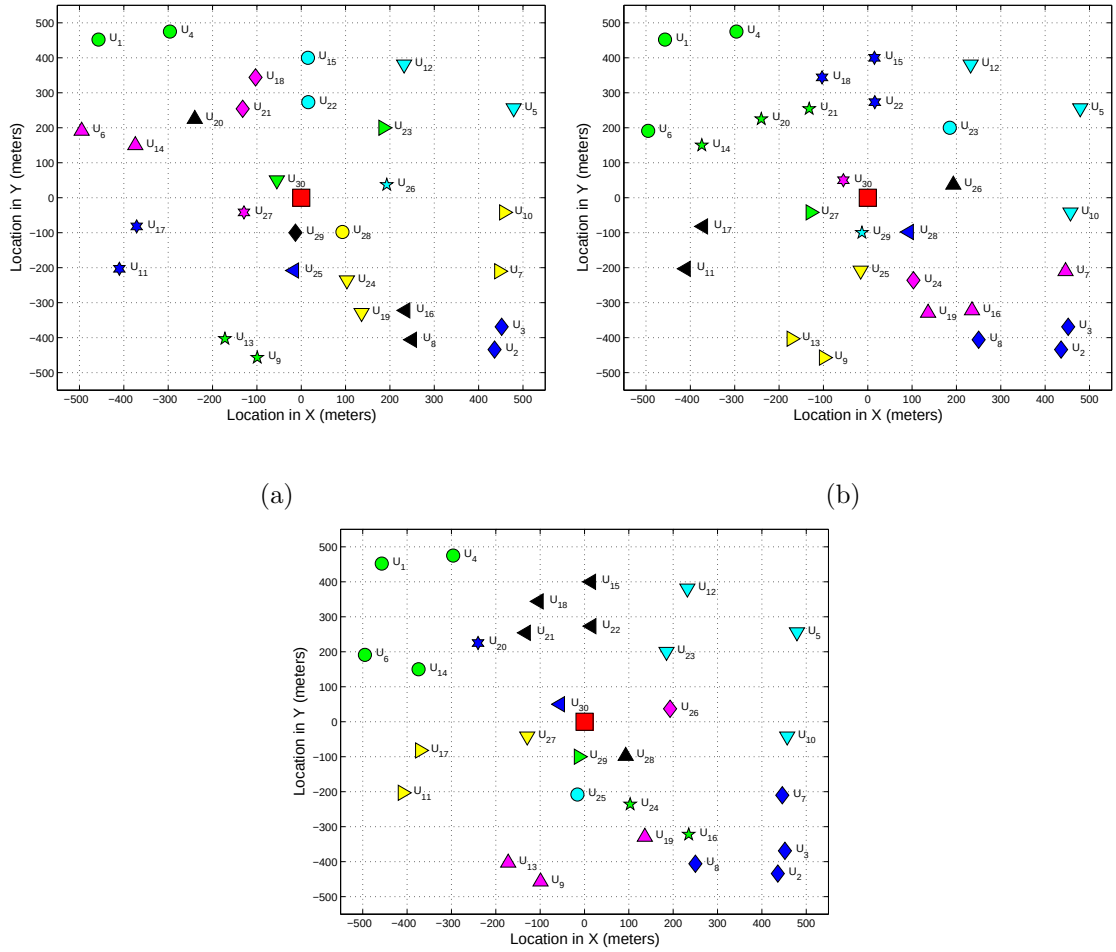

(a) (b)

(c)

Figure 5.8: Coalition structures (shape and color coded) for the same WNC network ($N = 30$) with different Max values: (a) $Max = 1$, (b) $Max = 2$, and (c) $Max = 3$. The associated network power savings are 3.09, 3.40, and 3.39 times, respectively.

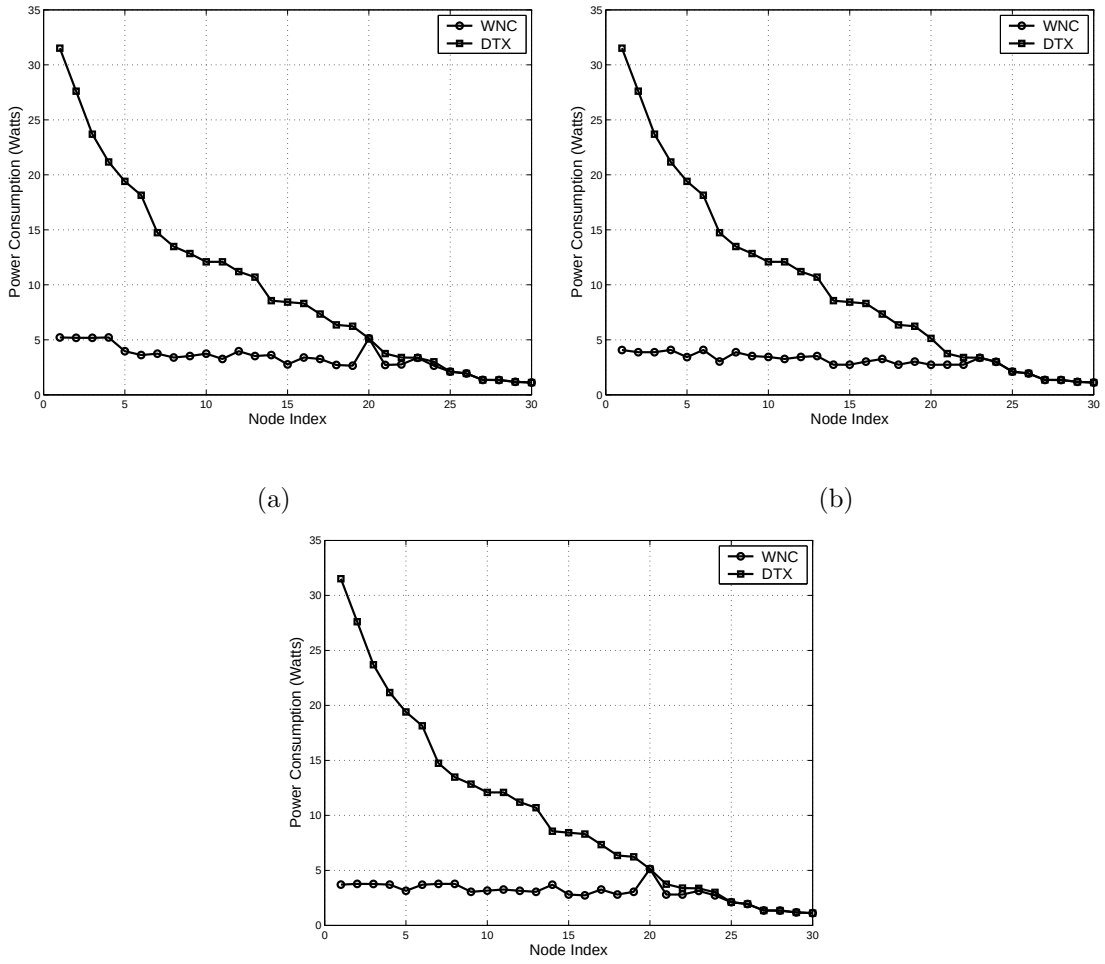

(a) (b)

(c)

Figure 5.9: Individual power savings for the same WNC network ($N = 30$) with different Max values: (a) $Max = 1$, (b) $Max = 2$, and (c) $Max = 3$.

potential in cooperation while a large value of Max may result in large overhead without providing any additional benefits.

Figure 5.9 shows the actual power consumption for individual user nodes in DTX and WNC networks for different coalition structures in Figure 5.8. From the figure, high power consumption is required for distant user nodes in the DTX network. This is due to the dependency of the required transmit power on the transmission distance in direct transmission. In contrast, there is a substantial reduction in power consumption of the WNC networks. This is due to the cooperation among the user nodes that helps reducing the required transmit power through the mean of spatial diversity. In addition, the power consumption profile in the WNC networks is very even, especially for the case of $Max = 2$, in which the power consumption for individual user nodes is very comparable. Clearly, beside helping reducing network power consumption, the proposed merge process also help improving network lifetime, defined as the time until the first node in the network dies.

Figure 5.10 shows the individual power saving for different coalition structures in Figure 5.8. Again, power saving is defined as a ratio between the power consumption in DTX network over that in WNC network. From the figure, the individual power savings for all individual user nodes are greater or equal to one . This clearly proves that the merge process would not cause additional power burden to individual nodes, as expected. From the figure, the individual power savings are comparable between $Max = 2$ and $Max = 3$. However, we see a large gap in individual power savings between $Max = 1$ and 2, especially for low user indexes. Again, the merge process with $Max = 1$ does not exploit the full potential of cooperation in this

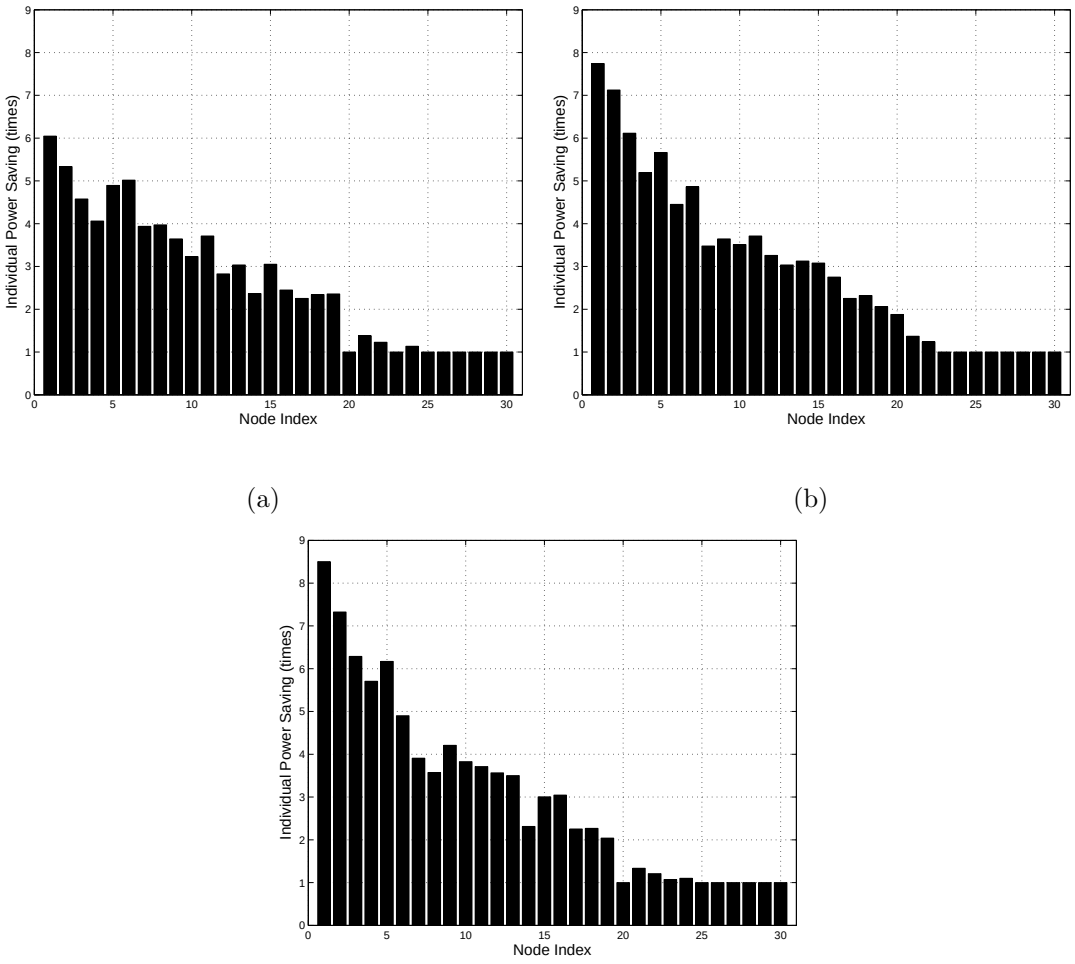

Figure 5.10: Individual power savings for the same WNC network ($N = 30$) with different Max values: (a) $Max = 1$, (b) $Max = 2$, and (c) $Max = 3$.

particular WNC network.

5.3 Summary

In this chapter, we examined the power consumption in WNC and DTX networks. The power consumption includes the processing power at the transmitter and receiver RF components and the transmit power accounting for PA energy efficiency and PAPR to convey information over the medium between the transmitter and receiver. The simulation shows that WNC does not always achieve power saving over DTX. In addition, for WNC networks associated with power saving, due to the additional power in reception and retransmission in cooperation, not all user nodes achieve individual power saving. To ensure energy efficient WNC networks, we proposed a TDMA-based merge process based on coalition formation games to orderly and efficiently form the cooperative groups in WNC networks. A node is merged into a cooperative group only if the merge leads to power saving for the group without causing additional power burden to the individual members. Simulation was provided to corroborate the energy efficient WNC networks. From the simulation, there is a substantial reduction in network power consumption when using the proposed merge process. In addition, the merge process also improves the network lifetime.

Chapter 6

Conclusions and Future Work

6.1 Conclusions

In this dissertation, we proposed a novel concept of wireless network cocast (WNC) and its associated STNCs to eliminate the issues of imperfect frequency and timing synchronization in cooperative communications while achieving full spatial diversity with low transmission delays. Due to the asynchronous nature of cooperation, the imperfect synchronization prevents cooperative communications emerging in practice. The WNC and its STNCs provide the mechanism to overcome such issues and would take cooperative communications into applications. More specifically, we addressed the following problems in this dissertation.

In Chapter 2, we described the novel concept of WNC and proposed a number of STNCs based on FDMA-like and CDMA-like combining techniques. We consider two general cases of multipoint-to-point (M2P) and point-to-multipoint (P2M), where user nodes transmit and receive their information to and from a common base node, respectively, with the assistance from relay nodes. Both DF and AF protocols in cooperative communications were considered. We derived the exact and the asymptotic SER expressions for general $\mathcal{M}$-PSK modulation for DF pro-

tocol. For AF protocol, we offered a conditional SER expression given the channel knowledge. The STNCs were then applied into networks, in which the user nodes are also relay nodes helping each other in their transmission. We studied the performance improvement of the WNC networks over DTX networks. Simulations show that given the same quality of service, WNC networks achieve a great improvement in terms of power saving, range extension, and transmission rate.

In Chapter 3, we proposed a number of location-aware cooperation-based schemes denoted as INC, MAX, and WNC to reduce the aggregate transmit power and achieve even power distribution among the user nodes in the network. The INC scheme utilizes single-relay cooperative communication, resulting in good reduction of aggregate transmit power and low transmission delay; however, power distribution is still uneven. In the MAX scheme, multi-relay cooperative communication is leveraged to provide incremental diversity to achieve even power distribution and substantial reduction in aggregate transmit power. However, transmission delay in the MAX scheme grows quadratically with the number of user nodes in the network. As a result, we utilized the concept of WNC to propose a location-aware WNC scheme that achieves incremental diversity as in the MAX scheme and low transmission delay as in the INC scheme. Performance evaluation in uniformly distributed networks showed that the INC, MAX, and WNC schemes substantially reduce aggregate transmit power while the MAX and WNC schemes also provide even power distribution.

In Chapter 4, a STNC based on transform-based coding, whose coding matrices take a form of Hadamard or Vandermonde matrices and compose a set of

parameters that are optimized for conventional signal constellations, was proposed to improve the spectral efficiency of the combining signals at relay nodes over that of the STNCs developed in Chapter 2. We analyzed the PEP performance of the proposed STNC and derived the design criteria of the network coding matrix to achieve full diversity. Simulations were conducted to validate the performance of the proposed STNC. In addition, performance comparison between the proposed STNC and a DSTBC scheme, which operated under timing synchronization errors, was investigated through simulations.

In Chapter 5, we first examined the power consumption in WNC and DTX networks. The power consumption includes the processing power at the transmitter and receiver radio-frequency components and the required transmit power to convey information over the medium between the transmitter and receiver. As shown in previous chapters, WNC networks and its associated STNCs provide spatial diversity to combat channel fading and thus dramatically reduce the required transmit power in comparison with DTX networks. However, due to the additional processing power in receiving and retransmitting each other's information, not all nodes and WNC networks result in energy efficiency. Thus we then offered a TDMA-based merge process based on coalitional formation games to orderly and efficiently form cooperative groups in WNC networks. A node is merged into a cooperative group only if the merge leads to power saving for the group without causing additional power burden to the individual members. Simulations were provided to corroborate the energy efficient WNC networks. From the simulation, there was a substantial reduction in network power consumption when using the proposed merge process.

In addition, the merge process also improved the network lifetime.

6.2 Future Work

In this dissertation, we provide a new framework for cooperation among single-antenna nodes in a network to overcome the issues of imperfect frequency and timing synchronization and to achieve spatial diversity for improvements in their communications performance. In WNC, each relay node combines overheard symbols in a unique signal to reduce the transmission delay. To further reduce the transmission delay in WNC networks, multiple transmission should be allowed. However, such relaxation can impact the performance of WNC networks due to the imperfect synchronization. Since STNCs provide spatial diversity to improve communication performance, the spatial diversity can be used to compensate the impact of the imperfect synchronization. For future work, we would like to investigate the performance tradeoffs in WNC networks when multiple simultaneous transmissions are permitted.

All the proposed STNCs assume coherent detection, in which detection of symbols at a receiver requires a full knowledge of channel coefficients. To acquire the channel information at a receiver, a preamble is usually inserted into the transmitted signal and channel estimation is utilized at the receiver. However, channel estimation is a challenging and costly task, especially in time-selective fading environments [69]. The amount of overhead due to the channel estimation becomes substantial in multinode wireless systems because the amount of training or convergence time

(if blind channel estimation is used) grows with the number of links. To bypass the channel estimation, distributed differential space-time coding schemes are proposed for multiple-relay networks in [70]. However, the differential coding schemes assume that simultaneous transmissions from multiple nodes are synchronized at the receiver. Such an assumption, as discussed in Chapter 1, is hard to achieve in practice. As a result, we will extend this work by deriving a differential STNC that helps to overcome the issues of imperfect frequency and timing synchronization as well as the burden of channel estimation.

Bibliography

[1] G. J. Foschini and M. J. Gans, "On the limits of wireless communications in a fading environment when using multiple antennas," *Wireless Personal Communications*, vol. 6, pp. 311–355, Mar. 1998.

[2] E. Telatar, "Capacity of multi-antenna Gausian channels," *Eur. Trans. Telecom.*, vol. 10, pp. 585–595, Nov. 1999.

[3] D. Tse and P. Viswanath, *Fundamentals of Wireless Communication*. USA: Cambridge University Press, 2005.

[4] V. Tarokh, N. Seshadri, and A. R. Calderbank, "Space-time codes for high data rate wireless communication: Performance analysis and code construction," *IEEE Trans. Inform. Theory*, vol. 44, pp. 744–765, Mar. 1998.

[5] S. M. Alamouti, "A simple transmit diversity technique for wireless communications," *IEEE J. Sel. Areas Commun.*, vol. 16, pp. 1451–1458, Oct. 1998.

[6] V. Tarokh, H. Jafarkhani, and A. R. Calderbank, "Space-time block coding from orthogonal designs," *IEEE Trans. Inform. Theory*, no. 5, pp. 1456–1467, Jul. 1999.

[7] W. Su, X. G. Xia, and K. J. R. Liu, "A systematic design of high-rate complex orthogonal space-time block codes," *IEEE Commun. Lett.*, vol. 8, pp. 380–382, Jun. 2004.

[8] H. Jafarkhani, "A quasi-orthogonal space-time block code," *IEEE Trans. Commun.*, no. 1, pp. 1–4, Jan. 2001.

[9] R. Blum, Y. Li, J. Winters, and Q. Yan, "Improved space-time coding for MIMO-OFDM wireless communications," *IEEE Trans. Commun.*, vol. 49, pp. 1873–1878, Nov. 2001.

[10] W. Su, Z. Safar, and K. J. R. Liu, "Full-rate full-diversity space-frequency codes with optimum coding advantage," *IEEE Trans. Info. Theory*, vol. 51, pp. 229–249, Jan. 2005.

[11] Z. Liu, Y. Xin, and G. Giannakis, "Space-time-frequency coded OFDM over frequency selective fading channels," *IEEE Trans. Signal Process.*, vol. 50, no. 10, pp. 2465–2476, Oct. 2002.

[12] W. P. Siriwongpairat, W. Su, M. Olfat, and K. J. R. Liu, "Multiband-OFDM space-time-frequency coding for UWB communication systems," *IEEE Trans. Signal Process.*, vol. 54, no. 1, pp. 214–224, Jan. 2006.

[13] K. J. R. Liu, A. K. Sadek, W. Su, and A. Kwasinski, *Cooperative Communications and Networking*. Cambridge, UK: Cambridge University Press, 2008.

[14] J. N. Laneman, D. N. C. Tse, and G. W. Wornell, "Cooperative diversity in wireless networks: efficient protocols and outage behavior," *IEEE Trans. Inform. Theory*, vol. 50, no. 12, pp. 3062–3080, Dec. 2004.

[15] A. Sendonaris, E. Erkip, and A. B., "User cooperation diversity-Part I and Part II," *IEEE Trans. Commun.*, no. 11, pp. 1927–1948, Nov. 2003.

[16] A. K. Sadek, W. Su, and K. J. R. Liu, "Multinode cooperative communications in wireless networks," *IEEE Trans. Signal Process.*, vol. 55, no. 1, pp. 341–355, Jan. 2007.

[17] K. G. Seddik, A. K. Sadek, W. Su, and K. J. R. Liu, "Outage analysis and optimal power allocation for multi-node relay networks," *IEEE Signal Processing Letters*, vol. 14, no. 6, pp. 377–380, Jun. 2007.

[18] A. Ibrahim, A. K. Sadek, W. Su, and K. J. R. Liu, "Cooperative communications with relay selection: when to cooperate and whom to cooperate with?," *IEEE Trans. Wireless Commun.*, vol. 7, no. 7, pp. 2814–2827, Jul. 2008.

[19] J. N. Laneman and G. W. Wornell, "Distributed space-time coded protocols for exploiting cooperative diversity in wireless networks," *IEEE Trans. Inform. Theory*, vol. 49, pp. 2415–2525, Oct. 2003.

[20] L. Venturino, X. Wang, and M. Lops, "Multiuser detection for cooperative networks and performance analysis," *IEEE Trans. Signal Process.*, vol. 54, no. 9, pp. 3315–3329, Sept. 2006.

[21] V. Mudumbai, D. R. Brown, U. Madhow, and H. V. Poor, "Distributed transmit beamforming: Challenges and recent progess," *IEEE Commun. Mag.*, vol. 47, no. 2, pp. 102–110, Feb. 2009.

[22] S. Jagannathan, H. Aghajan, and A. Goldsmith, "The effect of time synchronization errors on the performance of cooperative MISO systems," *Proc. IEEE GLOBECOM*, pp. 102–107, Dec. 2004.

[23] S. Wei, D. L. Goeckel, and M. Valenti, "Asynchronous cooperation diversity," *IEEE Trans. Wireless Commun.*, vol. 5, pp. 1547–1557, Jun. 2006.

[24] Y. Li and X. G. Xia, "A family of distributed space-time trellis codes with asynchronous cooperative diversity," *IEEE Trans. Commun.*, vol. 55, no. 4, pp. 790–800, Apr. 2007.

[25] M. Damen and A. Hammons, "Delay-tolerent distributed-TAST codes for cooperative diversity," *IEEE Trans. Info. Theory*, vol. 53, no. 10, pp. 2941–2956, Oct. 2007.

[26] D. Brown, G. Prince, and J. McNeill, "A method for carrier frequency and phase synchronization of two autonomous cooperative transmitters," *Proc. IEEE 6th Signal Process. Adv. Wireless Commun.*, pp. 260–264, Jun. 2005.

[27] T. Banwell, J. Dixon, J. Koshy, D. Waring, A. Scaglione, and M. Sharp, "Distributed carrier synchronization for HF cooperative communication employing randomized space-time block coding," *Proc. IEEE MILCOM*, pp. 1–7, Oct. 2009.

[28] H. Q. Lai and K. J. R. Liu, "Multipoint-to-point and point-to-multipoint space-time network coding," *Proc. IEEE ICASSP*, pp. 2878–2881, Mar. 2010.

[29] H. Q. Lai and K. J. R. Liu, "Space-time network coding," *IEEE Trans. Signal Proces.*, vol. 59, no. 4, pp. 1706–1718, Apr. 2011.

[30] H. Q. Lai and K. J. R. Liu, "Wireless network cocast: Cooperative communications with space-time network coding," *Proc. IEEE ICWITS*, Aug. 2010.

[31] H. Q. Lai, A. Ibrahim, and K. J. R. Liu, "Location-aware cooperative communications utilizing linear network coding," *Proc. IEEE GLOBECOM*, Dec. 2008.

[32] H. Q. Lai, A. Ibrahim, and K. J. R. Liu, "Wireless network cast: Location-aware cooperative communications with linear network coding," *IEEE Trans. Wireless Commun.*, vol. 8, no. 7, pp. 3844–3854, Jul. 2009.

[33] H. Q. Lai, Z. Z. Gao, and K. J. R. Liu, "Space-time network codes utilizing transform-based coding," *Proc. IEEE GLOBECOM*, Dec 2010.

[34] R. Ahlswede, N. Cai, S. R. Li, and R. W. Yeung, "Network information flow," *IEEE Trans. Info. Theory*, vol. 46, pp. 1204–1216, Jul. 2000.

[35] S. Y. R. Li, R. W. Yeung, and N. Cai, "Linear network coding," *IEEE Trans. Info. Theory*, vol. 49, no. 2, pp. 371–338, Feb. 2003.

[36] T. Ho, M. Medard, R. Koetter, D. Karger, M. Effros, J. Shi, and B. Leong, "A random linear network coding approach to multicast," *IEEE Trans. Info. Theory*, vol. 52, pp. 4413–4430, Oct. 2000.

[37] S. Verdu, *Multiuser Detection.* NewYork, USA: Cambridge University Press, 2005.

[38] L. L. Hanzo, L.-L. Yang, E.-L. Kuan, and K. Yen, *Single and Multi-Carrier DS-CDMA: Multi-User Detection, Space-Time Spreading, Synchronisation, Networking and Standards.* USA: Cambridge University Press, 2005.

[39] "IEEE Standard for Local and Metropolitan Area Networks - Part 16: Air Interface for Broadband Wireless Access Systems," *IEEE Std 802.16-2009.*

[40] X. Giraud, E. Boutillon, and J. C. Belfiore, "Algebraic tools to build modulation schemes for fading channels," *IEEE Trans. Info. Theory*, vol. 43, no. 3, pp. 938–952, May 1997.

[41] J. Boutros and E. Viterbo, "Signal space diversity: A power- and bandwidth-efficient diversity technique for the Rayleigh fading channel," *IEEE Trans. Info. Theory*, vol. 44, no. 4, pp. 1453–1467, Jul. 1998.

[42] Y. Xin, Z. Wang, and G. B. Giannakis, "Space-time diversity systems based on linear constellation precoding," *IEEE Trans. Wireless Commun.*, vol. 2, no. 2, pp. 294–309, Mar. 2003.

[43] "IEEE Standard for Local and Metropolitan Area Networks - Part 11: Wireless LAN Medium Access Control (MAC) and Physical Lyer (PHY) Specification," *IEEE Std 802.11-2007*.

[44] P. Merkey and E. C. Posner, "Optimum cyclic redundancy codes for noisy channels," *IEEE Trans. Info. Theory*, vol. 30, no. 6, pp. 865–867, Nov. 1984.

[45] M. K. Simon and M. S. Alouini, "A unified approach to the performance analysis of digital communication over generalized fading channels," *Proc. IEEE*, vol. 86, no. 9, pp. 1860–1877, Sep. 1998.

[46] A. Leon-Garcia, *Probability and Random Processes for Electrical Engineering*. USA: Addison Wesley Longman, 2nd ed., 1994.

[47] C. D. Meyer, *Matrix Analysis and Applied Linear Algebra*. USA: SIAM, 2000.

[48] Y. Cao and B. Vojcic, "MMSE multiuser detection for cooperative diversity CDMA systems," *Proc. IEEE WCNC*, vol. 1, pp. 42–47, Mar. 2004.

[49] E. Larsson and B. R. Vojcic, "Cooperative transmit diversity based on superposition modulation," *IEEE Commun. Lett.*, vol. 9, no. 9, pp. 778–780, Sep. 2005.

[50] L. Xiao, T. Fuja, J. Kliewer, and D. Costello, "A network coding approach to cooperative diversity," *IEEE Trans. Info. Theory*, vol. 53, no. 10, pp. 3714–3722, Oct. 2007.

[51] K. Ishii, "Cooperative transmit diversity utilizing superposition modulation," *Proc. IEEE Radio and Wireless Symposium*, pp. 337–340, Jan. 2007.

[52] T. Bui and J. Yuan, "Iterative approaches of cooperative transmission based on superposition modulation," *Proc. IEEE ISCIT*, pp. 1423–1428, Oct. 2007.

[53] G. Sun, J. Chen, W. Guo, and K. J. R. Liu, "Signal processing techniques in network aided positioning: A survey," *IEEE Signal Process. Mag.*, vol. 22, no. 4, pp. 12–23, Jul. 2005.

[54] A. H. Sayed, A. Tarighat, and N. Khajehnouri, "Network-based wireless location," *IEEE Signal Process. Mag.*, vol. 22, no. 4, pp. 24–40, Jul. 2005.

[55] W. Su, A. K. Sadek, and K. J. R. Liu, "Cooperative communications in wireless networks: performance analysis and optimum power allocation," *Wireless Personal Communications*, vol. 44, no. 2, pp. 181–217, Jan. 2008.

[56] J. G. Proakis, *Digital Communications*. New York, USA: McGraw-Hill, 4th ed., 2001.

[57] V. Tarokh, H. Jafarkhani, and A. R. Calderbank, "Space-time block coding for wireless communications: Performance results," *IEEE J. Sel. Areas Commun.*, no. 3, pp. 451–460, Mar. 1999.

[58] J. Li, J. Ge, Y. Tang, and X. Xiong, "Cooperative diversity based on Alamouti space-time code," *Proc. IEEE ICCSIT*, pp. 642–646, Sep. 2008.

[59] M. Ju, H. Song, and I. Kim, "Exact BER analysis of distributed Alamouti's code for cooperative diversity networks," *IEEE Trans. Commun.*, vol. 57, no. 8, pp. 2380–2390, Aug. 2009.

[60] B. M. Hochwald and S. T. Brink, "Achieving near-capacity on a multiple-antenna channel," *IEEE Trans. Commun.*, vol. 51, no. 3, pp. 389–399, Mar. 2003.

[61] R. A. Horn and C. R. Johnson, *Topics in Matrix Analysis*. New York, USA: Cambridge University Press, 2008.

[62] S. Siwamogsatham, M. P. Fitz, and J. Grimm, "A new view of performance analysis of transmit diversity schemes in correlated Rayleigh fading," *IEEE Trans. Info. Theory*, vol. 48, no. 4, pp. 950–956, Apr. 2002.

[63] W. Saad, Z. Han, and M. Debbah, "Coalitional game theory for communication networks," *IEEE Signal Process. Mag.*, pp. 77–97, Sep. 2009.

[64] W. Saad, Z. Han, M. Debbah, and A. Hjorungnes, "A distributed coalition formation framework for fair user cooperation in wireless networks," *IEEE Trans. Wireless Commun.*, vol. 8, no. 9, pp. 4580–4593, Sep. 2009.

[65] K. Apt and A. Witzel, "A generic approach to coalition formation," *Proc. Int. Workshop Computational Social Choice (COMSOC)*, Dec. 2006.

[66] S. Cui, A. J. Goldsmith, and A. Bahai, "Energy-constraint modulation optimization," *IEEE Trans. Wireless Commun.*, vol. 4, no. 5, pp. 2349–2360, Sep. 2005.

[67] S. Cui, A. J. Goldsmith, and A. Bahai, "Energy-efficiency of MIMO and cooperative MIMO techniques in sensor networks," *IEEE J. Sel. Areas Commun.*, vol. 22, no. 6, pp. 1089–1098, Aug. 2004.

[68] H. S. Kim and B. Daneshrad, "Energy-aware link adaptation for MIMO-OFDM based wireless communication," *Proc. IEEE MILCOM*, pp. 1–7, Nov. 2008.

[69] Q. Zhao and H. Li, "Differential modulation for cooperative wireless systems," *IEEE Trans. Signal Proces.*, vol. 55, no. 5, pp. 2273–2283, May 2007.

[70] Y. Jing and H. Jafarkhani, "Distributed differential space-time coding for wireless relay networks," *IEEE Trans. Commun.*, vol. 56, no. 7, pp. 1092–1100, Jul. 2008.